**UNIVERSITY OF CALIFORNIA,**
**IRVINE**

# Geometric Control of Macrophage Phenotype and Function: A Single Cell Analysis

DISSERTATION

Submitted in partial satisfaction of the requirements
for the degree of

DOCTOR OF PHILOSOPHY

in Biomedical Engineering

by

**Frances Y. McWhorter**

Dissertation Committee:
Professor Wendy F. Liu, Chair
Professor Abraham P. Lee
Professor Jered B. Haun

2015

# TABLE OF CONTENTS

## ACKNOWLEDGEMENTS

I would like to express my deepest gratitude to my advisor and committee chair, Professor Wendy Liu, for all her guidance and support over the last five years. Her continued optimism carried me through the many trials and tribulations of graduate school. She is one of the most understanding and kind person I have worked with, and is a great example of a successful female scientist. I would also like to thank my other committee members, Professors Jered Haun and Abe Lee, for taking time out of their busy schedules to provide me with fresh perspectives and insights into my project.

I would like to thank all the Liu Lab members, past and present, not only for insightful discussions about science but also for the numerous outside-of-lab excursions. I will cherish the laughters and camaraderie we shared for many years to come. In addition, I would like to especially thank the Edwards Lifesciences center manager Linda McCarthy for her technical expertise and many valuable advices on life.

Words cannot begin to express my gratitude to my mother, who has been my biggest supporter, best friend and cheapest therapist. Without her, I would not be where I am today. I also thank my father, Dan McWhorter, for his continued support of my education. Lastly, I thank my friends and families, near and afar, for sharing life's ups and downs with me.

# CURRICULUM VITAE

**Frances Y. McWhorter**

| | |
|---|---|
| **2015** | **Ph.D.** in Biomedical Engineering<br>*University of California, Irvine*, CA |
| **2013** | **M.S.** in Biomedical Engineering<br>*University of California, Irvine*, CA |
| **2010** | **B.S.** in Biomedical Engineering, with Honors<br>*The University of North Carolina at Chapel Hill*, NC |

**Publications**

1. **F. Y. McWhorter**, C. T. Davis, W. F. Liu, "Physical and mechanical regulation of macrophage phenotype and function." *Cell. Mol. Life Sci.* 72 (7), 1303-1316; Apr. 2015
2. K. S. Harker, E. Jivan, **F. Y. McWhorter**, W. F. Liu, & M. B. Lodoen, "Shear Forces Enhance Toxoplasma gondii Tachyzoite Motility on Vascular Endothelium," *mBio*, 2014; 5(2), e01111-13.
3. N. Ueno, K. S. Harker, E. V. Clarke, **F. Y. McWhorter**, W. F. Liu, A. J. Tenner, and M. B. Lodoen, "Real-time imaging of infected human monocytes under fluidic shear stress reveals rapid translocation of intracellular parasites across endothelial barriers," *Cell. Microbiol.* Nov. 2013
4. **F. Y. McWhorter***, T. Wang*, P. Nguyen, T. Chung, and W. F. Liu, "Modulation of macrophage phenotype by cell shape," *Proc. Natl. Acad. Sci.*, Oct. 2013; 110(43)
5. A. G. Pope, G. Wu, **F. Y. McWhorter**, E. P. Merricks, T. C. Nichols, T. J. Czernuszewicz, C. M. Gallippi, and A. L. Oldenburg, "Contrast-enhanced imaging of SPIO-labeled platelets using magnetomotive ultrasound," *Phys. Med. Biol.*, vol. 58, no. 20, pp. 7277-7290, Oct. 2013

# ABSTRACT

**Geometric Control of Macrophage Phenotype and Function:**

**A Single Cell Analysis**

By

Frances Y. McWhorter

Doctor of Philosophy in Biomedical Engineering

University of California, Irvine, 2015

Professor Wendy F. Liu, Chair

Macrophages are tissue-resident immune cells that play critical roles in development, metabolic regulation, maintenance of tissue homeostasis and defense against invading pathogens. To carry out their diverse functional roles, Macrophages rely on their remarkable plasticity to assume a continuum of different functional phenotypes in response to their ever changing microenvironment. Precise spatiotemporal regulation of macrophage phenotype is necessary as any abnormalities could lead to chronic inflammation, the hallmark of many diseases such as cancer and atherosclerosis. While it is thought that biochemical signals such as cytokines and chemokines are the primary regulators of macrophage phenotype polarization, evidence has begun to emerge that tissue architecture and physical cues in the extracellular microenvironment can also contribute to their phenotype and function. Here, we show that macrophage cell shape can similarly provide an instructive signal for macrophage phenotype polarization.

One of the major challenges in studying macrophages is to accurately identify phenotypic subsets within a heterogeneous population. Traditional bulk measurements of cellular attributes, such as ELISA, Western blot and PCR, can overlook these heterogeneities and the potential role of rare subsets in initiating an immune response. Furthermore, the effects of complex microenvironmental cues, both soluble and physical, on macrophage activation may be lost when only the average response of a cell population is examined. In order to tease apart the nuanced contributors to the functional variances among macrophages, single cell analyses of phenotype and function must be utilized. While flow cytometry combined with immunofluorescence and fluorescence in situ hybridization (FISH) has already been used in phenotying and genotyping single cells, functional assessment through secreted products remain challenging. Recent chip-based technologies have used micro-/nano- fabricated wells to physically isolate single T cells and B cells and examined their secreted products. However, these are non-adherent cells that are less sensitive to the physical and adhesive cues provided by the extracellular matrix. To examine adherent cells such as macrophages, we herein created a single cell cytokine detection platform that allows for controlled physical and adhesive microenvironment. We used this platform to examine single macrophage cytokine secretion under different soluble factors, on different adhesive substrates, and with different cell shape.

This work broadens our understanding of macrophage activation in the context of pathophysiological conditions. It further demonstrates the importance of physical and adhesive cues on macrophage activation and function, and the necessity to include these factors when studying macrophages *in vitro*. Our novel device allows precise control of macrophage adhesion and simultaneous detection of secreted products on a single cell level, which will facilitate future research on this topic.

## LIST OF FIGURES

# CHAPTER 1: Macrophage Biology and Mechanotransduction

## 1.1 Macrophage phenotype polarization

Macrophages are primarily tissue-resident immune cells that play critical roles in development, metabolic regulation, maintenance of tissue homeostasis and defense against

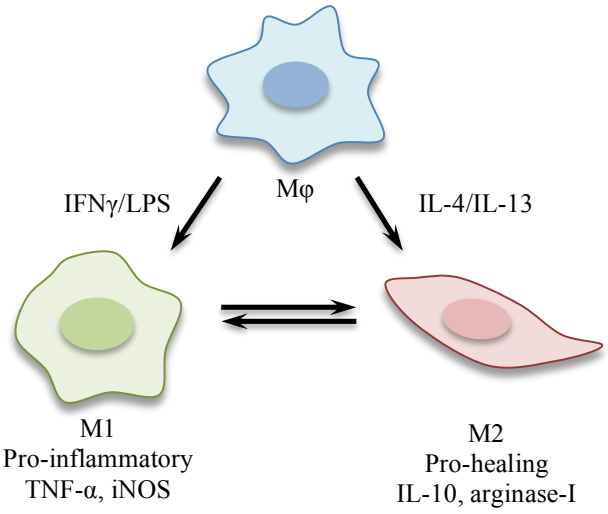


Figure 1. Schematic of macrophage phenotype polarization

invading pathogens. Most tissue-specific macrophages are derived from the yolk sac during embryonic development and maintained through self-renewal[1]. In adults, hematopoiesis continues in the bone marrow to give rise to circulating blood monocytes. These monocytes can be recruited and differentiated to replenish tissue macrophages, usually at sites of injury[2]. In their basal states, macrophages maintain tissue homeostasis through the clearance of apoptotic cells and assist in tissue repair. Most mature macrophages were thought to have little to no

proliferative potential and are only replenished through continued infiltration of monocytes into the tissue. However, some studies suggest that this may not always be true as in the case of microglial cells in the central nervous system[3].

Being prolific phagocytic cells, macrophages are indispensable in maintaining tissue homeostasis through the clearance of apoptotic cells and cellular debris left from tissue remodeling. While this process generally does not involve any immune signaling or other immune cell activities, some cellular debris may have receptors that present as danger signals. To carry out more specialized immune functions, macrophages can become activated and assume a diverse range of phenotypes in response to their microenvironment. It is now widely accepted that macrophage phenotypes can be viewed as a continuum[4], comprising of multiple distinct functional states and each with its unique transcriptional profile[5]. In the most simplistic form, macrophage activation is often categorized into two extremes: classically-activated (M1) and alternatively-activated (M2). (Fig.1) The macrophage activation states are named based on the traditional dichotomy of T-lymphocytes classification: Th-1 and Th-2. Th-1 lymphocytes release cytokines such as interferon-γ (IFN-γ) that induces M1 polarization in macrophages, while Th-2 cytokines such as Interleukin (IL) 4, 5, 13 induce M2 polarization[6]. In addition to T-cell derived cytokines, many other factors can lead to macrophage activation.

Classical (M1) activation of macrophages has been well-studied for decades and can be achieved through stimulation with IFN-γ alone or together with microbial products such as

lipopolysaccharide (LPS). It leads to secretion of high levels of cytokines tumor necrosis factor alpha (TNF-α), interleukin-12 (IL-12) and interleukin-23 (IL-23). This pro-inflammatory activation is also marked by intracellular production of nitric oxide (NO) and reactive oxygen intermediates (ROI), toxic agents that help fight pathogens. Alternative (M2) activation of macrophages is a more recent discovery in comparison. It refers to macrophages assuming any activation state other than the classically-activated M1 phenotype and includes three subtypes: M2a, M2b, and M2c[7]. In general, these macrophages are known for their ability to resolve inflammation and facilitate tissue repair by releasing anti-inflammatory cytokine interleukin-10 (IL-10) and various growth factors. IL-10 is known to directly inhibit the productions of inflammatory cytokines TNFα, IL-1, IL-6, and IL-12 via STAT-3 dependent pathways[8]. In addition to IL-10, murine M2 macrophages also produce high levels of arginase, an enzyme involved in collagen synthesis and thus tissue repair. Through the degradation of arginine, arginase facilitates the production of ornithine, which can be metabolized by proline to synthesize collagen[9]. Arginase and iNOS are known to act on the same substrate $_{L}$-arginine[10], which makes them good markers for M2 and M1 macrophages, respectively. M2 cells also highly express macrophage mannose receptor (MR) or CD 206 on their surfaces. CD 206 is important for phagocytosis of microorganisms by mediating binding and recognition[11]. It also enables macrophage fusion to one another and the formation of foreign body giant cells (FBGCs) during foreign body reaction[12].

Although majority of the properties of M1 and M2 macrophages are conserved between human and murine cells[7], there are some key differences. Most notably, arginase-I and Ym-1, which are strongly expressed in alternatively-activated murine macrophages, are not induced by IL-4 and IL-13 stimulation in human macrophages [13].

## 1.2 Macrophage plasticity and heterogeneity in diseases and tissue remodeling

### *1.2.1 Cancer*

Macrophages play a pivotal role in tumor progression and cancer. There is strong positive correlation between the number of tumor-associated macrophages (TAMs) and poor tumor prognosis[14]. TAMs isolated from human and murine tumors have been found to express low levels of pro-inflammatory chemokine receptors while producing anti-inflammatory cytokines IL-10 and TGFβ, suggesting that they are similar to the M2 phenotype[15]. In addition, these macrophages produce many growth factors and enzymes such as VEGF and MMPs to promote angiogenesis. Thus, not only do the anti-inflammatory TAMs have very little cytotoxic effects on tumor cells, they further tumor growth and metastasis[16]. Studies have already shown that switching the TAMs from an M2 to an M1 phenotype, such as through inhibition of IL-10 function, can restore anti-tumoral activities and improve tumor prognosis[17].

*1.2.2 Atherosclerosis*

Macrophages contribute significantly to the progression of atherosclerosis and comprise up to 60% of atherosclerotic lesion mass. Reducing the number of macrophages in mice has been demonstrated to impede disease progression[18]. Evaluation of macrophage phenotype in atherosclerotic plaques in apoE-KO mice revealed that M2 macrophages predominate in early plaques while M1 phenotype seems to take over in later stages[19]. The specific roles of M1 and M2 macrophages in atherogenesis are still unclear. M1 cells are generally considered atherogenic due to their inflammatory properties and involvement in generating foam cells[20]. They promote smooth muscle cell growth, release vasoactive nitric oxide, and produce reactive oxygen species that disrupt normal lipoprotein oxidation[21]. On the other hand, M2 macrophages are thought to be atheroprotective because of their role in resolving inflammation. Recent studies have shown that M2 cells have lower capacity for lipid uptake and foam cell transformation. Hindering the ability of M2 cells to clear apoptotic cells and tissue debris has strong positive correlation with atherosclerosis progression[22].

*1.2.3 Wound healing*

Macrophages are indispensable in wound repair as depletion of these cells significantly

disturbs the healing process. Wound macrophages also experience phenotypic change during the repair process. Macrophages isolated from 1-day-old murine wounds primarily secrete M1 inflammatory cytokines such as TNF-α and IL-6, whereas 7-day-old wound macrophages secrete predominantly M2 cytokine TGF-β[23]. The M1 macrophages are the initial responders to sites of injury. They set the stage for repair primarily through scarring. M2 macrophages arrive later to resolve inflammation and eliminate M1 cells. The repair mechanism of M2 macrophages results in much less scarring, due to their ability to decrease collagen deposition. Both phases, M1 and M2, are crucial for the repair process. Recent study shows that destruction of M1 macrophages in the early stage resulted in reduced overall healing response and excessive scar formation while depletion of M2 macrophages in the later stage resulted in reduced new tissue development[24].

*1.2.4 Tissue remodeling around implantable biomaterials*

The ultimate functional success of implantable biomaterials is dependent on its interaction with the host immune system. All biomaterials, when implanted, elicit the foreign body response (FBR), which is largely orchestrated by macrophages. The reaction begins with nonspecific adsorption of proteins from the blood and surrounding tissues, which facilitates macrophage adhesion to the material surface, and it invariably leads to the encapsulation of the material by

fibrotic tissues. Macrophages are involved in the every step of this process and therefore are critical in determining the outcome of a material's integration into the host. Current strategies for mitigating FBR-associated inflammation primarily focus on passivating material surfaces to minimize macrophage adhesion. This strategy has had limited success because macrophages have alternative activation mechanisms that do not require adhesion[12]. Macrophage plasticity has been observed during the foreign body reaction, and their phenotype may be an important predictor of material integration outcome. Early on post implantation, most macrophages assume the M1 phenotype to attack the foreign object. As time goes on, they gradually switch over to a more M2-like phenotype to assist in tissue repair[25]. It is important for this phenotypic switch to occur in a timely fashion as the failure to do can result in chronic inflammation. Conversely, a predominant M2 population present at earlier time points during the process is directly indicative of constructive remodeling and positive outcome[26,27]. Some studies have shown that many macrophages around biomaterials can concurrently express both M1 and M2 markers. However, increased expressions of M2 markers still correlate with less fibrosis and better neovascularization[28].

In all the processes discussed in this section, macrophage phenotypes are dynamically regulated, and they are capable of switching from one form to another in response to their constantly changing local environment. Dysregulation of macrophage phenotypic switch can

perpetuate inflammation, impede tissue repair and further disease progression. Alternatively, modulation of macrophage phenotype presents as a potential strategy for mitigating host immune response against biomaterials, as well as therapeutic approach for many diseases. Before this could be realized, a better understanding of what regulates macrophage phenotype is required. As with most cells, macrophages respond to a myriad of signals present in their extracellular microenvironment. Although soluble factors such as cytokines and chemokines are known to be the primary regulators and are fairly well-characterized, evidence has only begun to surface that physical and mechanical cues can also direct macrophage phenotype polarization.

## 1.3 Physical, mechanical and adhesive cues in regulation of cellular behaviors

### *1.3.1 Mechanotransduction in other cells*

The behavior of a cell, which includes proliferation, migration, differentiation and activation, is governed by a milieu of cues in its local microenvironment. A growing body of evidence suggests that physical and mechanical signals play an equally important role in governing cell behavior as biochemical signals. Cells sense mechanical signals through membrane mechanosensitive proteins and the cytoskeleton and convert them into biochemical signals in a process known as mechanostransduction[29]. Although this ability was initially thought to be

exclusive to certain specialized cells such as hair cells[30], it is now clear that most cells can respond to changes in their physical environment.

Many tissues in the body experience mechanical stress on a daily basis. Mechanical loading and strain are required for osteogenesis[31]. Hemodynamic forces such as shear stress and cyclic stretch are critical in maintaining structural integrity and proper functioning of cells in the cardiovascular system. Endothelial cells, when subject to physiologic shear stress, not only accelerate proliferation and capillary tube formation but also reorient and elongate in the direction of flow[32]. Cyclic stretch has been shown to induce proliferation and contractile protein synthesis in vascular smooth muscle cells[33]. Hemodynamic forces are also necessary for embryonic stem cell differentiation into vascular progenitor cells[34].

In addition to forces, architecture and mechanical properties of the extracellular matrix (ECM) can provide subtler cues to anchorage-dependent cells. Groundbreaking work in recent years have shown that substrate rigidity directs stem cell lineage commitment[35] and helps maintain stem cell self-renewal potential[36]. Changes in cell shape, which can be a direct consequence of substrate rigidity and topology, has been associated with changes in cell function for many years[37]. Various microfabrication and bioengineering tools have been developed to manipulate cell geometry individually and in groups. Using micro-contact printing, Chen et al. demonstrated that cell shape alone can regulate growth and apoptosis in endothelial cells[38]. Elongated cell shape proved to be a more potent regulator of embryonic mesenchymal stem cell

differentiation into smooth muscle cells than soluble factors[39]. Rectangular cell shape resulted in preferential stem cell differentiation into bone whereas square cells do not[40]. Mesenchymal stem cells micropatterned on small islands are able to better maintain multipotency, an effect that was attributed to decreased actin-myosin contractility[41].

### *1.3.2 Mechanotransduction in macrophages*

#### *1.3.2.1 Substrate topography and matrix architecture*

Much of our current understanding of how physical cues influence macrophage phenotype has come from the field of biomaterials. Macrophages are among the first cells to interact with implanted biomaterials and are key mediators of the host foreign body response. Macrophage phenotype polarization during FBR is critical as M2 phenotype has been shown to be indicative of constructive remodeling around implanted materials[26,42]. Therefore, the ability to modulate macrophage phenotype toward M2 polarization has emerged as a promising design strategy for biomaterials. Toward this end, many groups have attempted to exploit the material surface topography as a passive, alternative approach to biochemical surface modification (Fig. 2).

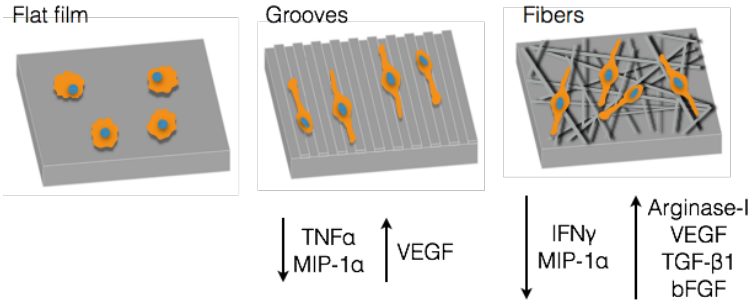


Figure 2. Substrate topography such as micro- and nano- grooves and fibers can affect macrophage adhesion, spreading and activation.[43–45] Reproduced from [46]

It has long been observed that macrophages prefer to adhere to rough surfaces rather than flat[47]. More recently, researchers have examined whether surface roughness plays a role in macrophage secretion of inflammatory cytokines. In the absence of LPS stimulation, sandblasting and acid etching roughened titanium surfaces were shown to increase TNF-α secretion while decreasing production of chemoattractants monocyte chemotactic protein 1 (MCP-1) and macrophage inflammatory protein-1α (MIP-1α) in RAW264.7 macrophages. When activated with LPS, surface roughness synergistically upregulates secretion of all inflammatory cytokines including TNF-α, IL-1β, IL-6, MCP1, and MIP-1α. The surface roughness enhanced secretion was generally observed at the 24 h or 48 h time point but not at an earlier, 6h, time point, implying a temporal dependence of the topographical effect[48]. Contrarily, in murine J744A.1 macrophages, sandblasted and acid etched roughness in titanium showed no significant effect on the production of IL-1β, IL-6, IL-10 and nitric oxide (NO)[49]. However,

nano-roughened titanium surfaces resulted in mitigated expression of TNF-α, IL-1β and NO in J744A.1 macrophages. In addition, nanorough substrates also restricted macrophage migration through reduction in migration speed and distance[50]. These seemingly incongruent findings may be attributed to differences in cell line, experimental time points, and perhaps the rather imprecise control of surface topology through roughening.

Using lithographic methods to more precisely control surface topography, studies have examined macrophage response to various polymers imprinted with grooves or gratings. On poly(methyl methacrylate) containing 10 μm-wide and 0.5 μm-deep grooves, murine P388D1 macrophages exhibit substantial cellular elongation and align along the grooves and ridges. The patterned substrate enhanced macrophage migration in terms of speed, distance and persistence[51]. Additionally, microgrooves promote phagocytosis of polystyrene microbeads by increasing the number of phagocytic cells as well as the number of phagocytosed beads per cell[52]. Intriguingly, groove depth, rather than width, was suggested to be the predominating factor influencing migration and phagocytosis. RAW264.7 cells cultured on nanogrooves (250 nm - 2 μm in width) imprinted in polymers also display elongated morphologies (Fig. 2). Macrophage response to various groove widths, in terms of both morphology change and cytokine secretion, appeared to be biphasic. Flat substrates and gratings less than 500 nm in width had little to no effect on macrophages, whereas cells cultured on 1μm lines exhibit most elongated shape and show marked reduction in inflammatory cytokine secretion. Overall, the grooves appear to

require longer durations to influence macrophage cytokine secretion profile, as the reduced secretion was only seen after 48 h[43]. *In vivo* studies using the same substrates reported similar findings in that microscale grooves reduce cell adhesion and foreign body giant cell formation when compared to planar substrates.

Alternative to surface patterned materials are electrospun polymer meshes, which more closely recapitulate native microenvironments. Saino et al.[44] investigated the activation of RAW264.7 cells on electrospun poly(L-lactic) (PLLA) fibrous materials (Fig. 2). Both fiber diameter and alignment were found to affect macrophage adhesion and activation. Aligned fibers, of either micro- (~1.6 μm) and nano- (~600 nm) scale, appeared to enhance macrophage adhesion when compared to randomly aligned or flat PLLA substrates. In the presence of LPS, macrophages secreted less inflammatory cytokines on fibrous PLLA than on flat PLLA films. Unlike microgrooved substrates, the attenuation in activation caused by aligned fibers was only observed during the first 24 h, and not at the later 7 d time point. Similarly, electrospun polydioxanone (PDO) scaffolds containing larger fiber/pore size not only mitigated M1 activation but also skewed macrophage polarization toward an M2 phenotype, with increased expressions of arginase-1, VEGF, TGF-β1, and bFGF[45]. Implantation of random and aligned polycaprolactone (PCL) nanofibers in rats led to thinner fibrous capsules when compared to flat PCL films[53], suggesting reduced inflammation and enhanced wound healing around the fibrous materials. Consistent with these findings, Sanders et al. examined a variety of different polymers

and fiber sizes and demonstrated that in all materials, smaller fiber (1-5 μm diameter) resulted in thinner fibrous capsule formation when compared to larger fibers (11-15 μm diameter) [54].

While the majority of the studies investigating the effect of substrate topology on macrophage function have been carried out on 2D engineered materials, it has been argued that cells can behave very differently in 3D microenvironments[55]. By embedding electrospun poly(lactic-co-glycolic acid) (PLGA) within a hydrogel, one group created a nanofibrous hydrogel system for investigating the effect of 2D versus 3D substrate architecture on human macrophages derived from peripheral blood mononuclear cells (PBMC). In accordance with previous studies, they report that 2D flat hydrogels stimulate secretion of inflammatory cytokines TNF-α and IL-1β. Interestingly, 3D nanofibrous hydrogels not only downregulate these inflammatory cytokines but also encourage production of pro-angiogenic chemokines IL-8 and MIP-1β[56]. This presents an important consideration for tissue engineering applications, and perhaps is also suggestive of a disease mechanism, as macrophages are known to promote angiogenesis in densely fibrillar tumor matrices[57]. 3D matrix architecture can also profoundly impact macrophage migration. While most leukocytes migrate via an amoeboid migration mode, macrophages employ both amoeboid and mesenchymal migration modes[58]. Using 3D fibrillar and gelled type I collagen, it has been demonstrated compellingly that matrix architecture dictates macrophage migration modes[59]. In gelled collagen, a dense matrix with few distinct fibrils, human monocyte-derived macrophages adopt the mesenchymal migration

mode. On the other hand, in fibrillar collagen, macrophages migrate via the amoeboid mode. Remarkably, when presented with matrices of variable stiffness and architecture, macrophages adopt migration modes primarily based on architecture, thus establishing it as the dominant factor.

*1.3.2.2 Stretch*

Certain tissues in the body, such as bones, vasculature and lungs, undergo substantial mechanical loading and stretch as part of their normal function. While physiological levels of mechanical stimulation are important for growth and maturation of cells in those tissues, abnormal stimulation has been associated with inflammation and disease[60,61]. Macrophages present in these tissues are also exposed to these mechanical stimuli and have been known to respond to them. Osteoclasts, which belong to a special class of macrophages only found in bone tissues, increase their bone resorbing activities when exposed to cyclic stretch[62]. In both human alveolar and THP-1 monocyte derived macrophages, cyclic stretch alone induced secretion of IL-8. When applied concurrently with LPS stimulation, stretch enhanced LPS-mediated secretion of TNF-α, IL-6 and IL-8[63]. Primary rat peritoneal macrophages subjected to static stretch increased expression of inflammatory genes including inducible nitric oxide synthase (iNOS), cyclooxygenase-2 (COX-2), IL-1β, IL-6, MIP-1α, and MIP-2[64]. Stretch can also affect ECM integrity by upregulating macrophage production of matrix metalloproteinases such as

MMP-1, MMP-3, MMP-9, and TIMP-1[63,65]. Cyclic stretch has also been shown to synergistically affect macrophage phenotypic polarization along with other biophysical cues. In human PBMCs seeded on electrospun elastomeric scaffold, a moderate 7% cyclic strain was shown to increase the ratio of M2/M1 macrophages over a 7-day period when compared to unstretched control. However, a more extensive 12% strain resulted in marked reduction in M2/M1 macrophages over the time course[66]. This biphasic effect perhaps reinforces the concept that an optimal or physiological level of stretch can promote tissue homeostasis, whereas abnormal stretch leads to inflammation.

*1.3.2.3 Substrate Stiffness*

In addition to applied forces, the stiffness of the surrounding tissue can also contribute to the mechanical environment of cells. The interstitial matrix surrounding cells can possess wide range of mechanical properties *in vivo*. In recent years, the rigidity of the underlying substrate has been shown to be critically important for cellular behaviors ranging from adhesion and contractility to migration[67] and differentiation. For instance, bone ECM features drastically different elastic modulus than neural tissues, and is an important differentiation cue for stem cells during development[35]. Tissue stiffness also changes dramatically during aging and the development of diseases. The progression of cancer and atherosclerosis are both accompanied by the stiffening of normal tissue. Using techniques such as the indentation test and atomic force

microscopy to measure the elastic moduli of normal and diseased tissues, it has subsequently been shown that increase in ECM stiffness is critical for tumorigenesis[68] and atherogenesis[69]. In addition to its contribution to disease progression, stiffness also plays a role in the host response to implanted biomaterials as most synthetic materials have very different elastic moduli than native tissue.

Considering the extensive role of macrophages in diseases and mediating tissue-biomaterial interactions, there have been numerous investigations examining the effect of substrate stiffness on macrophage phenotype. Using Arg-Gly-Asp (RGD) -functionalized poly(ethylene glycol) (PEG) hydrogels, Blakney et al.[70] tuned the compressive moduli of the substrate without changing the amount of cell adhesion ligands. Although it has been previously shown that RAW264.7 cells seeded onto PEG hydrogel with gradient elasticity preferentially adhere to the stiffer parts of the hydrogel[71], this group found no significant difference in adhesion on substrate stiffness ranging from 130 kPa to 840 kPa. They then examined the effect of stiffness on phenotypic polarization of murine bone marrow derived macrophages (BMDMs), and found no significant differences in the absence of soluble co-stimulants. However, in the presence of LPS, the expression of TNF-$\alpha$, IL-6, IL-1$\beta$ and IL-10 all increased with increasing rigidity. In accordance with these *in vitro* results, subcutaneous implantation of stiff hydrogels in mice elicited a more severe foreign body response, evidenced by the recruitment of more inflammatory macrophages, than soft hydrogels.

In studies using human macrophages, the elastic modulus of the substrate and surface adhesion ligand density have also been shown to affect adhesion and cytokine secretion. Macrophages differentiated from human THP-1 cells were examined on PEG-coated polyacrylamide gels of stiffness ranging from 1.4 kPa to 348 kPa. Without any RGD adhesion peptide modification, human macrophages preferentially adhered to stiffer substrates when compared to soft substrates. On RGD peptide-modified surfaces, the same trend of more adhesion on the stiffer substrates remained, although the differences were less pronounced. Interestingly, TNF-α secretion by adherent human macrophages was found to be inversely proportional to the substrate stiffness: cells secreted most TNF-α on 1.4 kPa substrate and least on 348 kPa. It is important to note that this result was obtained by normalizing the bulk population secretion to the number of adherent cells, and without normalization, there was no difference in TNF-α secretion. In contrast to TNF-α, the IL-8 secretion profile appeared to be biphasic in that secretion was low on 1.4 kPa and 348 kPa but high on the intermediate 10 kPa substrate[72].

In a separate study, murine and differentiated human macrophages were investigated side by side on polyacrylamide gels with elastic moduli ranging from 0.3 kPa to 76.8 kPa. Cell adhesion over this stiffness range was not significantly different. Without LPS activation, substrate rigidity appears to have little effect on TNF-α secretion in both RAW264.7 and human U937 macrophages. However, with LPS stimulation, TNF-α production inversely correlated

with rigidity in both cell types. Increasing stiffness also enhanced opsonization-mediated macrophage phagocytosis in both RAW264.7 and human alveolar macrophages (AM)[73].

The effect of substrate rigidity on macrophage adhesion and activation may still be up for debate. Experimentally, the effect of stiffness on macrophage adhesion and cytokine secretion need to be clearly demarcated, as secretion profile for adherent and non-adherent macrophages are likely different. Similar to stretch, there may be one or more optimal range of stiffness that is ideal for homeostasis. Moreover, various tissue-specific macrophages are accustomed to ECMs of different elasticity *in vivo*, and therefore stiffness-dependent effects on macrophage phenotype may be ontogenetic.

## 1.4 Signaling pathways in mechanotransduction

### *1.4.1 Cellular mechanotransduction*

In general, cells bind to their substrates through integrins, transmembrane proteins that link the cytoskeleton to the ECM proteins. Integrin is arguably the most implicated membrane protein in mechanotransduction. Not only does it provide the physical link between extracellular and intracellular spaces, its binding initiates a cascade of intracellular signaling that lead to changes in cytoskeletal dynamics and ultimately cell behavior. ECM-binding causes physical

deformation in integrins that result in conformational changes in its cytoplasmic structure, unveiling binding sites for actin cytoskeleton and other signaling proteins involved in the formation of focal adhesions (FA). Focal adhesions are large multi-protein complexes that include talin, which binds directly to actin, and vinculin, which binds to actin as well as the actin-crosslinking protein α-actinin. The size and structure of FAs are direct consequences of ECM substrate and cell contractility[74,75]. Cells on stiff substrates form large robust focal adhesions that are accompanied by increase in actin polymerization and actin-myosin contractility, whereas cells on soft substrates have smaller and more dynamic focal adhesions[76]. It has been shown in endothelial cells that the amount of focal adhesions is proportional to the degree of cell spreading and is independent of the ECM area the cell is exposed to[77].

Upon integrin binding, focal adhesion kinase (FAK) activate through tyrosine phosphorylation, and is responsible for modulating focal adhesion assembly[78]. FAK subsequently activates and recruits other tyrosine kinase proteins such as src to focal adhesion complex and serves as a dock for cytoskeletal proteins such as paxillin and vinculin to bind. FAK also activates Rho-GTPases Cdc42 and Rac, which lead to actin polymerization.

The Rho family of GTPases, a subclass of the Ras superfamily, is an important class of signaling proteins that includes well-known members RhoA, Rac1, and Cdc42. Their activation modulates numerous cell functions including proliferation, differentiation, and migration, but more importantly they regulate the signaling pathway between membrane receptors and actin

cytoskeleton[79]. Rac activation leads to assembly of actin mesh near the cell periphery, which leads to the development of lamellipodia. Cdc42 mediates the formation of actin-rich cell surface protrusions known as filopodia. RhoA is responsible for the assembly of actin-myosin contractile filaments, more commonly known as stress fibers. Crosstalk between different members of the Rho family is not uncommon. For example, Cdc42 can activate Rac, and Rac can activate RhoA. Although these proteins are most studied in fibroblasts, there is strong evidence suggesting that their functions are conserved in most eukaryotic cells[79]. In several cell types, Rac1 or Cdc42 and RhoA have been observed to have antagonizing effects on the degree of cell spreading[80–82]. For instance, Rac1 and Cdc42 are generally associated with cell expansion through the formation of protrusive elements whereas Rho is commonly linked with cell contraction. In macrophages, activation of Rac1 and Cdc42 also lead to formation of lamellipodia and filapodia[83]. However, activated RhoA promotes only assembly of actin-myosin filaments and not focal adhesions, which causes macrophage cells to round up. This feature is also observed in neuronal cells but not in fibroblasts[81,83]. RhoA activity is also implicated in mediating cell shape induced stem lineage commitment, suggesting that physical cues in the cellular microenvironment may be transduced via RhoA[84]. All Rho proteins have an active form when bound to GTP and are inactive in the form of Rho-GDP. Rho activity is regulated by two proteins: guanine nucleotide exchange factor (GEF) and GTPase activating protein (GAP). GEFs

activate Rho by facilitating the release of GDP and replacement with GTP. GAPs inhibit Rho by hydrolyzing GTP to GDP[85].

Rho-associated kinase (ROCK) is a known downstream effector of Rho. Activation of ROCK inhibits myosin light chain phosphatase, which induces phosphorylation of myosin light chain (MLC) and increases interaction between actin filaments and myosin[83]. This is necessary for the induction and maintenance of actin stress fibers and focal adhesions[86]. Rho-ROCK expression is nearly universal throughout the body. However, it is most often studied in the cardiovascular and nervous systems[87].

### *1.4.2 Macrophage intracellular mechanics*

3D-reconstructed confocal stacks of phalloidin-stained rat alveolar macrophages (AMs) show that the majority of the macrophage actin cytoskeleton are cortical and form a thick submembranous stratum[88], as opposed to organized stress fibers observed in many adherent cells. Stiff substrates have been shown to increase actin polymerization and filopodial projections[70,73,88]. Murine macrophages plated on microgrooved substrates exhibit higher overall F-actin content and also along the edges of the microridges[51]. Several studies have noted differences in actin organization between M1 and M2-polarized macrophages[89,90]. M1 cells display more clustered F-actin structures that are more likely to be found around the nuclei,

whereas M2 cells present more diffused actin organization that are perhaps more around the periphery of the cells, suggestive of lamellipodia formation.

A few studies have implicated intrinsic changes in stiffness and elasticity of macrophage cells as a possible mechanism for sensing changes in the physical microenvironment[73,88]. Rat AMs cultured on stiff substrates exhibit increased cellular elastic modulus. Surprisingly, this phenomenon cannot be attributed to an increase in actin polymerization, as treatment with inhibitor cytochalasin D failed to abolish the difference in cellular stiffness due to substrate rigidity. Using magnetic twisting cytometry (MTC), AMs were shown to have minimum internal tension. Although not detectable by MTC, it is possible for macrophages to generate local stress points that co-localize with punctated podosomes and actin structures, especially during actin-mediated tasks such as migration and phagocytosis[88]. This seems to be consistent with the general understanding that podosome assembly does not require intracellular tension but rather depend on extracellular cues such as substrate flexibility[91]. These results, together with the lack of observable actin stress fibers, allude to a macrophage mechanotransduction mechanism that may be distinct from most other tissue cells.

Evidence strongly suggests that macrophage elasticity is linked to its activation and function. Using colloidal force microscopy, LPS-activated human macrophages were shown have an average Young's modulus that is three times less than that of unstimulated resting

macrophages. The same study also found that stimulation with LPS stimulation caused an increase in adhesion strength of macrophages[92]. In murine RAW264.7 cells, LPS and IFN-γ stimulation increased cellular elasticity, unlike in human macrophages. However, LPS increased macrophage adhesion strength, as was also shown with human cells [73,93]. A more rigid substrate increases elasticity, similar to stimulation with LPS and IFN-γ, and this increased elasticity corroborates with enhanced phagocytosis and reactive oxygen species (ROS) production. However, contrary to the study in rat AMs[94], this particular study demonstrated that actin polymerization was required for murine macrophage elasticity while actin-myosin contractility has minimal involvement[73]. It has been previously suggested that cellular stiffness is regulated by both cell shape and substrate rigidity[95]. Although the exact mechanics remains elusive, there is emerging evidence supporting the idea that biophysical regulation of macrophage behavior is mediated by alterations in cell stiffness and shape.

### *1.4.3 Molecular mechanism of macrophage mechanotransduction*

For macrophages to be mechanically activated, they must be able to probe and discern changes in the mechanical properties of their environment and transduce these changes into biochemical signals that ultimately lead to differential gene and protein expressions. To date, most studies in mechanotransduction have been performed on low motile tissue cells with

highly polymerized actin organization. In contrast, macrophages are derived from non-adherent monocytes. Once activated, they become adherent and migrate through tissue to reach the site of injury or inflammation. Macrophage adhesion to the extracellular matrix environment is mediated by various types of integrins, as well as scavenger receptors. Interestingly, macrophages have been known to deploy different modes of adhesion to type collagen I that may be dependent on species, cell source, or the context of adhesion. Generally, $\beta_1$ integrin is thought to be the main receptor for macrophage adhesion to collagen[96]. In rat alveolar macrophages (AMs), CD18, the $\beta_2$ subunit of integrin, was shown to be main regulator of adhesion to type I collagen, whereas CD11b, the $\alpha_M$ subunit, did not participate in adhesion[88]. In RAW264.7 macrophages, neither $\beta_1$ nor $\beta_2$ subunits are involved in adhesion to denatured type I collagen. Instead, it was largely modulated by class A macrophage scavenger receptor (SR-A)[97]. SR-A has also been implicated in mediating macrophage adhesion to a number of other modified ECM components, including glycated[98], proteoglycan-[99] and cigarette smoke-[100] modified ECM, suggesting a possible disease mechanism in which modified ECMs associated with disease progression may enhance macrophage adhesion through SR-A.

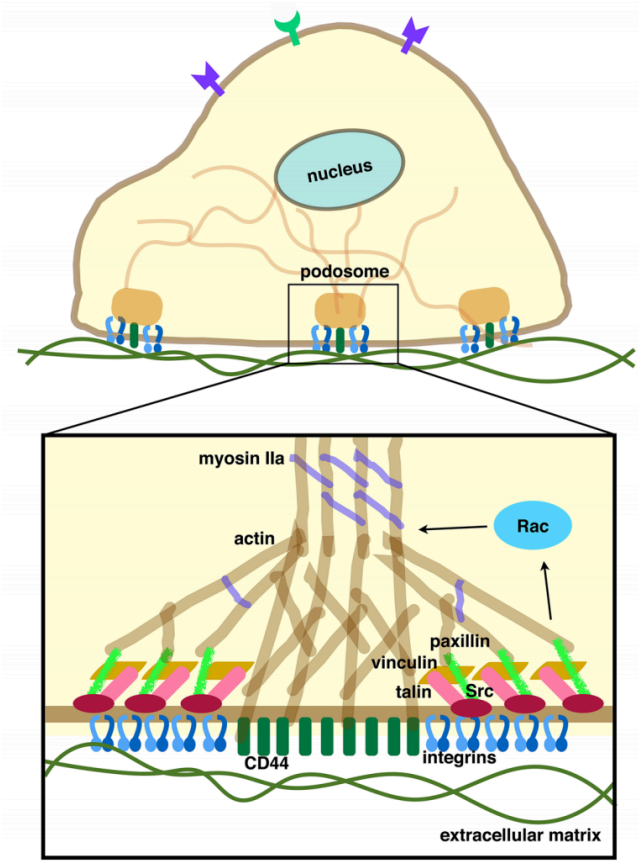


Figure 3. Schematic of macrophage mechanotransduction pathway. Podosomes, which contain focal adhesion proteins, mediate macrophage adhesion and links the actin cytoskeleton to the ECM. Reproduced from [46]

Once adherent, membrane adhesion receptors of most cells cluster and recruit additional proteins to form focal adhesions (FA), which are linked to the cytoskeleton and provide a signal transduction pathway for physical cues from extracellular space. In place of FAs, macrophages form punctated focal complexes known as podosomes, which are similar to FA in protein composition but different in structure and dynamics. Podosomes are cylindrical structures that contain an actin-rich core and form perpendicular to the membrane rather than

tangential (Fig. 3). They are more dynamic and unstable than FAs, which may play a key role in macrophage migration, invasion and degradation of surrounding matrices[91]. The distribution, size and shape of these focal complexes vary and are a reflection of changes in macrophage adhesion and morphology. The peripheries of podosomes are composed of integrins, the specific types of which are tissue-dependent[101,102]. The cores of podosomes also contain CD44, a protein that can modulate macrophage adhesion through its affinity to hyaluronan, collagen and matrix metalloproteases. Adherent, well-spread macrophage cells generally develop larger podosomes[103], and the traction force generated by podosomes are sensitive to substrate rigidity, which is the reason that they are often considered mechanosensors[104]. Studies on macrophage podosome dynamics in 3D collagen gels recapitulate results from 2D, suggesting similar macrophage mechanosensing mechanisms in 2D and 3D[105].

Adhesion can also lead to integrin clustering and subsequently activate focal adhesion kinase (FAK)[106,107]. Downstream of that are the Rho family of GTPases, which include RhoA, Rac, and cdc42. These signaling proteins, generally activated following FAK phosphorylation, are the key regulators of actin cytoskeletal dynamics and are directly involved in the assembly of actin stress fibers (RhoA), lamellipodia (Rac), and filipodia (cdc42)[79]. The importance of these proteins in mechanotransduction has been well-documented in many cell types, and they have been implicated in mediating adhesion, spreading, phagocytosis, and podosome assembly in macrophages[81,83,108,109]. More recently, several studies have highlighted the significance of Rac in

modulating macrophage morphology, migration and phenotype polarization. Among the three highly conserved isoforms of Rac, Rac1 is ubiquitous in all mammalian cells including macrophages, whereas Rac2 is only found in hematopoetic and endothelial cells. Deletion of Rac1 and Rac2 in mice has been shown to alter macrophage cell shape. Comparing to wildtype, $Rac1^{-/-}$ BMDMs display elongated morphologies and reduced spread area. $Rac2^{-/-}$ cells also exhibited an elongated cell shape, though to a lesser extent than $Rac1^{-/-}$ cells, but did not show difference in cell spreading. Rac2 knockout also completely abolished podosome formation in BMDMs, whereas Rac1 knockout only led to abnormal podosome assembly. Surprisingly, abnormal podosomes due to Rac1 deletion did not affect macrophage migratory abilities. Rac2 deletion reduced the number of migratory cells but did not affect their migration speed[110]. In mouse tumor models, Rac2 was implicated in mediating macrophage migration into tumors via integrin $\alpha_4\beta_1$. It was subsequently shown that Rac2 activation regulates macrophage polarization to tumor-associated M2 phenotype both *in vitro* and *in vivo*[111].

Taken together, these studies overwhelmingly support the notion that macrophages respond to changes in the physical microenvironment, although different activation states may result in differential sensitivity to mechanical cues. LPS or M1-like activation has been demonstrated to enhance cell adhesion in both human and murine macrophages[73,89,93]. Macrophage-1 antigen (Mac1), an integrin family receptor composed of both CD11b and CD18, is well-known for mediating phagocytosis[106] and is upregulated in murine macrophages

stimulated with LPS and IFN-γ. Additionally, these cells upregulate adhesion receptors lymphocyte function associated antigen-1 (LFA-1), CD29, and CD11a, which may partially explain their enhanced adhesion[89]. As adhesion proteins are a major component of macrophage membrane mechanosensor, it is not surprising that podosome assembly can also be modulated by phenotypic states. The cytokine CSF-1, which is known to steer macrophage polarization toward an M2-like phenotype[112], has been shown to increase the assembly and alter the distribution of podosomes in BMDMs[113]. IL-4 – polarized human macrophages form podosome rosettes, which are not seen in IFNγ-induced M1 or unstimulated resident macrophages. The formation of these rosettes is linked to increased degradation and migration through the ECM by M2 macrophages, and may also explain the ability of M2 cells to adopt a mesenchymal migration mode[114]. Murine M1 macrophages also exhibit increased cellular elastic modulus, which correlates with their enhanced ability to uptake tissue fragments[89] and opsonized particles[73,93]. In addition to phagocytosis, intrinsic cell stiffness can affect other cytoskeleton-mediated macrophage behavior such as migration. It is thought that migration speed is inversely correlated with intracellular tension[91], and consistent with this, M2 primary murine macrophages are seen as more motile than M1 cells in the absence of chemoattractant[89]. Alterations in cellular elasticity and podosome assembly, underlied by differential activation of RhoA and Rac, may also explain the different macrophages migration modes, as 3D matrix architecture and stiffness are thought to modulate mesenchymal versus amoeboid modes of migration by macrophages[59]. While the

underlying molecular mechanism for mechanically induced macrophage phenotype and function remains to be determined, various studies have implicated molecules including integrins[106,107], FAK-src activation[50,103], actin polymerization[73,90,94], actin-myosin contractility[90,104], and Rho GTPases RhoA[59,89], Rac[59,89,110,111,115] and cdc42[73].

### 1.5 Overview of Dissertation Research

Although physical and mechanical cues have been previously shown to influence macrophage activation and function, the exact mechanism is still largely unknown, and the field is far from reaching consensus. Our exploration into the effect of cell shape on macrophage polarization in the following chapter offers a more unifying explanation to some of the observations and findings in the literature. In the process, we have encountered challenges in pinpointing nuanced contributors to macrophage activation amidst confounding factors such cellular heterogeneity, a problem likely faced by all researchers in the field. To address that, we created a single cell cytokine detection device that allows for precise manipulation of the adhesive microenvironment on a single cell level. We used this device to demonstrate that adhesive cues can influence macrophage secretion on a single cell level. This device may enable future discoveries of macrophage biology that are not possible via traditional molecular techniques.

# CHAPTER 2: Modulation of Macrophage Phenotype by Cell Shape

## 2.1 Introduction

While it is thought that cytokines and chemokines are the primary regulators of macrophage polarization state[116], previous work have shown that the underlying tissue architecture and physical cues in the extracellular microenvironment can also contribute to their function[59]. Tissue topography and architecture are critical in steering cells toward tissue-specific phenotypes and functions. It is precisely the loss of normal tissue architecture that leads to the development of many diseases[117]. The pathogenesis of previously mentioned atherosclerosis and cancer are accompanied by not only changes in the soluble milieu but also changes in architecture and mechanical properties of the surrounding tissue. For instance, tumor ECM is comprised of densely aligned collagen fibers, as opposed to reticular collagen in normal tissue, to facilitate tumor cell migration and metastasis[118]. Using intravital microscopy, tumor-associated macrophages (TAMs), which are M2-like, have been observed to elongate and migrate along the collagen fibers in tumor ECM, much like tumor cells[119]. The trademark of atherosclerosis is the development of a collagen-rich fibrous cap and stiff plaques[20]. Although the plaques comprises of a heterogeneous population of macrophages, M1 macrophages are found to predominate in rupture-prone shoulder regions of plaques, whereas M2 cells preferentially reside in the collagen

rich fibrous cap and exhibit an elongated morphology[20,120]. Most cells can relay changes in ECM architecture and stiffness into reorganization of its own cytoskeleton, and subsequently transform mechanical signals into biochemical signals that lead to differential gene expression. Thus, cell function is intimately linked to its interactions with the ECM, and often that is done through changing its own shape.

As cells probe and migrate through their surrounding matrix, their morphologies inevitably changes. Alterations in cell shape have been associated with changes in cell function for many years[37]. Moreover, many of the physical cues discussed in Chapter 1, including topography, stretch, and stiffness, can profoundly influence macrophage cell shape. Cyclic biaxial stretch increased macrophage cell area[63], whereas uniaxial stretch led to cellular elongation along the direction of stretch[121]. Multiple studies investigating the effect of substrate stiffness have shown that macrophages are more spread and flattened on rigid substrates, and more rounded on soft[70,72,88]. This rigidity-dependent cell spreading seems to be inversely correlated with cell height. Furthermore, stiffer substrates tend to encourage the formation of long protrusive actin structures such as filapodia[73,88]. Polymers imprinted with micro- and nano- scale grooves are capable of directing macrophage cells to exhibit elongated morphologies both *in vitro* and *in vivo*[43,52].

Macrophages also undergo morphological changes in response to soluble factors. A number

of groups have observed that when murine bone marrow-derived macrophages (BMDMs) are stimulated with lipopolysaccharide (LPS) and interferon-γ (IFNγ), they adopt a circular and flatten morphology. However, in the presence of M2-inducing cytokines interleukin-4 (IL-4) and interleukin-13 (IL-13), they exhibit much more elongated morphologies[90,110]. The activation of microglial cells, which are the resident macrophages of the central nervous system, occurs in concert with distinct morphological changes[122]. It was subsequently shown that soluble factors secreted by adipose-tissue-derived mesenchymal stem cells (ASCs) lead to elongated cell shape in microglia, which is also accompanied by a noninflammatory phenotype characterized by low TNFα and IL-6, and high Arginase-I production[123]. Cell shape has also been linked to polarization state in human macrophages. In one study examining the effects of stretch and electrospun scaffold on PBMC-derived macrophages, it was observed that $CCR7^+$ M1 macrophages were small and rounded, whereas $CD206^+$ M2 cells exhibited more actin protusions[66]. Human THP-1 derived macrophages cultured on substrates such as glass, polyurethane, modified chitosan and hyaluronic acid (HA) have been shown to display distinctly different morphologies in 3D. Cells on glass are most spread out, and possess the largest total surface area and volume. Interestingly, these cells also secreted the most amount of TNFα. Cells on chitosan and HA were nearly spherical and have the smallest surface area and volume, which correlated with low TNFα secretion. Finally, cells on polyurethane were less spread than glass, and present intermediate surface area, volume as well as TNFα secretion[124].

In our previous *in vitro* studies, we observed that cytokine-induced M1 and M2 murine macrophages adopted markedly different cell morphologies. Specifically, bone marrow-derived macrophages stimulated with LPS and in IFN-γ, known M1 polarizing agents, assumed round pancake-like shapes. On the other hand, macrophages stimulated with M2 polarizing cytokines IL-4 and IL-13 took on an elongated cell shape (Fig. 4 A & D). The degree of cell elongation was quantified by an elongation factor, which is the ratio of the major (long) axis length and the minor (short) axis length of the cell. M2 cells clearly exhibited much higher degree of cell elongation when compared to M1 and control, unstimulated cells, while cell spreading across the three phenotypes remained relatively the same (Fig. 4 B & C). To confirm the polarization states, the expressions of iNOS and arginase-I, which are established murine M1 and M2 markers respectively, were examined by immunofluorescence and Western blots (Fig. 4 D & E). M1 macrophages expressed only iNOS, whereas M2 macrophages only expressed arginase-I. Furthermore, dose response of IL-4 and IL-13 stimulation shows that arginase-I expression increases with increasing cytokine stimulation (Fig. 5A). Interestingly, the degree of cell elongation also increases with increasing M2 cytokine stimulation (Fig. 5B), which seems to suggest that cell elongation correlates with M2 macrophage polarization state. Despite evidence suggesting that macrophage cells adopt different geometries both *in vitro* and *in vivo*, how these changes in cell shape might influence their functional phenotype has not been previously explored.

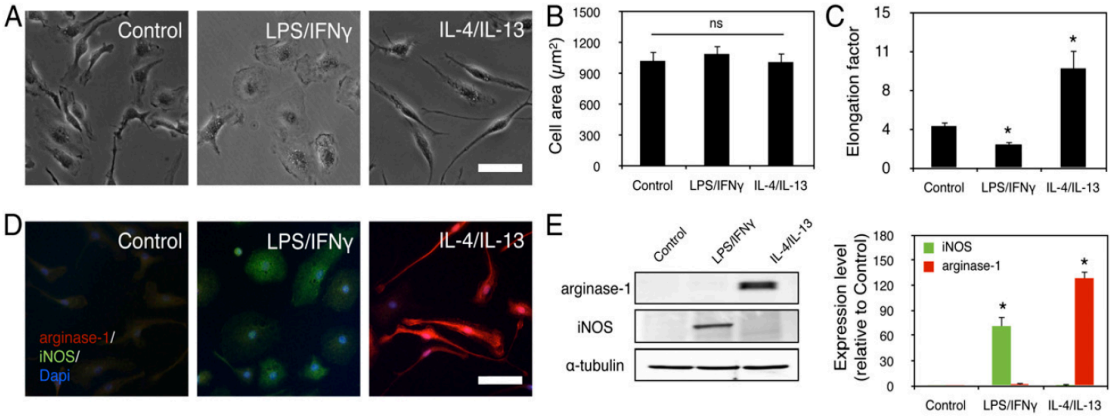


Figure 4. Polarization of macrophages toward an M2 phenotype is associated with an elongated cell shape. A) Phase contrast images of BMDMs left untreated (*left*) or treated with LPS/IFN-γ (*Center*) or IL-4/IL-13 (*Right*). (Scale bar: 50 μm). (B) Quantification of area for control, LPS/ IFN-γ-treated, and IL-4/IL-13-treated cells. (C) Quantification of elongation, or length of the long axis divided by length of the short axis, for control, LPS/ IFN-γ-treated, and IL-4/IL-13-treated cells. (D) Fluorescence images of cells immunostained for iNOS (grean) and arginase-1 (red) and Hoechst nuclear conterstain (blue) of control, LPS/ IFN-γ-treated, and IL-4/IL-13-treated cells. (Scale bar: 50 μm). (E) Representative Western blot of iNOS, arginase-1 and α-tubulin of control, LPS/ IFN-γ-treated, and IL-4/IL-13-treated cells and quantification of average across three separate experiments. Error bars indicate the SEM for three separate experiments. $^{*}P < 0.05$ compared with control cells as determined by the Student *t* test. ns, not significantly different. Reproduced from [90]

The development of various microfabrication and bioengineering tools in recent years has enabled unprecedented control over cell geometry, either singularly or in groups, in order to specifically study the effect of cell shape on function. Using these technologies, cell shape has been demonstrated to be an important regulator of growth and apoptosis in endothelial cells[38], differentiation and multipotency in mesenchymal stem cells[39,40], collagen synthesis in fibroblasts[125], and proliferation[126] and contractility[127] in vascular smooth muscle cells.

The goal of this study is to investigate the effect of cell shape on macrophage polarization with and without the addition of exogenous cytokines. Macrophages were micropatterned on on

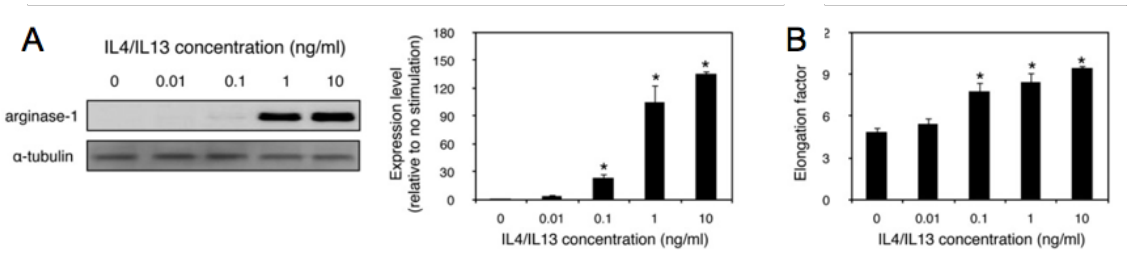


Figure 5. A) Representative Western blot of arginase-1 and α-tubulin in response to different dosage of IL-4/IL-13 and quantification of average across three separate experiments. (B) Quantification of cell elongation for macrophage treated with different IL-4/IL-13 dosages. Error bars indicate the SEM for three separate experiments. $*P < 0.05$ compared with control cells as determined by the Student *t* test. Reproduced from [90]

20 μm-wide lines of ECM proteins to induce cellular elongation, and the effect of elongation on macrophage polarization without any cytokine stimulation was examined. In addition, the effect of cell elongation on macrophage polarization in the presence of M1 and M2 inducing cytokines was characterized. Lastly, underlying molecular mechanism of shape-mediated polarization was explored through pharmacological inhibition of acto-myosin contractility.

## 2.2 Materials and Methods

### *2.2.1 Macrophage cell isolation and culture*

Bone marrow-derived mouse macrophages (BMDMs) were harvested from femurs of 6-12 week old female C57BL/6J mice (Jackson Laboratory). All procedures involving animals were performed in accordance with UC Irvine Institute for Animal Care and Use Committee (IACUC) approved protocols. Bone marrow was flushed out of the femurs with DMEM

supplemented with 3% heat-inactivated FBS (both from Invitrogen) to collect bone marrow cells. Cells were treated with ACK lysis buffer to rid of red cells, centrifuged, seeded in DMEM supplemented with 10% heat-inactivated FBS, 1% penicillin/streptomyocin (Invitrogen) and 1% conditioned media containing macrophage colony stimulating factor (M-CSF) to induce differentiation to macrophages. After 7 d in culture, BMDMs were collected using cell dissociation buffer (Invitrogen) and seeded onto experimental substrates.

*2.2.2 Cell micropatterning*

Silicon wafers containing arrays of 20-μm and 50-μm microgrooves were fabricated using standard photolithography. Polydimethylsiloxane (PDMS; Dow Corning) stamps were replica-molded from the silicon wafers. Stamps were sonicated and cleaned with 70% ethanol and then dried in a nitrogen stream. The clean stamps were then coated with 20 μg/mL human fibronectin (BD Biosciences) at room temperature (RT) for 1 h, rinsed with deionized water, and

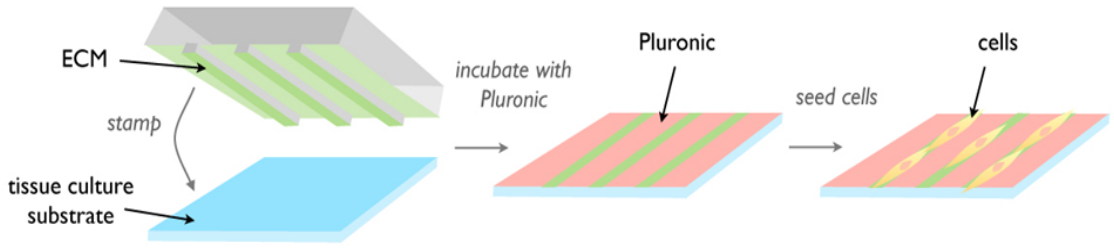


Figure 6. Schematic of method used to micropattern cells by microcontact printing of arrays of fibronectin lines of various widths. Adapted from [90]

dried with a nitrogen stream. PDMS-coated substrates were treated with UV Ozone (Jelight) for 7 min, and fibronectin was transferred from the stamps to the PDMS surface. The freshly stamped substrates were blocked with a 0.2% Pluronic F-127 solution (Sigma–Aldrich) for 1 h at RT and then washed with PBS prior to cell seeding. (Fig. 6)

*2.2.3 Analysis of cell morphology*

Phase contrast images of cells were captured using a Nikon Eclipse TE300 inverted microscope. Using ImageJ software (National Institutes of Health), the long axis and short axis of each cell were manually traced and measured. The long axis was defined as the longest length of the cell, and the short axis was defined as the length across the nucleus in a direction perpendicular to the long axis. The ratio of the two axes was determined to be the elongation factor. The area of each cell was determined by tracing cell outline.

*2.2.4 Western blotting*

Cells were rinsed with PBS before applying a lysis buffer, which is a combination of radioimmunoprecipitation assay buffer and 1% protease inhibitor mixture (both from Sigma–Aldrich). The cells were scraped off the substrates, placed on an agitator at 4 °C for 20 min, and

spun at 16873 × g for 10 min to pellet the cellular components. Proteins were denatured in a Laemmli sample buffer (Biorad) at 95 °C for 5 min and then separated by standard SDS/PAGE using 7.5% polyacrylamide gels. Proteins were transferred from the gels onto nitrocellulose membranes by electroblotting (Biorad) at 4 °C overnight. Membranes were rinsed with 1× Tris-buffered saline with Tween 20 (TBST) buffer and blocked at RT for 2 h with either 4% BSA or 10% nonfat milk in 1× TBST. After 1 h of washing, membranes were probed with primary antibodies at 4 °C overnight, rinsed, and then incubated with secondary antibodies at RT for 2 h. For detection, Immobilon chemiluminescent HRP substrate solution (Millipore) was applied to the nitrocellulose membrane, which was imaged immediately using a ChemiDoc XRS System (Biorad).

*2.2.5 Flow cytometry*

BMDM cells were seeded onto patterned and unpatterned substrates for 48 h before flow cytometry analysis. Cells stimulated with 20 ng/mL IL-4 and IL-13 24 h before analysis were used as a positive control. Cells were removed from substrates with Cell Dissociation Buffer (Invitrogen) and fixed with 90% methanol for arginase-1 or 2% paraformaldehyde for CD206 and Ym-1. After blocking with anti-CD16/32 antibodies (Biolegend) and resuspended in a wash buffer (1% BSA and 0.1% saponin in 1× PBS), cells were incubated for an additional 30 min with

primary antibody. For the isotype control groups, cells were incubated with the appropriate normal IgG/FITC rat anti-mouse IgG2a/2b (BD Pharmingen), normal goat IgG (Santa Cruz Biotechnology), or normal rabbit IgG (Santa Cruz Biotechnology). Following thorough washing to remove excess unbound primary antibodies, the arginase-1 and Ym-1 samples were further incubated with secondary antibodies. Flow cytometry was performed on a BD LSRII flow cytometer using BD FACSDiva software (BD Bioscience). Data analysis and quantification of mean fluorescence intensity were performed using Cyflogic software, version 1.2.1 (www.cyflogic.com).

*2.2.6 Cytokine array*

Supernatants from cells cultured on control and experimental substrates were collected and concentrated to 500 μL using 3-kDa centrifugal filters. Concentrated supernatants were tested for cytokines using Mouse Cytokine Antibody Array Panel A (R&D Systems) according to the manufacturer's protocol. Briefly, supernatants were incubated with a detection antibody mixture at RT for 1 h. Membranes containing preprinted anti-cytokine antibodies were blocked with blocking buffer for 1 h and then incubated with the supernatant-detection antibody mixture at 4 °C overnight. After repeated washing, the membranes were incubated with streptavidin/HRP at RT for 30 min. Following more washes, the membranes were developed

with Chemi Reagent Mix and imaged using a ChemiDoc XRS System (both from Biorad). The pixel density of each spot on the arrays was analyzed using ImageJ (National Institutes of Health).

*2.2.7 Immunofluorescence imaging and cytometry*

Samples were fixed with 100% methanol on ice for 15 min and then blocked with 5% donkey serum in 1× PBS at 4 °C overnight. Primary antibodies diluted to 4 μg/mL in 5% donkey serum (Sigma–Aldrich) were applied to the samples at RT for 1 h and washed, and samples were then incubated with secondary antibodies diluted 1:500 in PBS at RT for 1 h. Cells were counterstained with Hoechst 33342 dye (Invitrogen) and washed before imaging using a Nikon Eclipse E800 upright microscope. Mean fluorescence intensity was quantified using CellProfiler software (Massachusetts Institute of Technology Broad Institute).

*2.2.8 Statistical analysis*

Data were presented as the mean ± SEM, unless otherwise indicated, across at least three independent experiments. For experiments where individual cells were assayed by microscopy, at least 100 cells were examined in each experiment. Comparisons were performed by means of a

two-tailed Student t test, and $P < 0.05$ was considered significant.

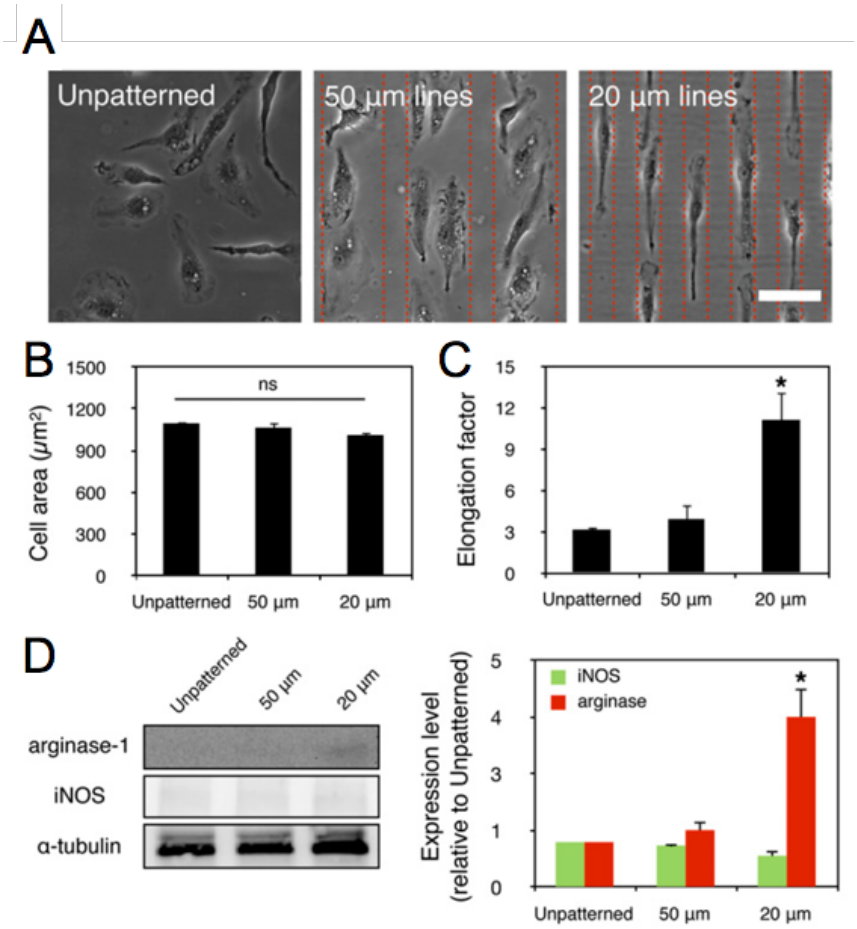


Figure 7. Elongation of cells by micropatterning drives macrophage polarization. A) Phase contrast images of unpatterned cells and cells patterned on 50-µm and 20-µm wide lines. (Scale bar: 50 µm.) B) Quantification of cell area of unpatterned cells and cells patterned on 50-µm and 20-µm wide lines. C) Quantification of elongation factor of unpatterned cells and cells patterned on 50-µm and 20-µm wide lines. D) Representative Western blot of iNOS, arginase-1, and α-tubulin of unpatterned and patterned cells and quantification across three separate experiments. Error bars indicate the SEM for three separate experiments. *$P < 0.05$ compared with unpatterned cells as determined by the Student *t* test. ns, not significantly different. Reproduced from [90]

## 2.3 Results

### *2.3.1 Macrophage elongation stimulates polarization towards an M2 phenotype*

To explore whether macrophage cell shape play a direct role in regulating their phenotype polarization, we employed a micropatterning approach to directly control the geometry of cell adhesion. (Fig. 6) Macrophages were cultured on micropatterned substrates containing 50- or 20-μm wide fibronectin lines separated by 20-μm wide areas coated with Pluronics F127, a nonadhesive surface that prevents cell adhesion. Cells adhered and spread only along the fibronectin lines and did not migrate or spread to the regions coated with Pluronics F127 (Fig. 7A). By comparing to cells patterned on 50 μm-wide lines and unpatterned cells, we show that the degree of cell elongation, as measured by the elongation factor, can be modulated. Across the three conditions, while cell area remained relatively constant, the degree of cell elongation was highest when cultured on the 20 μm-wide lines. In fact, the 20 μm-wide micropatterned cells elongated to a similar degree as IL-4/IL-13-stimulated cells, whereas cells cultured on 50-μm wide lines were not more elongated than cells on control, unpatterned surfaces. (Fig. 7 B & C) Next, we examined whether the changes in cell elongation, as controlled by micropatterning, induced changes in expression of macrophage phenotype markers.

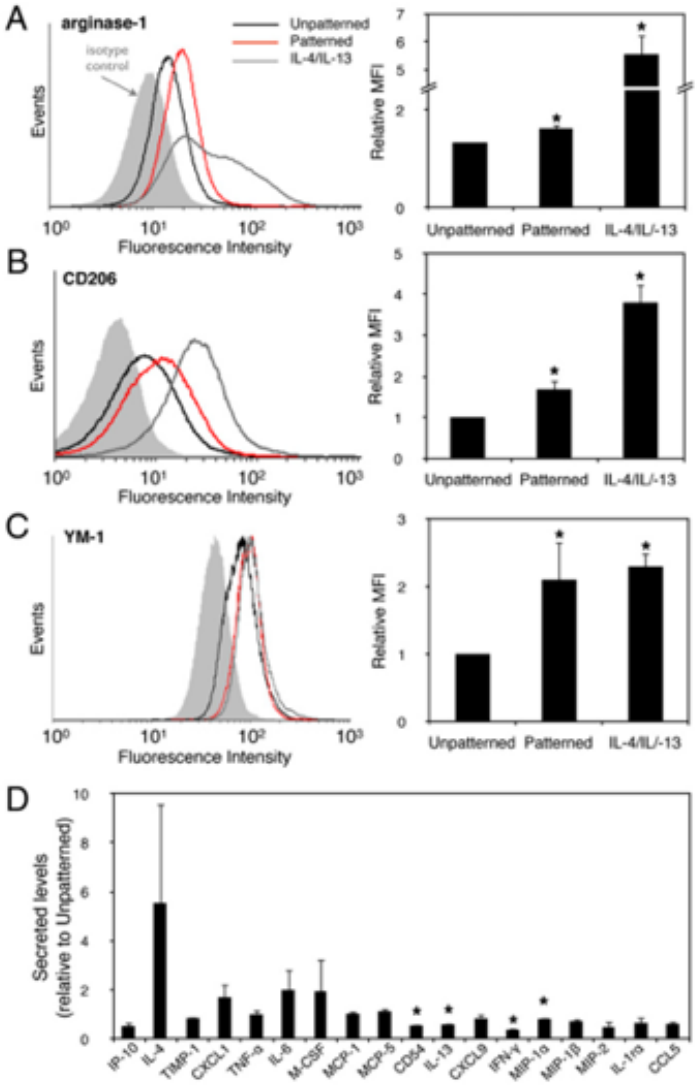


Figure 8. Macrophage elongation up-regulates markers of M2 polarization and reduces secretion of proinflammatory cytokines. Representative flow cytometry histograms (*Left*) and average relative mean fluorescence intensity (MFI) across three separate experiments (*Right*) of arginase-1 (*A*), CD206 (*B*), and YM-1 (*C*) for unpatterned cells and cells patterned on 20-μm wide lines and for cells treated with IL-4/IL-13. (*D*) Graph of secreted levels of indicated cytokines for patterned cells relative to unpatterned cells. Error bars indicate the SEM for three separate experiments. *$P < 0.05$ compared with unpatterned cells as determined by the Student *t* test. CCL5, chemokine (C-C motif) ligand 5; CXCL, chemokine (C-X-C motif) ligand IP-10, interferon gamma-induced protein 10; MCP, monocyte chemotactic protein; M-CSF, macrophage-CSF; TIMP-1, TIMP metallopeptidase inhibitor 1. Reproduced from [90]

Cells were cultured on unpatterned and patterned (50-μm and 20-μm wide lines) surfaces for 24h, and iNOS (M1 marker) and arginase-I (M2 marker) expressions were evaluated by Western blotting. iNOS expressions were similarly low across the three conditions. However, cells micropatterned on 20 μm-wide lines expressed significantly higher levels of arginase-I compared with cells cultured on 50 μm-wide lines or unpatterned cells (Fig. 7 D). These data suggested that cell elongation promotes macrophage polarization toward a prohealing, M2 phenotype and does not influence inflammatory activation. To further examine how cell elongation influences macrophage phenotype and function, the expressions of arginase-1, as well as additional M2 markers CD 206 (macrophage mannose receptor) and Ym-1 were examined by flow cytometry. Cells were seeded on upatterned and patterned (20 μm-wide lines) surfaces for 24h. Then, they were removed from the substrate and stained with primary and fluorescently labeled secondary antibodies. We found that patterned cells expressed higher levels of arginase-I, CD 206 and Ym-1 than control, unpatterned cells, although the expression of all three markers was not as high as levels achieved with IL-4/IL-13 cytokine stimulation (Fig. 8 A-C). In addition, upon analysis of the cytokines secreted from patterned and unpatterned cells, we found that elongation of cells in general reduced the secretion of proinflammatory cytokines, including CD54, IFN-γ, and macrophage inflammatory protein-1α (Fig. 8 D).

Together, these data demonstrate that elongated cell shape can stimulate macrophage polarization toward an M2 phenotype, enhancing markers associated with a prohealing

phenotype and abrogating secretion of proinflammatory cyotkines. These results suggest that cell shape, independent of soluble cues, plays a role in the regulation of the phenotypic polarization of macrophages.

*2.3.2 Macrophage elongation synergizes with cytokines to regulate polarization*

Considering the macrophages are likely to be exposed to a mixture of soluble and adhesive

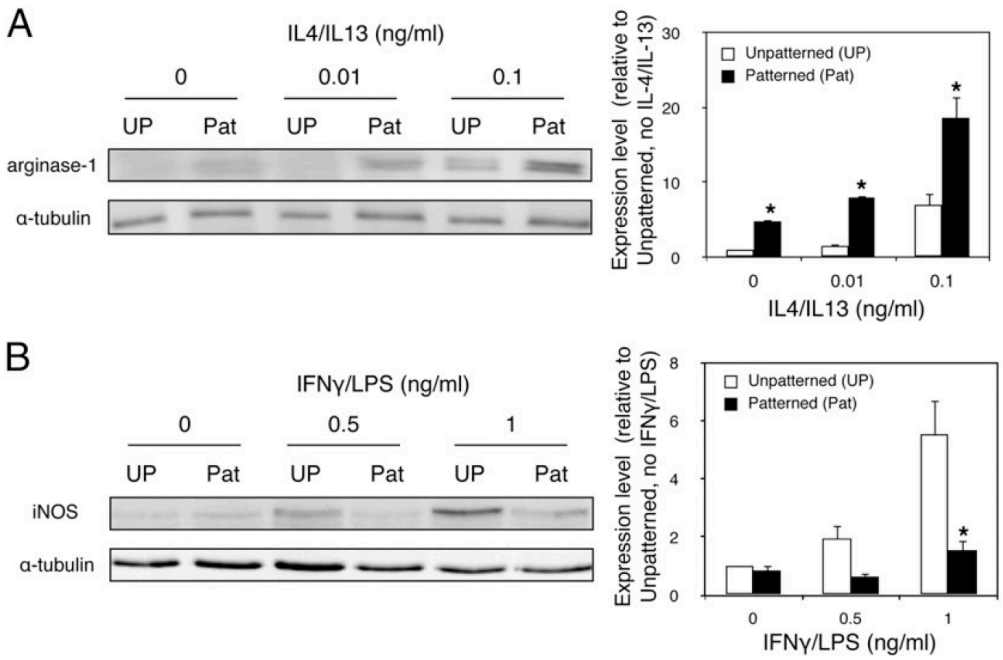


Figure 9. Shape and cytokines synergize to modulate macrophage polarization. (A) Representative Western blot of arginase-1 and α-tubulin in unpatterned (UP) cells and cells patterned (Pat) on 20-μm wide lines treated with the indicated concentration of IL-4/IL-13 (*Left*) and quantification of average across three separate experiments (*Right*). (B) Representative Western blot of iNOS and α-tubulin in unpatterned cells and cells patterned on 20-μm wide lines treated with the indicated concentration of IFN-γ and LPS (*Left*) and quantification of average across three separate experiments (*Right*). Error bars indicate the SEM of three separate experiments. $*P < 0.05$ compared with unpatterned cells treated with the same dose of cytokines as determined by the Student *t* test. Reproduced from [90]

cues in their native in vivo microenvironment, we next examined the combined effect of cell shape and cytokine stimulation. Macrophages were first seeded onto unpatterned and micropatterned (20 μm-wide lines) surfaces overnight, and they were then incubated for an additional 24h with low doses of IL-4/IL-13, which were found to cause undetectable or low levels of arginase-1 expression (Fig. 5A). We found that elongation of cells indeed enhanced the effects of IL-4/IL-13 stimulation. For each dosage of IL-4 and IL-13, the expression of arginase-1 was higher in patterned cells compared with unpatterned cells (Fig. 9 A), suggesting that elongation synergizes with IL-4/IL-13 to enhance M2 polarization. However, when patterned and unpatterned cells were treated with IFNγ/LPS to stimulate iNOS expression, we found that patterned cells that were stimulated with 1 ng/mL IFNγ/LPS exhibited significantly lower levels of iNOS compared with unpatterned cells (Fig. 9 B). These data demonstrate that cellular elongation protects macrophages from M1 polarization by inflammatory stimuli. Finally, we examined whether restricting macrophages from spreading by patterning on 50- x 50-μm discrete square adhesive islands prevents the upregulation of arginase-1 by IL-4/IL13 stimulation (Fig. 10 A). We found that cells that were restricted from spreading and elongating exhibited lower levels of arginase-1 compared with cells cultured on unpatterned surfaces, even when they were administered the same amount of IL-4/IL-13 (Fig. 10 B). This suggest that IL-4/IL-13-mediated polarization requires, at least in part, the elongation of cells.

Together, our data show that elongation enhances the expression of arginase-1 induced by IL-4/IL-13 and mitigates the expression of iNOS induced by IFNγ/LPS. Moreover, preventing cell elongation inhibits the full activation of the M2 polarization program induced by IL-4/IL13.

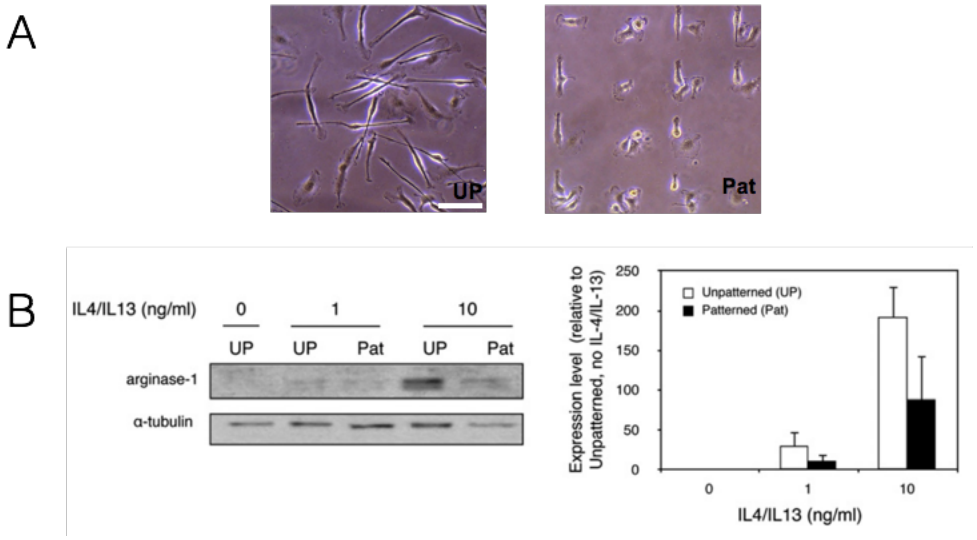


Figure 10. Inhibition of cell elongation mitigates IL-4/IL-13-induced arginase-1 expression. (A) Phase contrast images of unpatterned cells (UP, *Left*) and cells patterned (Pat, *Right*) on 50-μm x 50-μm squares and treated with 10 ng/mL IL-4/IL-13. (Scale bar: 50 μm.) (B) Representative Western blot of arginase-1 and α-tubulin in unpatterned (UP) cells and cells patterned (Pat) on 50-μm x 50-μm squares and treated with indicated concentrations of IL-4 and IL-13 (*Left*) and quantification of average across two separate experiments (*Right*). Error bars indicate the SEM. Adapted from [90]

### *2.3.3 Shape-induced polarization of macrophages requires cytoskeletal contractility*

To begin to explore potential molecules that might transduce cell shape into biochemical signals that regulate macrophage polarization, we examined the actin cytoskeleton, which has been implicated in transducing shape in other cell types[77,84]. Unpatterned, patterned, and cytokine-stimulated macrophages were fixed and stained with phalloidin, and then evaluated by

immunofluorescence microscopy. We found that cells stimulated with IL-4/IL-13, as well as patterned cells, exhibited higher fluorescence signal compared with control unpatterned, unstimulated cells or LPS/IFN-γ-stimulated cells (Fig. 11 A). The unpatterned, unstimulated cells exhibited clusters of actin or podosomes, which were not observed in the other conditions. We further examined the effect of pharmacological inhibitors that prevent actin and actin-associated signaling pathways. Cells were incubated with blebbistatin to inhibit myosin phosphorylation, cytochalasin D to inhibit actin polymerization, Y27632 to inhibit Rho-associated kinase (ROCK), and ML-9 to inhibit myosin light chain kinase (MLCK), and actin cytoskeleton was evaluated by phalloidin staining. We found that the level of phalloidin intensity was generally reduced with treatment of inhibitors in unpatterned cells, patterned cells, and cells treated with IL-4/IL-13 (Fig. 11 B).

We then asked whether actin and actin-associated contractility is required for shape-induced macrophage polarization. We developed an immunofluorescence cytometry method to evaluate arginase-1 expression by microscopy and confirmed that the results from immunofluorescence cytometry correlated well with the data obtained by flow cytometry (Fig. 12). Cells were seeded on unpatterned and patterned surfaces, treated with the aforementioned drugs to inhibit actin and actin-associated contractility, and then evaluated for cell shape and arginase-1 expression. The degree of spreading was not affected and cells were still able to acieve significant elongation on patterned surfaces when cultured in the prescence of drugs (Fig. 11 C and D). However,

treatment with all drugs abrogated the up-regulation of arginase-1 in patterned cells and led to expression levels similar to those of unpatterned cells (Fig. 4E). For the most part, inhibition of cytoskeletal contractility did not affect IL-4/IL-13-induced changes in cell shape or arginase-1 expression, suggesting that although IL-4/IL-13 appears to alter the cytoskeleton, cytoskeletal contractility is not required for cytokine-induced macrophage polarization. These data suggest that actin polymerization and myosin-dependent cytoskeletal contractility are required for macrophages to sense shape and mediate shape-induced polarization, and that cytokine-induced and shape-induced polarization pathways are likely to be distinct.

**2.4 Discussion**

In this study, we revealed a role for cell elongation in the regulation of macrophage phenotype polarization. We found that the elongation of macrophages led to higher levels of arginase-1, CD206, and YM-1, which are markers of M2 polarization. Although elongation had no effect on the expression of iNOS, a marker of M1 polarization, the secretion of proinflammatory cytokines were reduced. The degree of elongation required to induce expression of M2 markers was similar to the elongation levels elicited by IL-4/IL-13 stimulation. M2 marker expression stimulated by cell shape was not as high as expression in cells stimulated with high doses of cytokines, but patterned cells stimulated with low dose of IL-4/IL-13 exhibited

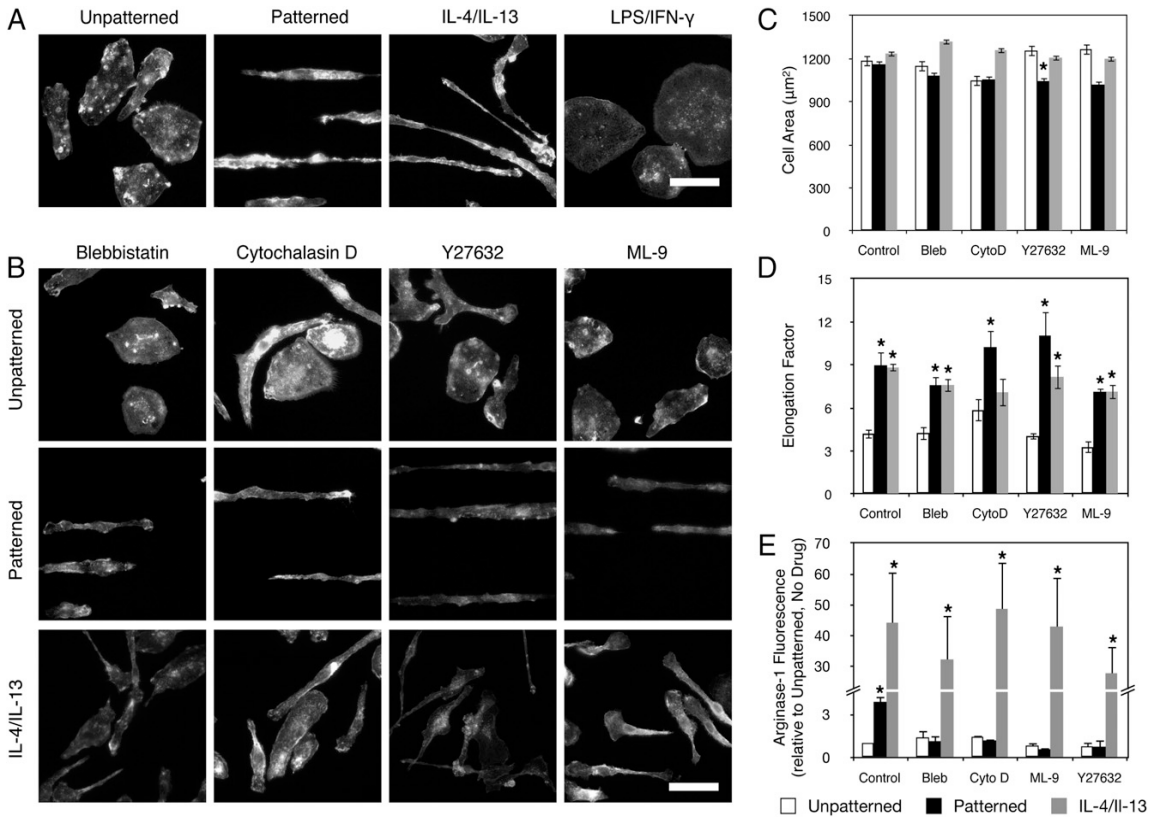


Figure 11. Cytoskeletal contractility is required for shape-induced M2 polarization. (A and B) Fluorescence images of phalloidin-labeled unpatterned cells and cells patterned on 20-μm wide lines treated with the indicated pharmacological agents or soluble stimuli. (Scale bar: 50 μm.) Quantification of cell area (C) and quantification of cell elongation (D) of cells shown in A and B. (E) Relative arginase-1 expression of cells shown in A and B, as measured by immunofluorescence cytometry. Error bars indicate the SEM for three separate experiments. *$P <$ 0.05 compared with unpatterned cells treated with the same drug as determined by the Student $t$ test. Bleb, blebbistatin; CytoD, cytochalasin D. Reproduced from [90]

higher levels of arginase-1 expression compared with unpatterned cells subjected to the same soluble conditions. Together these results suggest that cell shape itself polarizes macrophages toward an M2 phenotype and that cell shape synergizes with cytokines to enhance their effects on polarization state.

Macrophages are instrumental in facilitating collagen deposition during wound

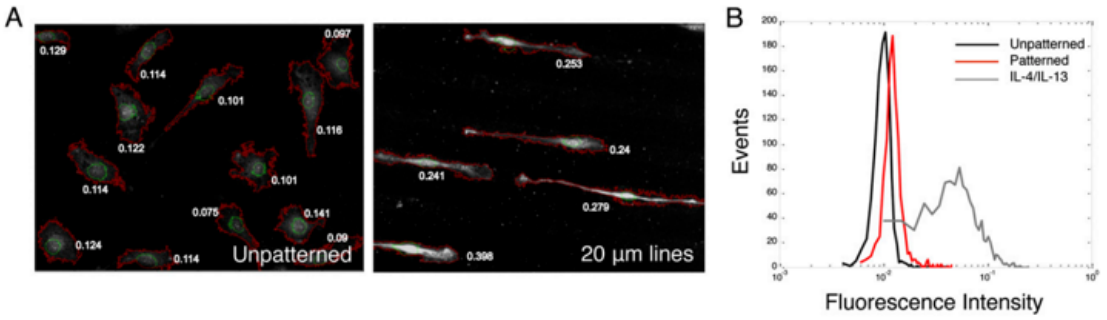


Figure 12. Immunofluorescence cytometry correlates with flow cytometry as a method to evaluate arginase-1 expression. (A) Representative immunofluorescence images of unpatterned (*Left*) and patterned (*Right*) cells stained for arginase-1 and analyzed for fluorescence intensity by CellProfiler software. Cells were outlined, and total pixel intensity was quantified. (B) Representative histogram of fluorescence levels in at least 1,000 cells quantified by immunofluorescence cytometry shows that the results obtained correlate well with the flow cytometry method used in Fig. 8. Reproduced from [90]

healing[128], and it is thought that arginase-1, an enzyme that metabolizes arginine to form proline, is involved in this process. Interestingly, however, it has also been shown that expression of arginase-1 prevents excessive collagen deposition by depleting arginine, which is needed T cell-mediated inflammation and fibrosis[129]. Together, these data suggest that tight control of arginase-1 levels is likely needed to achieve an optimal wound healing response with minimal fibrosis or scar formation. Our study suggests that changes in the physical extracellular microenvironment associated with collagen remodeling may feed back to regulate arginase-1 expression in macrophages. In addition, our data might help explain why macrophages of different phenotypes can be located in close proximity, where local tissue architecture may be different but soluble cues are likely to be similar[20,130]. Although the recruitment of distinct precursor populations may contribute to this phenomenon, our data provide compelling

evidence that adhesive cues in the local environment can modulate the phenotypic polarization of macrophages.

We demonstrate that contractility within the actin cytoskeleton is a key mediator of shape-induced macrophage polarization. Overall levels of F-actin were higher in M2 and micropatterned cells compared with unpatterned cells, although dramatic changes in cytoskeletal organization were not observed. Although such differences in the cytoskeleton with the macrophage polarization state have been previously reported[114], the functional role of actin in macrophage has been primarily associated with phagocytosis[131], podosome formation[132], or fusion events[133], and little is known about the role of cytoskeleton in macrophage polarization. We found that abrogation of actin polymerization and actin/myosin contractility, as well as ROCK and MLCK activities, completely eliminated shape-induced effects on polarization, suggesting a critical role for actin in the modulation of macrophage polarization by cell shape. Actin and actin-associated contractility have previously been implicated in transducing shape signals to changes in function in numerous cell types, including endothelial cells, smooth muscle cells, fibroblasts, and stem cells. It is interesting to note that M2 cells, which exhibit elevated actin, have also been shown to demonstrate other characteristics typical of mechanosensitive cells, including a mesenchymal, as opposed to amoeboid, migratory mode[59]. However, we found that cytoskeletal contractility was not required for IL-4 and IL-13 to induce arginase-1 expression. Nontheless, the evidence suggests that although macrophages are derived from a

nonadherent monocytic lineage, these cells, particularly those that adopt an M2 phenotype, may indeed be regulated by adhesive interactions with the ECM microenvironment.

How the cytoskeleton transduces physical signals to regulate biochemical cues that modulate the macrophage polarization state remains unknown. Because administration of Y27632 abrogated shape-induced polarization, it is possible that activation of GTPase signaling could participate in pathways that control polarization. In addition, alterations of cell shape may directly influence transcription of M1 or M2 gene programs, because recent evidence has demonstrated a critical role for mechanical signals on transcription factor activity[134]. Cellular elongation has been shown to influence nuclear organization, chromatin condensation, and histone modification[135,136], which could indeed have an impact on genetic programs associated with macrophage phenotype. Furthermore, an important area of future work is to elucidate the effect of elongation on macrophage function.

Dissecting the role of physical cues in macrophage polarization will have broad implications in the treatment of numerous pathological conditions[137]. Interestingly, disease characterized by chronic macrophage activation, including atherosclerosis and cancer, are often associated with alterations in the ECM architecture and mechanics, which are thought to play a critical role in disease progression[69,138]. Physical properties of the ECM lead to changes in adhesive interactions, integrin and cytoskeletal organization, and thus intracellular signaling pathways that are thought to promote cell transformation[139]. A better understanding of how

these microenvironmental cues regulate specific disease-associated macrophage functions will be critical for developing immune-targeted therapies for treatment of many diseases. In addition, the ability to modulate immune cell phenotype by the physical environment will be critical for encouraging wound healing in regenerative medicine. The immune response to tissue-engineered scaffold materials is critical to their success, and as such, investigators have explored whether physical factors, such as substrate topology, influence macrophage behavior. Interestingly, it has been observed that surface features indeed affect macrophage morphology and cytokine secretion profiles[44,45,140], as well as the overall fibrotic responses[53], although the mechanisms underlying these responses have so far remained elusive. Our data suggest that topological cues might lead to different macrophage responses by influencing their shape and cytoskeleton. Ultimately, encouraging the appropriate immune response to enhance healing will be needed to achieve tissue integration and optimal regeneration.

In the grand scheme of macrophage biology, although it is evident that morphology is strongly linked to phenotype in certain macrophages, the phenomenon is not universal. While we and others have observed that while M2-polarized BMDMs and microglia exhibit dramatic cellular elongations, many other macrophages do not. For example, in our experience, human macrophages derived from peripheral blood mononuclear cells (PBMC) do not exhibit significant elongation when stimulated with IL-4 and IL-13. Nevertheless, morphological changes are inevitably rooted in cytoskeletal reorganization and regulated by underlying

signaling pathways, which may suggest a mechanotransductive pathway that extends to other macrophages

# CHAPTER 3: Investigation of Single Macrophage Secretion in Controlled Adhesive Microenvironment

## 3.1 Understanding immune cell heterogeneity

The immune system is composed of a complex network of cells that interact through densely overlapping connections, resulting in coordinated immune responses. Until recently, studies have primarily examined immune cells at a population level. As our understanding of immune cell subtypes and activation states deepened, there is an increased appreciation for immune cell complexity and heterogeneity. For instance, CD4+ T cells were thought to have only two subtypes, Th1 and Th2, in the early 1980s. Five additional subgroups have since been recognized[141]. Similarly, alternative activation program of macrophages was not discovered until the early 1990s. Now, it is widely accepted that macrophage activation states far exceeds just the two extreme and instead exist on a spectrum[142]. Examples of this could be found across the immune system, as individual types of leukocytes can be subcategorized based on lineages, differentiation, phenotypic or functional states[143]. Clinical samples of single immune cell type show remarkable heterogeneity and present distinct phenotypic (cell surface or intracellular markers), functional (secreted products) and genetic signatures across multiple subsets. All of this complicates our efforts to understand immune regulation. Traditional bulk measurements of

cellular attributes, such as protein content by Western blot, secreted products by ELISA, and RNA and DNA by PCR, would most certainly overlook these heterogeneities. Even our own study presented in Chapter Two does not take into account macrophage heterogeneity. The M1-M2 simplistic model used to describe macrophage polarization does not take into account the fact that even *in vitro* stimulation with known M1 or M2 polarizing cytokines can lead to very differentially activated cells. *In vivo* studies have shown that macrophages in close proximity to one another can exhibit very different phenotype markers. Some can even expressed established markers for both M1 and M2 phenotypes[144]. It is still unclear whether these macrophages are simply a transient intermediate state as a product of undergoing phenotypic transition or that they are actually a stable, distinct phenotype in their own right. Emergent evidence in T cells seem to support the latter[145]. Furthermore, while the micropatterning technique allowed us to increase the average degree of elongation within a cell population, there was still substantial variation from cell to cell. All of these factors conflate to potentially confound our conclusions, especially considering that we only observed modest changes in the average population response due to changing cell shape.

While the importance of immune cell heterogeneity has been increasingly underscored in the literature, it was not until recent years, with the advancement in single cell technologies, that it was conclusively proven. To be fair, some of the early claims of immune cell heterogeneity could probably be attributed to the lack of awareness of the many functional subtypes, of which

we are still continuing to discover to this day. Heterogeneity was also initially attributed to enabling immune cell recognition of massive amount of pathogens through variability and plasticity[141]. It was not until last year, in an elegant study published in Nature, cellular heterogeneity was shown be perhaps a strategy for controlling population response. Shalek et al.[146] used a single cell RNA-seq technique to examine single dendritic cell transcriptome under different stimulation conditions and over various time courses. They discovered that as early as one hour after LPS challenge, there already appeared to be several precocious cells that express high levels of *Ifnb1* and *Ifit1*. It was subsequently shown that IFN-β secretion in precocious cells at early time points lead to the gradual expression of a core antiviral module in all cells within the population via paracrine signaling. Blocking cell-to-cell communication downregulates single cell expression of inflammatory genes as well as population level response. This is a remarkably interesting finding as the ability for a few precocious cells to influence the behavior of a whole population of cells present an efficient strategy for immune activation. Although it also suggests the activation of these precocious cells must be stringently regulated, as inadvertent activation of a few cells may result in unwanted population response. This perhaps also suggest the need for there to be immune regulators of different strengths. While most immune cells are known to be strongly affected by a robust extracellular cytokine signal, in the absence of robust soluble stimuli, the more subtle regulators such as physical and adhesive cues may play a deterministic role in the population response of immune cells. Thus, studies such as this highlights not only

the importance of heterogeneity in immune populations, but also the need for using more single cell analytical tools in examining immune systems. Traditional bulk assays would certainly overlook these rare subsets that are capable of initiating an immune response. Furthermore, the effects of complex microenvironmental cues on cellular activation may be lost when only the average response of a population is examined. Therefore, in order to tease apart the nuanced contributors to the functional variances among immune cells such as cell adhesion and cell shape, we must be able to accurately assess their phenotype and function on a single cell level.

### 3.2 Single cell analytical tools for examining immune cell heterogeneity

Most single cell techniques can be categorized based on the cellular components under study: protein content, RNA, and DNA. Although multiple components are beginning to be incorporated into newer technologies in order to provide a more complete whole cell picture. Flow cytometry is arguably the current gold standard for single cell analyses. However, similar to many other traditional molecular assays, it samples cells that were cultured in bulk and allowed to interact with one another and their external environment in an uncontrolled way. This type of methodology only averages the effects of cell-cell and cell-matrix interactions, which could be crucial to cellular activation and function. Moreover, while flow cytometry combined with immunofluorescence and fluorescence in situ hybridization (FISH) has already been used in

phenotyping and genotyping single cells[147], functional assessment through secreted products remain problematic. Detection of cytokines by flow requires protein transport inhibition followed by intracellular staining. Disruption of protein transport can affect cell migration[148] and potentially other cellular functions. In our experience, the addition of monensin and bredfeldin A to cultured cells changes macrophage cell shape. Enzyme-Linked ImmunoSpot (ELISPOT) is another immunoassay common for single cell cytokine detection. The assay requires cells to be sparsely seeded onto a bed of capture antibodies, and secretion is detected via enzymatic colorimetric method. The ease with which actively secreting single cells can be enumerated led to wide adoption of this assay in clinical settings. However, using this method means that cells would be cultured in bulk and on antibodies instead of extracellular matrix. Additionally, it is nearly impossible to quantify and correlate secreted products with secreting singles cells, which has limited its usefulness in basic research.

As secreted proteins are central to cell-to-cell communication and coordinated immune responses, several recent technologies set out to overcome the limitations of flow cytometry and ELISPOT by using microfabricated platforms. Love et al.[149] first demonstrated a technique termed microengraving, which uses an array of microwells to physically isolate single cells. A glass substrate immobilized with capture antibodies covers the wells during cellular interrogation and is removed afterwards for analyte quantification by immunofluorescence. Subnanoliter wells present an attractive platform for single cell analyses as they completely eliminate paracrine

signaling, provide a uniform extracellular microenvironment across thousands of single cells, and are conducive to registrations of multiple measurements for each cell. By increasing well size and combining with an antibody barcode array detection strategy, the microwell platform has since been improved to allow simultaneous detection of 42 secreted proteins on a single cell level[150]. However, in both of these studies, the microwells were blocked with bovine serum albumin (BSA) prior to cell seeding to prevent cell adhesion. While these have been great tools in studying T cells and B cells, which are non-adherent cells, they neglect the need for cell-matrix interactions that are important for adherent immune cells such as macrophages.

As previously discussed, macrophages activation and function are influenced by both biochemical cues and physical and adhesive cues in the extracellular microenvironment[46]. Biomaterials studies have shown that different material surface topography can affect macrophage morphology and their secretion of a number of different inflammatory cytokines including TNF$\alpha$, IFN$\gamma$, and MIP-1$\alpha$[46]. It has also been known for a while that extracellular matrix composition can lead to macrophage activation. For instance, matrix proteins fibronectin and fibrinogen are known to activate macrophage inflammatory pathway through Toll-like Receptor 4 (TLR4)[151,152]. In the case of fibronectin, it has been postulated that fibronectin proteins contain cryptic sites that are exposed only in certain conformations. However, when exposed and in contact with cells, they lead to inflammatory activation in immune cells. In the previous chapter, we primarily examined the effect of cell shape on macrophage phenotype

expression. While those studies gave us a sense of what changing shape does to the macrophages themselves, we need to also know how macrophage secretion is affected to understand the system level response. We performed an enzyme-linked immunosorbent assay (ELISA)-based secretion screening on micropatterned macrophages cultured in bulk, looking for approximately fifty different chemokines and cytokines. To our disappointment, we only observed statistically significant effect in four of the secreted proteins. Cell elongation led to a reduction in inflammatory cytokines CD54, IFNγ, and MIP-1α (Fig. 8 D). While these are promising initial findings, we believe that the results may be confounded by the fact that these macrophages were cultured in bulk and their shapes non-uniformly controlled. Therefore, we are interested in examining the effect of cell shape on macrophage secretion on a single cell level. However, delineating the effects of these factors on macrophage cytokine secretion on a single cell level is impossible with existing technologies mentioned previously.

### 3.3 Extracellular matrix influences macrophage secretion of inflammatory cytokines via TLR4

Extracellular matrix proteins, especially those associated with injury, have been thought to elicit immune responses by pathologists for many years. However, only recent studies have begun to reveal the mechanisms through which these occur. Fibrin/fibrinogen deposition resulting from extravascular coagulation can stimulate macrophage adhesion and secretion of

monocyte chemotactic protein 1 (MCP-1, also known as CCL2) *in vivo*[152]. The extra domain-A (EDA) present in alternatively spliced fibronectin molecules can promote similar cellular responses as LPS. Interestingly, both fibrinogen and fibronectin can lead to macrophage activation and secretion through Toll-Like Receptor 4[151,152].

MCP-1 is a protein secreted by many cells types, including monocytic, endothelial, fibroblasts, epithelial, and smooth muscle cells[153]. Although monocytes and macrophages are found to be the major producers of MCP-1. It induces chemotactic migratory behaviors in monocytes, macrophages and basophils, and does not affect neutrophils and eosinophils. It is largely responsible for monocyte/macrophage infiltration into tissues. Various reports have suggested that MCP-1, alone or in combination with other cytokines, not only attract but also activate macrophages[154].

In humans, MCP-1 proteins are known to bind to at least two different receptors. In fact, many chemokine receptors, such as CCR2, respond to several different ligands. Therefore, understanding the chemokine-receptor interactions remains a challenge[153]. For the most part, MCP-1 mediates its effect through receptor CCR2, which are expressed in less cells than MCP-1. Interestingly, in addition to being a monocyte chemoattractant, MCP-1 also act as a potent polarizing agent for directing $Th_0$ cells towards a $Th_2$ phenotype and enhancing IL-4 production by $Th_2$ cells.

MCP-1 has been linked to the pathogenesis of many diseases. Absence of MPC-1 in mice

resulted in substantial reduction in lipid deposition and atherosclerosis. MCP-1 is highly expressed in tumor tissues, and its expression is directly correlated with the extent of tumor-associated macrophage (TAM) infiltration, angiogenesis and poor survival. The seemingly opposite effects of MPC-1 in atherosclerosis and cancer is perhaps not surprising as CCR2 receptor has been shown to exhibit both proinflammatory and anti-inflammatory properties. The proinflammatory roles are generally carried out by antigen presenting cells (APCs) and T cells, whereas the anti-inflammatory roles are dependent on regulatory T cells.

The secretion of both MCP-1 and TNFα can be instigated by TLR4 binding. However, the signaling pathways differ slightly. The gene expression of MCP-1 is regulated by transcription factor NF-κβ, along with other inflammatory cytokines IL-1 and IL-8. The secretion of TNFα can be both NF-κβ-mediated and MAP kinase-dependent, which involves the activation of ERK1/2 and JNK. Other inflammatory cytokines such as IL-6 and RANTES employ a similar signaling cascade[155]. Although these are the ways through which TLR4 activation lead to the secretion of these two cytokines, these are by no means the only ways these cytokines can be secreted by a cell. For example, the secretion of both cytokines can also be elicited by the binding of the receptor for advanced glycation endproducts (RAGE), and MCP-1 expression can also be regulated by JNK and AP1[156].

### 3.4 A microwell system for detection of cytokine secretion by single adherent macrophages

To address the shortcomings in currently available technologies and further enable our own investigation into the effect of adhesive cues on macrophage function, we set out to create a novel single cell analytical tool that allows for controlled physical microenvironment of single cells and simultaneous detection of their secreted products. We drew our inspiration from the microengraving tool developed by Love et al.[149]. Our device employs a modular design composed of three components in a sandwich format. The bottom level consists of an adhesive substrate that could be modified with desired ECM proteins, topography and rigidity. The middle level is a thin PDMS membrane with arrays of micrometer openings. By combining the bottom and middle layers, an array of microwells is formed. The PDMS membrane can be easily microfabricated to contain openings of different shapes and sizes to control cell shape and cell spreading. The top level is a glass substrate that has been covalently conjugated with capture antibodies. A machined acrylic holder is used to fasten the three components together during cellular interrogation. We used this device to demonstrate that ECM proteins and macrophage cell shape can affect macrophage secretion of inflammatory cytokines on a single cell level. We compared the single cell results with bulk cell measurements via enzyme-linked immunosorbent assays. Together, we demonstrate that this device is a viable and also necessary platform for studying the effect of physical and adhesive cues on macrophage function.

## 3.5 Materials and methods

### *3.5.1 Photolithography of high aspect ratio microfeatures on silicon wafers*

All microfabrications were carried out in the UC Irvine INRF BiON facility. Transparency masks for photolithography were designed in AutoCAD and printed emulsion down by Cad Art Services (Bandon, OR). Test grade, three inch diameter silicon wafers (University Wafer) were immersed in 2% hydrofluoric acid to remove the oxide layer. Wafers were rinsed thoroughly with DI water and dried with $N_2$ stream. Wafers were further dried in a dehydration oven of at least 120°C for 15 min minimum. Thirty minutes is recommended for ideal results. A nitrogen gun was used to remove any visible dust particles left on the wafer surface. Each wafer was secured on a spin coater (Laurell Technologies), and approximately 2 mL of SU-8 50 (Microchem) were dispensed onto the center of the wafer. The spin speed and duration depends on the desired final thickness of the SU-8. To generate 50 μm thick PDMS with through openings, features on the wafers were designed to have a height of approximately 80 μm. To achieve that, SU-8 50 was spun at 500 rpm for 30 sec, followed by 1500 rpm for 1 min. After, the wafers were soft baked on a hot plate at 65 °C for 5 min and then in a 95 °C oven for 2 h. For UV exposure, Microchem protocol recommends 485 mJ/cm$^2$ to achieve an 80 μm thickness. Depending on UV flood lamp intensity, the exposure time will be approximately 45

sec. Soft baked wafer was centered under the lamp, and transparency mask was placed on top with the right side up. A high quality quartz plate that is transparent to UV light is placed on top to press the transparency mask flat against the wafer. After exposure, the wafers undergo post exposure bake on a hotplate at 65 °C for 3 min and 95 °C for 10 min. The mask patterns should start appearing in the SU-8 during post exposure. If not, the wafer might be underexposed. For SU-8 development, wafers were immersed in SU-8 developer (Microchem) for approximately 5 min. For optimal results, the developer solution should be 50:50 fresh developer and used developer. During development, the container was gently swirled every 30 sec to facilitate the removal of unpolymerized SU-8. Wafers were rinsed thoroughly with isopropanol to remove SU-8 developer. The appearance of white streaks during this step would signify that the wafer is underdeveloped. If everything was clear, wafers were further rinsed with DI water and dried with $N_2$ stream. The final step in the process requires baking the wafers at 200 °C for at least 30 min to finish curing the SU-8. Wafers were placed on hotplates, and the temperature of the hotplate was slowly ramped to 200 °C so as to not buckle the SU-8 layer with sudden temperature change. Once the wafer fabrication was complete, the wafer was placed into a silanization desiccator with 10 μL (Tridecafluoro-1,1,2,2-Tetrahydrooctyl) Trichlorosilane (Gelest) for at least 4 h.

*3.5.2 Fabrication of microwells*

Support rings for the polydimethylsiloxane (PDMS; Dow Corning) membranes were fabricated from a PDMS slab that is approximately 2-3 mm thick. Large circular pieces were punched out of the PDMS slab using a 5/8 inch diameter die. Within each 5/8 inch circle, a 1/2 inch circle was punched out, leaving a PDMS ring with an inner diameter of 1/2 inch. Silicon wafers containing 80 μm-tall posts of 33 μm x 33 μm, 20 μm x 50 μm, or 10 μm x 100 μm cross-sectional area were fabricated using standard SU-8 photolithography. PDMS were spin-coated onto the wafers to form an even 50 μm-thick membrane with through holes. While the PDMS was still wet, PDMS rings were placed around the features and cured with the membranes. Sterile glass coverslips were UV Ozone treated for 15 min before being adsorbed with either 20 μg/mL human fibronectin (BD Biosciences) or 2% Pluronics F-127 (Sigma Aldrich) for 1 h at room temperature (RT). After briefly drying with $N_2$ stream, PDMS membranes and glass coverslips were exposed to UV Ozone for 15 min and then adhered together to form an array of microwells. The microwells were incubated with a 2% Pluronics F-127 solution (Sigma Aldrich) at RT for 1 h while being desiccated to remove air bubbles from the wells. The microwells were rinsed thoroughly with PBS prior to cell seeding.

*3.5.3 Modification of antibodies*

For maximal conjugation of either biotin or Oregon green, antibodies stock solutions should be at least 500 μL and have a concentration of at least 500 μg/mL. LEAF-purified antibody pairs for specific target proteins were purchased from Biolegend. For biotinylation, antibodies, PBS, sodium bicarbonate and Sulfo-NHS LC Biotin (Thermo Scientific) were mixed thoroughly in an epitube. For Oregon Green conjugation, antibodies, PBS, sodium bicarbonate, dimethylformamide (DMF), and NHS-Oregon Green (Thermo Scientific) were mixed thoroughly in an epitube. Both reactions were allowed to take place at RT for 3 h on a gyromini. Afterwards, each reaction were put through Zeba desalting columns three times to remove unreacted linkers. Final concentrations of the modified antibodies were obtained using a NanoDrop spectrophotometer (Thermo Scientific).

*3.5.4 Modification of detection substrates*

Standard 25 mm x 75 mm glass microscope slides were cleaned with concentrated $H_2SO_4$ and autoclaved in sterile pouches. Clean slides were wiped with isopropanol and UV Ozone treated for 15 min. The slides were then silanized with a 4% (3-Mercaptopropyl)trimethoxysilane solution (Sigma Aldrich) at RT for 1 h. Meanwhile, NeutrAvidin proteins (250 μg/mL) were

conjugated with Sulfo-SMCC crosslinkers (both from Life Technologies) at RT for 30 h. Silanized glass slides were washed thoroughly with 100% ethanol and dried with $N_2$ stream. They were further baked dry in a 70 °C oven for 30 min. Once dry, a liquid blocker super pap pen was used to carefully mark the edges of the slides. A clean silicone gasket of 10 miliwells was sealed onto the slide about two thirds way down. The maleimide-activated NeutrAvidin was added to a 2 mL 7 kDa Zeba desalting column (Thermo Scientific) and centrifuged at 2000 rmp for 3 min to remove excess crosslinkers. The collected maleimide-activated NeutrAvidin was diluted to 10 μg/mL and incubated on the silanized slide at RT for 1 h. Following washing and blocking with 1% bovine serum albumin (BSA; MP Biomedicals) in PBS, the slides were incubated with 5 μg/mL of biotinylated LEAF purified capture antibodies (TNFα: Clone 6B8; MCP-1: Clone 2H5; Both from Biolegend) at 4°C overnight. Prior to cytokine interrogation, the detection slides were washed and blocked with 1% BSA for 30 min at RT.

*3.5.5 Cell seeding and cytokine interrogation*

Bone marrow derived macrophages (BMDMs) were harvested from 6- to 12- week old female C57BL/6J mice (Jackson Laboratory). Briefly, bone marrow cells were flushed out of the femurs with DMEM supplemented with 3% heat-inactivated (HI) FBS, and treated with ACK lysing buffer to remove red blood cells (all from Life Technologies). The remaining bone marrow

cells were cultured in a macrophage differentiation media consisting of DMEM supplemented with 10% HI FBS, 1% penicillin/streptomycin, 2 mM L-glutamine, and 1% conditioned-media containing macrophage colony stimulating factor (M-CSF). After 7 days, BMDMs were removed from culture using cell dissociation buffer (Life Technologies) and seeded into the microwells at 25,000 cells per well in a 12-well plate.

BMDMs were allowed to adhere and spread into the shapes of the microwells overnight. Immediately before cytokine interrogation, cells were stimulated with 10 ng/mL of lipopolysaccharide (LPS) and Interferon-γ (IFNγ) (both from Biolegend), and stained with 2.5 μg/mL of Hoechst (Life Technologies). Two 12 mm coverslip microwells were inverted over one detection slide. A PDMS-coated half slide were inverted over that to create a slide sandwich and seal the wells for the duration of cytokine interrogation. The seal can be obtained by either using four binder clips per 25 mm x 75 mm slide or a machined acrylic holder with thumb screws. Each detection substrate also contains a protein standard. To accomplish that, a silicone gasket with 3 mm wells (Grace Bio-Labs) was placed onto each detection slide, and the wells were loaded with known concentrations of recombinant mouse TNFα or MCP-1 (Both from Biolegend). Upon completion of interrogation, the detection substrates were removed and stained with 5 μg/mL of Oregon Green-conjugated detection antibodies (TNFα: Clone MP6-XT22; MCP-1: Clone 4E2; Both from Biolegend). A quick spin down of the detection antibody stock solution is necessary to minimize background noise in the final fluorescent images. Slides

were thoroughly washed with PBS, and a 25 mm x 60 mm cover glass was mounted onto each slides using fluoromountG (SouthernBiotech).

*3.5.6 Imaging and analysis*

All imaging were carried out on an Olympus IX2 inverted microscope equipped with an automated stage and the Micro-Manager software package of ImageJ (NIH). Live cells were imaged during interrogation while they were confined in the wells and inside the holders. For both cells and detection substrates, entire applicable areas of the slide or coverslip were scanned. The general microscope settings for nuclei imaging were: lamp intensity = 100, exposure = 5 ms, gain = 180, binning = 2x2. The nuclei images of the cells in microwells were stitched back together using ImageJ software (National Institutes of Health). Single cells in wells were identified based on nuclei size and distance from neighboring nuclei using a homemade Python script. The detection substrates were imaged using a 40x oil objective to enhance detection limit. The general microscope settings for nuclei imaging were: lamp intensity = 100, exposure = 15 ms, gain = 255, binning = 8x8. The stacks of fluorescent images were then processed to subtract out common background noise and stitched together using a homemade Python script. At least 20 matching sets of landmarks were manually registered using ImageJ in each pair of cell nuclei and cytokine detection images. A Python script then measures the fluorescence intensity in the

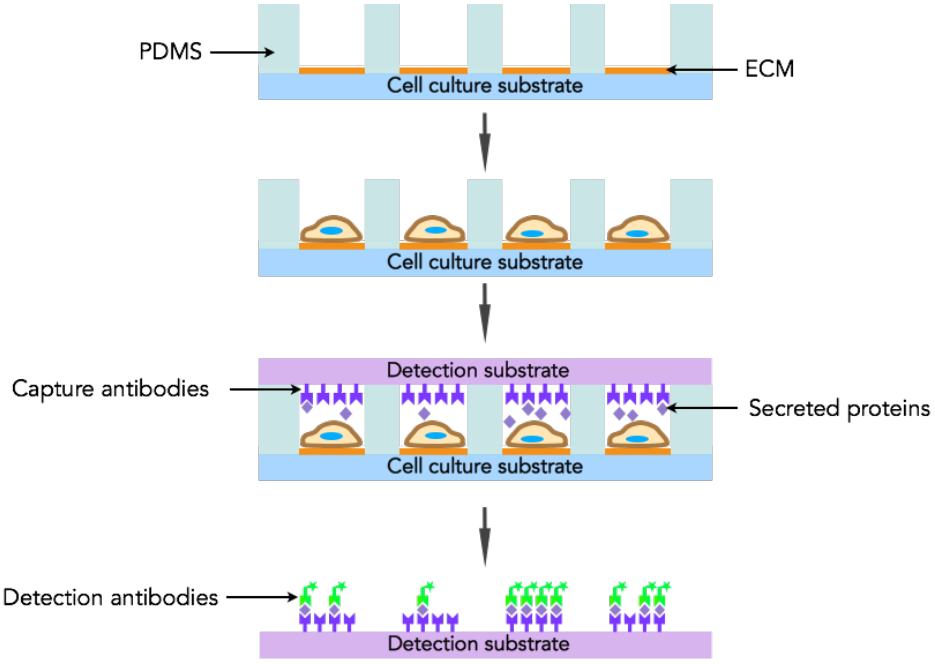


Figure 13. Schematic of the microwell system for single cell cytokine detection

detection image at each location where a single cell was found in the nuclei image. Each of the 3 mm miliwells of protein standards were also imaged with the exact same microscope setting as the cell detection substrates. They are stitched together the same way as detection substrates. The average fluorescence intensity at each protein concentration was measured using ImageJ (NIH), and a standard curve was created to transform the mean fluorescence intensity of the detection substrate into protein concentrations.

## 3.6 Results

### *3.6.1 Design of the microwell system*

We employed a modular design for our single cell cytokine detection platform (Fig. 13). We started with a cell culture substrate, which can be any surface that supports cell adhesion. For our initial experiments, we simply used 12 mm circular glass coverslips. We can adsorb various ECM proteins onto the glass. In the case of no ECM, we simply block the glass surface with Pluronics F127 to prevent cell adhesion. This design would allow us to easily switch out the glass surface for other materials with either chemical or physical surface modifications in order to investigate the effects of those modifications on cell secretion. The next component in the device is a 50 μm-thick PDMS membrane with micrometer size openings. The membrane is fabricated using a combination of standard photolithography and replica molding. PDMS was spin-coated onto silicon wafers containing 80 μm-tall posts to create a membrane with a uniform thickness of 50 μm. The posts can be designed to have cross sections of different shapes and sizes (Fig. 14 B) in order to control single cell shape and spread area (Fig. 14 C). They can also be used to compare the secretion of pairs of cells versus single cells, where the shape and area of each cell and the degree of cell-cell contact are kept constant (Fig. 14 A).

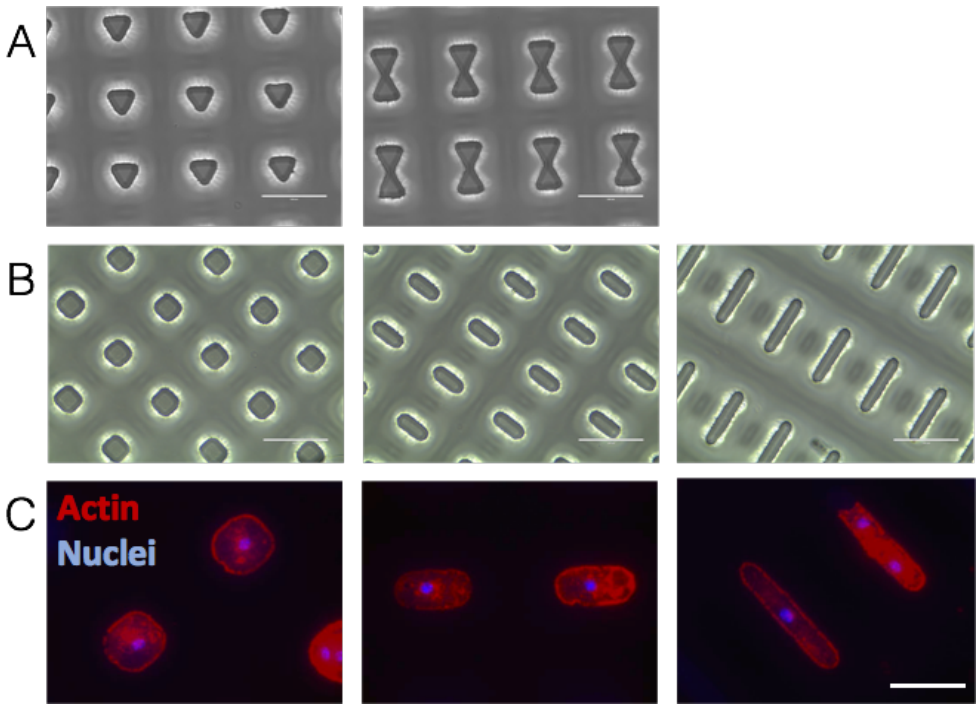


Figure 14. Microwells of various shapes and sizes to control single cell shape and spreading. (A) Microwells of 1000 μm$^2$ area (*Left*) and 2000 μm$^2$ area (*Right*) allows direct comparison of single cell and paired cell secretion where the degree of cell-cell contact is controlled. (Scale bar: 100 μm) (B) Microwells of the same 1000 μm$^2$ area but different aspect ratios: 33x33 μm (*Left*), 20x50 μm (*Middle*), and 10x100 μm (*Right*). (Scale bar: 100 μm) (C) Single macrophage shape and area are controlled using the microwells in (B). BMDMs are stained with Phalloidin to show actin cytoskeleton (Red) and counterstained with Hoechst to identify the nuclei (Blue). (Scale bar: 50 μm)

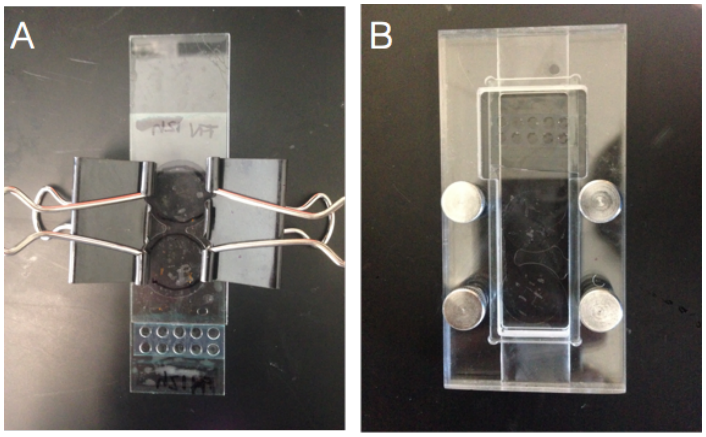


Figure 15. Housing units for the single cell detection platform. (A) Microwells can be sealed against a detection slide using a PDMS-coated glass slide and binder clips to apply pressure. (B) Second generation housing unit consists of two acrylic pieces with carved out space for detection slide. Pressure is applied using four thumb screws.

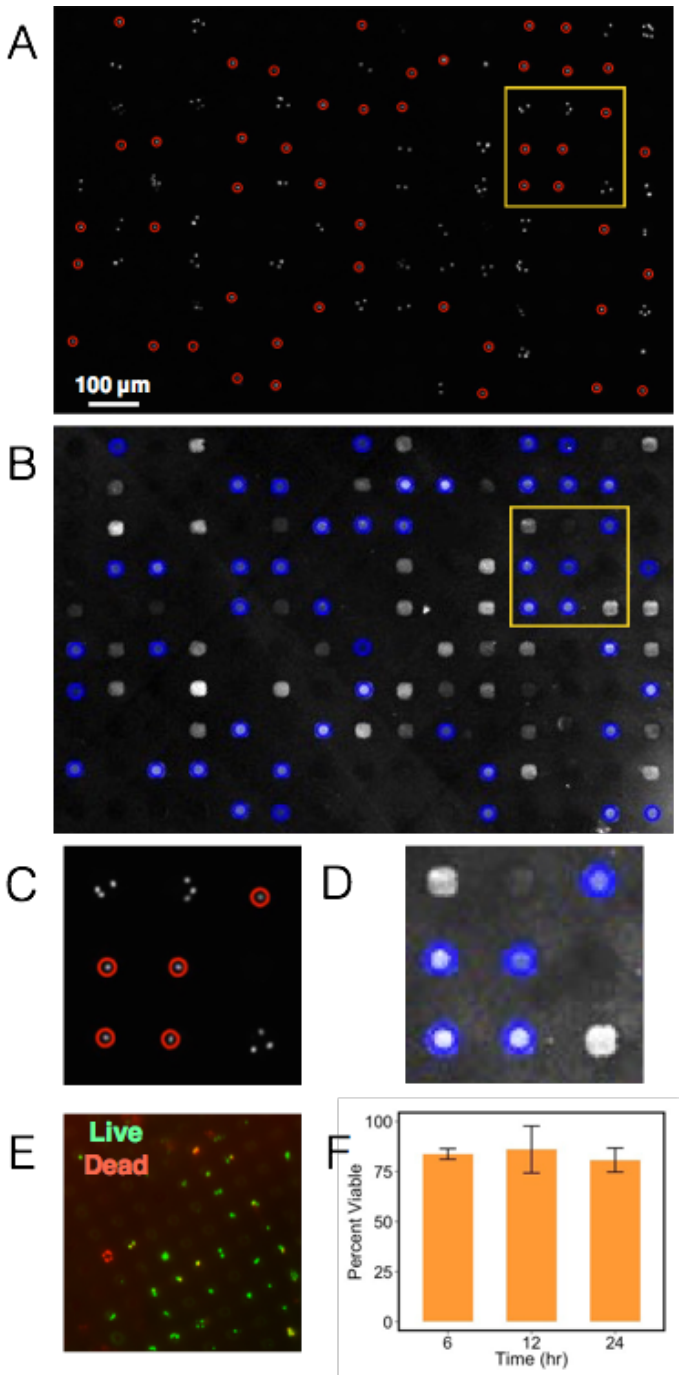


Figure 16. Macrophage secretion and viability in the microwells. (A) Fluorescent image of Hoechst-stained BMDMs in the microwells. Red circles identify the single cells in wells. (Scale bar: 100 µm) (B) Fluorescent image of MCP-1 secretion by BMDMs in (A). Blue circles identify secretion by single macrophages in wells. (C) Expanded view of the region in yellow in (A). (D) Expanded view of the region in yellow in (B) and corresponding region of (C). (E) Fluorescent image of macrophages labeled with calcein-AM (green, live) and ethidium homodimer-1 (red, dead) in the microwells. (F) Viability of macrophages in microwells over the course of 6h, 12h, and 24h.

Combining the cell culture substrate and the PDMS membrane with through holes together, an array of microwells that are only adhesive on the bottom of each well is formed. We further blocked the remainder areas of the microwell array with Pluronics F127 to ensure that the cells would only adhere to the bottom of the wells. The last component of the system is the detection substrate. To ensure maximal conjugation of capture antibodies and minimize noise in the detection, the substrate must be a very clean glass slide. Cleaning with a strong organic solvent such the 'Piranha" solution or concentrated sulfuric acid has yielded better results than with just 100% ethanol. After cleaning, we autoclave the slides to generate a nanosmooth glass surface, as steam has been shown to remove micro- and nano- topographical features on glass[157]. For conjugation of capture antibodies, we use a covalent conjugation strategy in which glass surface is first functionalized with a mercaptosilane and subsequently allowed to react with NeutrAvidin proteins via a NHS-ester and maleimide crosslinker. When compared to direct adsorption of proteins, this approach is more permanent and yields more proteins on the glass surface.

To combine all three components, the microwell arrays were inverted over the detection surface. Pressure is applied to seal the wells against the detection substrate through one of two ways. Initially, we simply placed a PDMS-coated glass slide on top of the microwells and against the detection slide and clamped everything together with binder clips (Fig. 15 A). Although the method works, it is cumbersome, and the applied pressure may not be uniform as it resulted in the leaking of certain wells. After some redesign, we created machined acrylic holders that can be

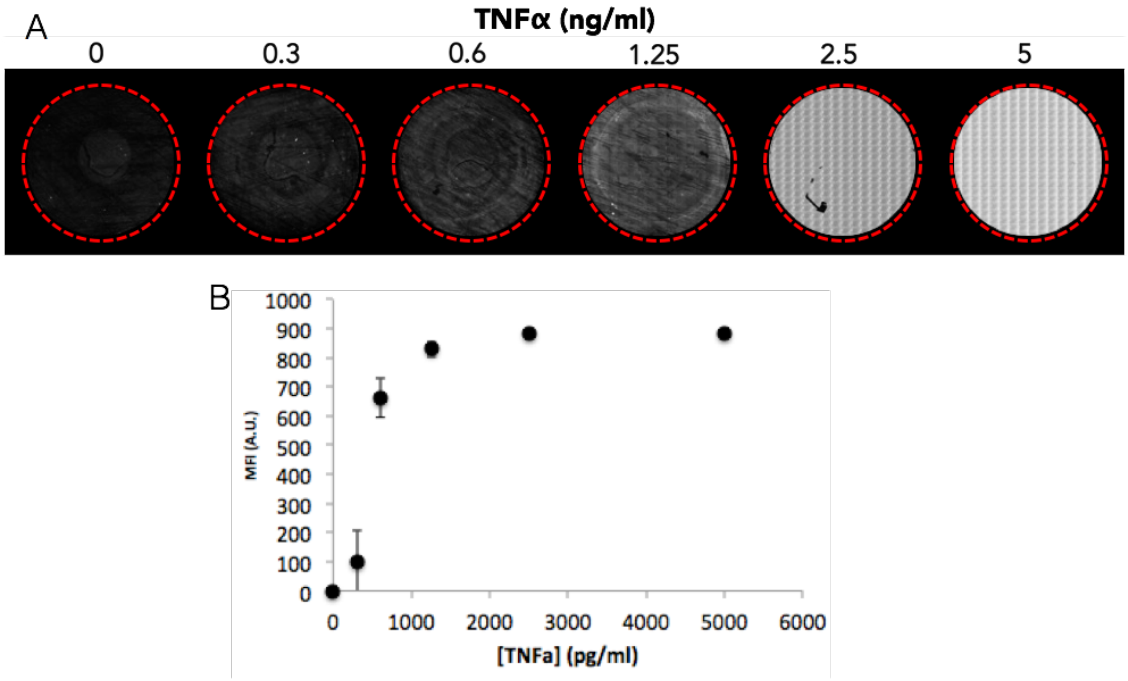


Figure 17. Sensitivity of fluorescence-based detection strategy. (A) 3mm-diameter miliwells were created on each detection substrate and loaded with recombinant target proteins of known concentrations. The entirety of each miliwell is imaged the same way that cell secretions are imaged. (B) A standard curve correlates the mean fluorescence intensity (MFI) of each miliwell and the protein concentration. Error bars indicate standard deviation of technical replicates from one experiment.

easily tightened with thumb screws to apply a more uniform pressure across all wells (Fig. 15 B). To test the system out in its entirety, BMDMs were seeded into the microwells. The cells were stimulated with 10 ng/mL LPS and IFNγ and introduced to Hoechst nuclei stain prior to interrogation. The wells were sealed with a MCP-1 detection substrate for 12 h. During which, the acrylic housing unit was placed directly under the microscope and scanned for Hoechst stain to identify cells in wells (Fig. 16 A). Following interrogation, the detection substrate is removed from the housing unit and stained with a fluorescent detection antibody. Fluorescent micrograph of the detection substrate was taken using an 40x oil objective (Fig. 16 B), and the detection

micrograph was correlated to the micrograph of cells in microwells (Fig. 16 C & D). To confirm the viability of the cells following interrogation, a time course experiment was conducted. At the end of 6 h, 12 h, and 24 h of interrogation, cells in the microwells were simultaneously stained with calcein-AM (green) and ethidium homodimer-1 (red) to differentiate live and dead cells (Fig. 16 E). The total viability of cells in microwells remained relatively constant (~80%) over the 24 h period, suggesting that the system is suitable for monitoring cell secretion over a 24 h period.

A final feature we wanted to include in this device is absolute quantification of secreted proteins. On every detection substrate, we placed a silicone gasket with 3 mm circular openings to form an array of miliwells. In these wells, we load known concentrations of recombinant target proteins and incubate for the same duration as cell interrogation. The detection substrate is processed the exact same way as previously described, and these protein standard wells are imaged the same way as cell secretion (Fig. 17 A). Once we obtain the mean fluorescence intensity (MFI) of each protein concentration, we can create a standard curve to correlate the MFI of cell secretion to protein concentration (Fig. 17 B).

*3.6.2 Extracellular matrices influence bulk macrophage secretion of cytokines*

Although it has been shown in the literature that certain extracellular matrix proteins can activate immune cells, we wanted to demonstrate that in our cells and with our particular

stimulation conditions. To test the effect of ECM on both classical activation and alternative activation, we chose to examine three cytokines that are highly secreted by macrophages. Tumor necrosis factor alpha (TNFα) and monocyte chemotactic protein 1 (MCP-1) are both inflammatory cytokines that are secreted by macrophages upon LPS and IFNγ challenge. IL-10 is arguable the only well-established anti-inflammatory cytokine that is produced as a result of IL-4/IL-13 stimulation and in the presence of LPS.

For our initial experiments, we examined at murine RAW264.7 macrophage secretion on fibronectin, matrigel, fibrinogen, and pluronics (control). We included four different soluble stimulation conditions: 1) Unstimulated (control) 2) 10 ng/mL LPS 3) 20 ng/mL IL-4 + 20 ng/mL IL-13 4) 10 ng/mL LPS + 20 ng/mL IL-4 + 20 ng/mL IL-13. The cells were seeded onto the different adhesive substrates for approximately 18 h and then stimulated with the appropriate soluble stimuli. After 24 h, we collected the supernatants of the cultures and looked the target cytokines by ELISA. As we expected, the presence of LPS significantly increased the secretion of inflammatory cytokines TNFα and MCP-1 (Fig. 18 A & B). Although we did not see significant differences in inflammatory cytokine secretion on different ECMs when LPS is present. This could be attributed to the fact that we were using near saturating levels of LPS stimulation (10 ng/mL), which may have masked the effect of ECM proteins. Interestingly, in the absence of LPS (unstimulated and IL-4/IL-13 stimulated), there is a significant increase in TNFα and MCP-1 secretion on fibrinogen.

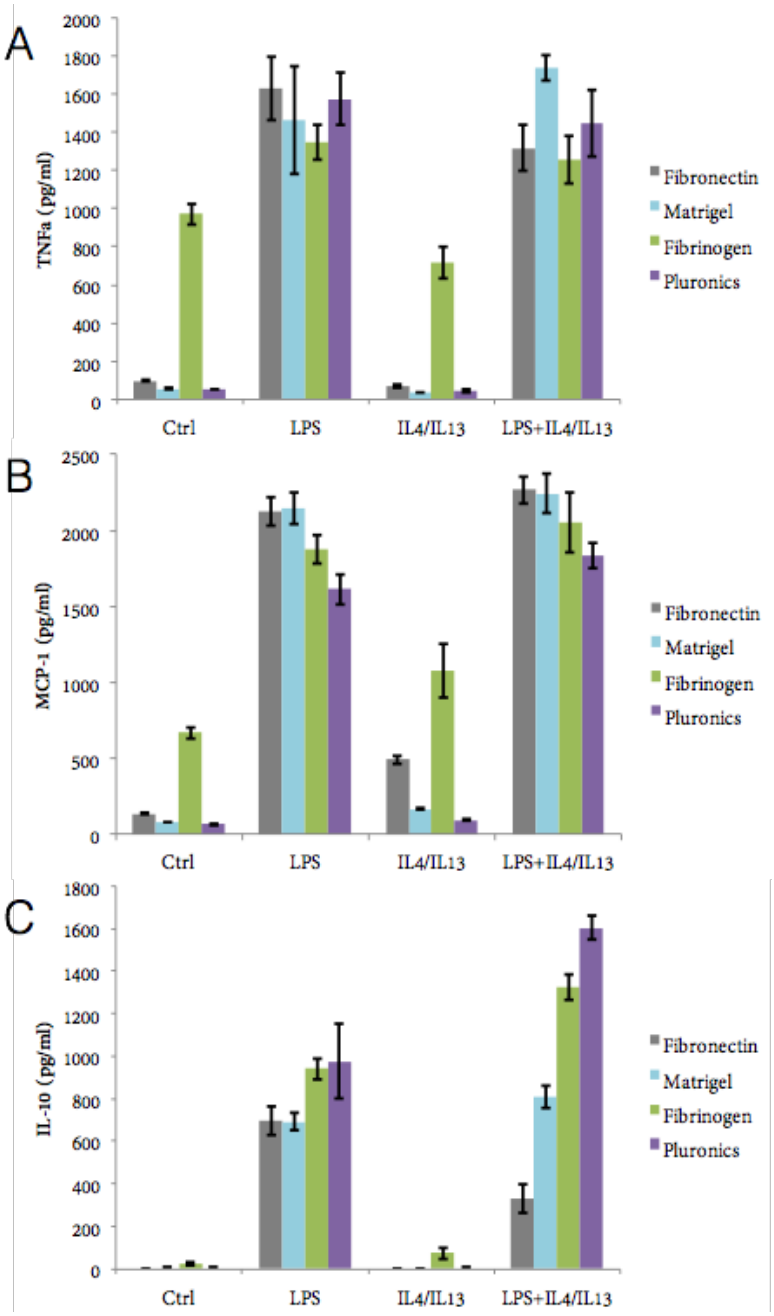


Figure 18. ECM proteins affect bulk RAW264.7 macrophage secretion of inflammatory and anti-inflammatory cytokines. (A) RAW264.7 macrophage secretion of TNFα. (B) RAW264.7 macrophage secretion of MCP-1. (C) RAW264.7 macrophage secretion of IL-10. Error bars indicate standard deviation of technical replicates from one experiment.

The levels of these secretion are more than half of the levels seen in the presence of LPS. Contrarily, on all other ECMs, the secretions of inflammatory cytokines in the absence of LPS were less than 10% of LPS stimulated conditions. This is perhaps not surprising as fibrinogen primarily appear during early phases of wound healing and blood clotting, where an inflammatory response is necessary to ensure that infection is kept at bay. A closer look at the LPS-less conditions show that TNFα and MCP-1 secretions are slightly higher on fibronectin than on matrigel or pluronics. This increase due to fibronectin is much less than on fibrinogen but is nonetheless visible, especially in MCP-1 secretion. Although IL-10 is considered an anti-inflammatory cytokine, we show that it would not be secreted with IL-4/IL-13 stimulation alone. In fact, LPS seems to be a much stronger inducer of IL-10 secretion, as only it only appears in the presence of LPS, either alone or in conjunction with IL-4/IL-13 (Fig. 18 C). Huge variations in IL-10 secretion on different ECMs in the presence of both LPS and IL-4/IL-13 is observed, and there is currently no good explanation for that. However, considering that LPS or TLR4 activation is required for IL-10 secretion, and we have previously established that fibrinogen lead to inflammatory activation similar to LPS, it is interesting that we observe slight increase in IL-10 production on fibrinogen in the absence of LPS. Together, these results establish fibrinogen as a potent immune activator.

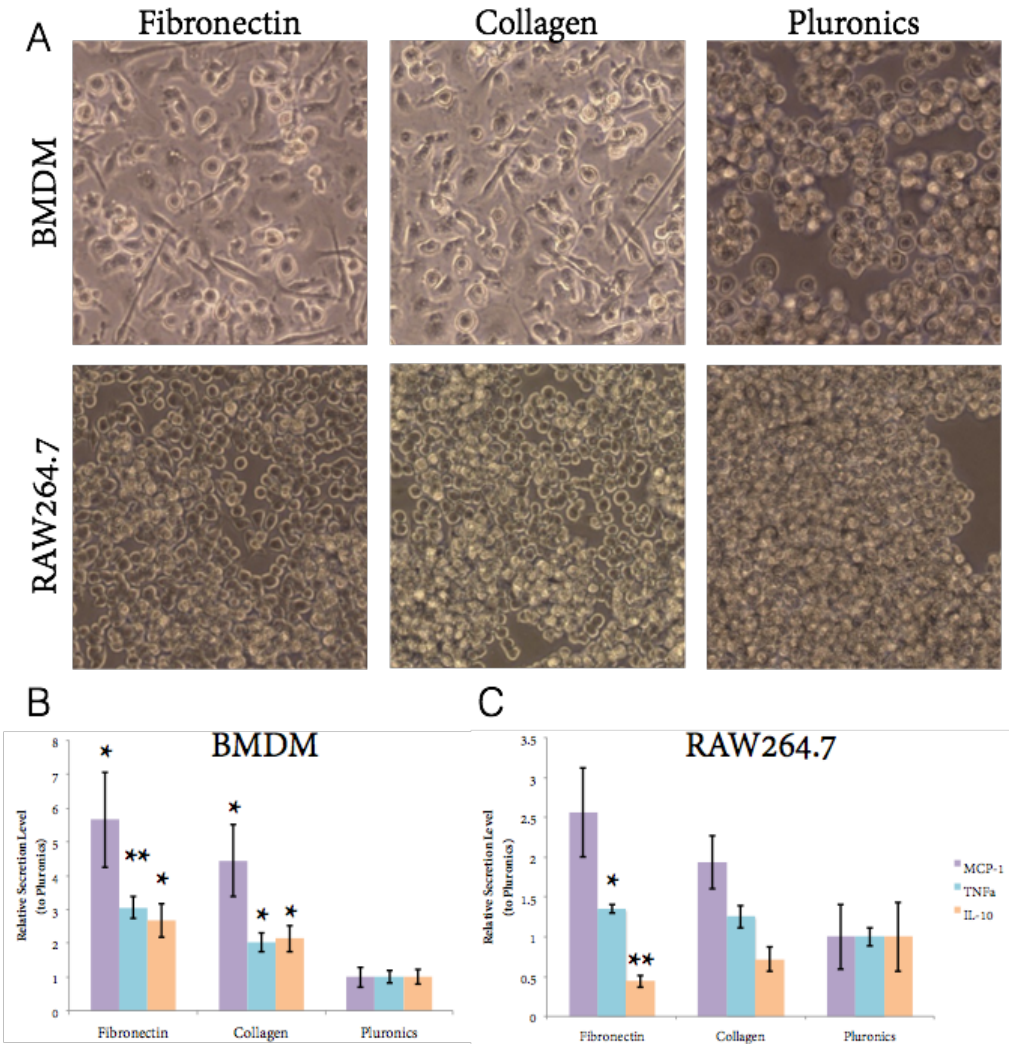


Figure 19. Bulk macrophage secretion on different ECMs and under various soluble conditions. (A) Phase contrast images of BMDM (*Top*) and RAW264.7 (*Bottom*) macrophages on different ECM proteins. (B) BMDM secretion of MCP-1, TNFa, and IL-10 on different ECMs. (C) RAW264.7 secretion of MCP-1, TNFa, and IL-10 on different ECMs. All secretion levels are normalized to the corresponding Pluronics condition. Error bars indicate the SEM for at least three separate experiments. *$P < 0.05$ and ** $P < 0.01$ compared with cells on pluronics under the same soluble condition as determined by the Student *t* test.

To further investigate the effects of matrix proteins on macrophage activation and secretion, we made a few changes to our experimental conditions. First, we wanted to study both primary BMDMs and RAW264.7 macrophages. Second, we narrowed down the adhesive

conditions to just fibronectin, collagen, and pluronics (control). We included collagen because it is the most abundant ECM protein in the body, while fibronectin is the second most abundant. Thirdly, we adjusted our soluble stimulation conditions since high dose of LPS may have confounded the effect of certain ECM proteins in the previous experiments. For the inflammatory cytokines TNFα and MCP-1, we stimulated both BMDMs and RAW264.7 macrophages with 1 ng/mL LPS, which is 10x less than the previous experiments. For IL-10 secretion, we stimulated BMDMs with 1 ng/mL LPS and RAW264.7 cells with 10 ng/mL LPS in addition to 20 ng/mL IL- 4/IL-13 for both cell types. We observed that both types of macrophages are most adherent to fibronectin in that they are most spread out on those surfaces. While both cells appeared to tether to collagen, they were much more rounded. As we would expect, neither macrophage type adhered to the pluronics substrates. All of the cells were rounded and floating in media in those conditions (Fig. 19 A). In terms of secretion of inflammatory cytokines, lowering of LPS stimulation seems to highlight the activating effect of fibronectin. In both macrophages, fibronectin significantly increased the secretion of both TNFα and MCP-1 (Fig. 19 B & C). This effect is much more prominent in the primary BMDMs than in RAW264.7 cells, and the increase in MCP-1 is more than TNFα. These experiments have been repeated at minimum three times, and the effect of fibronectin on BMDM secretion show statistical significance. Even collagen seems to significantly affect BMDM secretion of both TNFα and MCP-1, which has not been reported in the literature. Comparing to the pluronics

control, collagen also increases secretion of inflammatory cytokines, although not to the same degree as fibronectin. The same trend is observed in RAW264.7 cells, but the differences are much smaller and therefore not statistically significant. Interestingly with IL-10 secretion, we observe the exact opposite trend in BMDMs versus RAW264.7 cells. In BMDMs, IL-10 production is highest on fibronectin and lowest on pluronics, which is the same as the inflammatory cytokines. The differences between ECM proteins and pluronics are statistically significant. However, in RAW264.7 cells, IL-10 secretion is lowest on fibronectin and highest on pluronics, although these effects are not statistically significant. We are not sure what contributes to these differences. Nevertheless, these results conclusively prove that different adhesive conditions can affect macrophage secretion of both inflammatory and anti-inflammatory. However, whether the differences in secretion are due to the specific adhesive proteins, cell adhesion, cell spread area, or a combination of these factors is still unclear. Single cell studies where we can control single macrophage adhesion and cell spreading will likely aid in our understanding of these contributing factors on macrophage cytokine secretion.

*3.6.3 Single macrophage secretion under different soluble conditions*

To validate our single cell cytokine detection platform, we first wanted to examine whether we can detect differences in secretion levels when cells are under with different levels of soluble stimuli. For simplicity sake, we used two different stimulation conditions: 1) 1 ng/mL

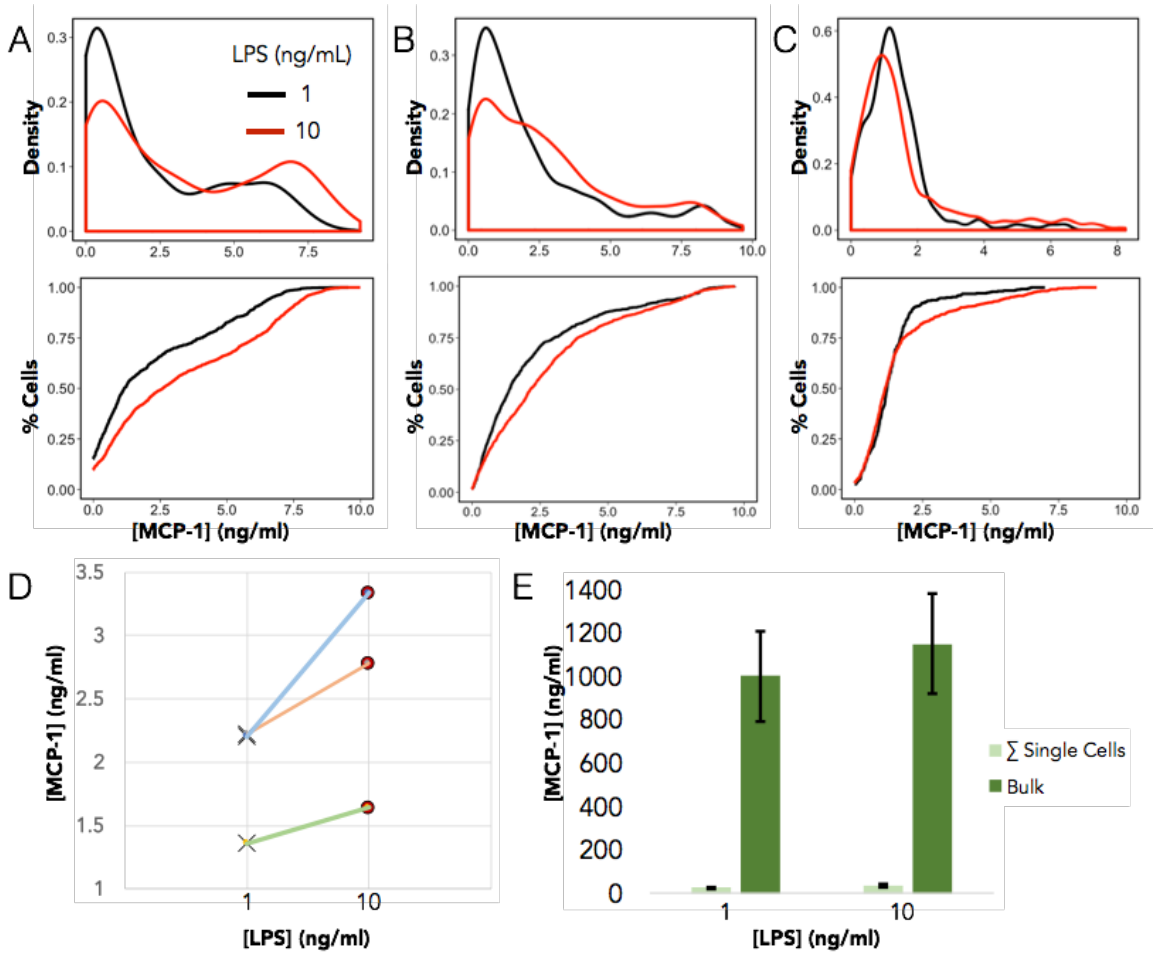


Figure 20. Single BMDM secretion of MCP-1 under different soluble stimuli. BMDMs were stimulated with either 1 ng/mL LPS or 10 ng/mL in addition to 10 ng/mL IFN-γ, and interrogated for MCP-1 secretion for 6 h. (A), (B), and (C) show results from BMDMs derived from three different mice. Probability density (*Top*) and cumulative distribution (*Bottom*) show single cell secretion heterogeneity under different LPS stimulation. (D) Average single cell secretion of MCP-1 from each of the three experiments. (E) Comparison of MCP-1 secretion from sum of single cells and bulk ELISA results in BMDMs under the same conditions.

LPS + 10 ng/mL IFN-γ, and 2) 10 ng/mL LPS + 10 ng/mL IFN-γ. BMDMs were seeded into 33 x 33 μm fibronectin –coated microwells. The cells were allowed to adhere and spread into the shape of the wells for 12 h. Afterwards, cells were stimulated with the two different simulation conditions and immediately sealed against detection substrates modified with MCP-1 capturing antibodies. The activated cells were interrogated for MCP-1 secretion for 6 h. The secretion of at

least 1000 cells were analyzed for each stimulation condition. We plotted the single cell secretion in histogram form to show population level secretion heterogeneity (Fig. 20 A-C top), as well as the cumulative distribution plots to directly compare the percentage of cells secreting at all MCP-1 concentrations (Fig. 20 A-C bottom). This experiment has been repeated three times with primary BMDMs harvested from three different mice. Although the baseline cell secretion level from different mice are likely to be different, as one of the experiments show much lower average single cell secretion than that other two. We still observed higher average single cell secretion of MCP-1 under higher LPS stimulation, which is what we would expect (Fig. 20 D). Finally, we compared the single macrophage secretion with bulk ELISA results. To do so, we took the average single cell secretion from the single cell experiments, and adjusted for volume differential between the single microwell and single tissue culture well (50 pL vs. 2 mL). We also multiplied the single cell secretion by 500,000, as that was the number of cells cultured in each bulk culture well. Surprisingly, the sum of the single cell secretion ($\Sigma$ single cell) was much less than that of bulk secretion. Although the same trend of increasing MCP-1 secretion with increasing LPS simulation is observed, $\Sigma$ single cell secretion is consistently about 50 times less than bulk secretion (Fig. 20 E). This is a potentially interesting finding as it alludes to the fact that paracrine signaling may be at play to amplify secretion in bulk.

*3.6.4 Single macrophage secretion on different adhesive substrates*

Next, we wanted to examine the effect of cell adhesion on secretion using our single cell device. For simplicity sake, we chose to test only fibronectin and pluronics, which are the two substrates that resulted in the biggest difference in BMDM MCP-1 secretion in the bulk assays (Fig. 19 B). In addition, we also wanted to examine secretion over a time course to reveal the secretion dynamics of these macrophages. BMDMs were seeded into 33 x 33 μm microwells coated with either fibronectin or pluronics. The cells were allowed to adhere and spread into the shape of the wells for 12 h. Afterwards, cells were stimulated with 10 ng/mL LPS and 10 ng/mL IFN-γ and immediately sealed against detection substrates modified with MCP-1 capturing antibodies. The activated cells were interrogated for MCP-1 secretion for 6 h, 12 h, or 18h. The secretion of at least 1000 cells were analyzed for each experimental group. This experiment has been repeated three times with primary BMDMs harvested from three different mice. Representative probability distribution plots (Fig. 21 A-C top) and cumulative distribution plots (Fig. 21 A-C bottom) from one experiment are shown. As we would expect, the average population secretion increases with increasing duration of interrogation. The single cell results also corroborate with the bulk ELISA data shown in Fig. 19, in that there is more BMDM MCP-1 secretion on fibronectin than Pluronics at each time point. In general, the probability distribution curves all have one tall peak signifying a large population of average, relatively low secreting cells. The fibronectin curves generally have higher number of high secreting cells,

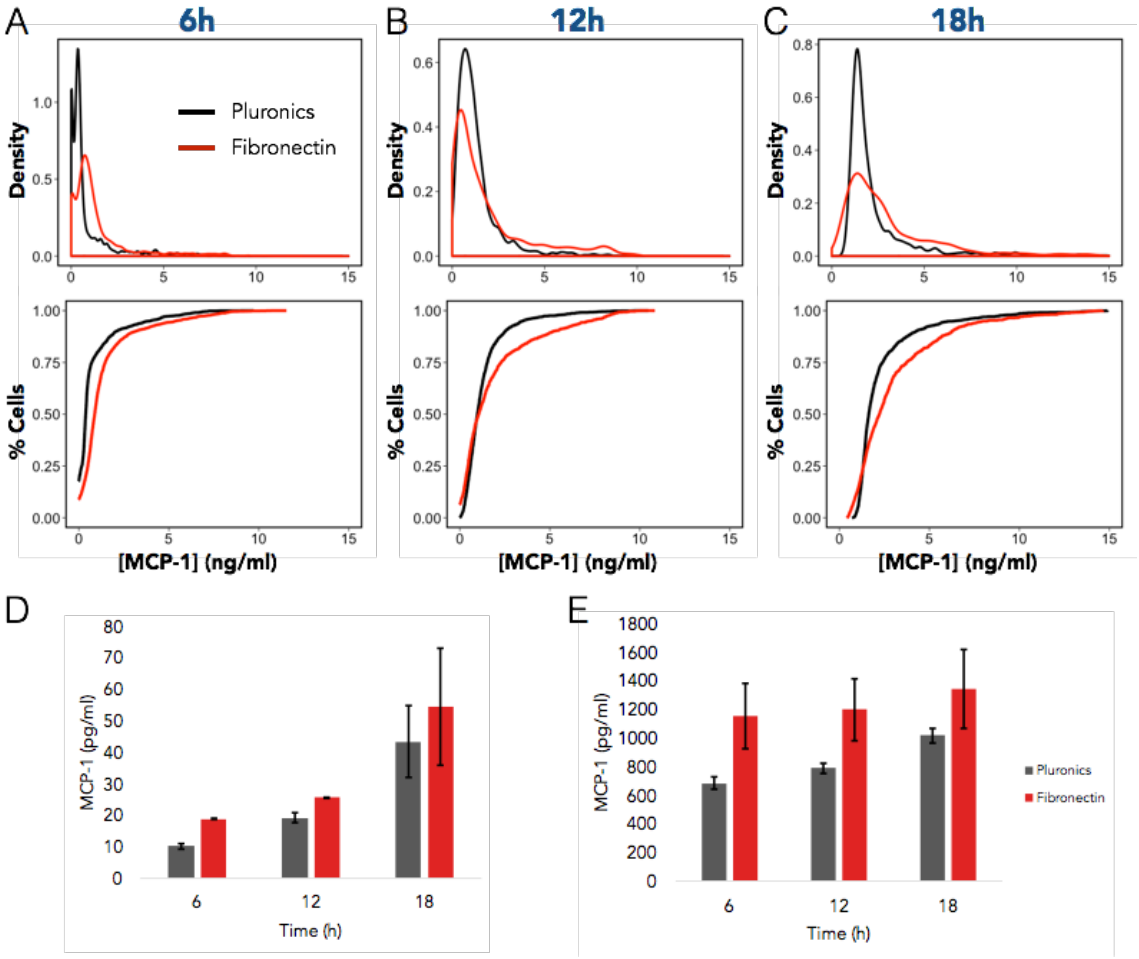


Figure 21. Single BMDM secretion of MCP-1 on different adhesive substrates. BMDMs were seeded on either fibronectin or pluronics, and stimulated with 10 ng/mL LPS and IFNγ. MCP-1 interrogations were carried out for 6h, 12h, and 18h. Representative probability density plot (*Top*) and cumulative distribution plot (*Bottom*) from one experiment at 6h (A), 12h (B), 18h (C). (D) Sum of single cell secretions of MCP-1 from average of two experiments. Error bars indicate SEM from two separate experiments. (E) Bulk BMDM secretion of MCP-1 measured by ELISA. Error bars indicate standard deviation from one experiment.

which leads to higher average secretion level than pluronics. More interestingly, the fibronectin probability distribution curves are also generally wider and more spread out, signifying the secretion range of single cells are more varied. This is especially true in the 18 h time point case (Fig. 21 C top), which suggests that ECM protein may actually contribute to the observed population heterogeneity. This is also supported by the cumulative distribution curves. The

fibronectin cumulative distribution curves are less steep and further become less steep as time goes on, implying increased heterogeneity. Whereas pluronics curves retain roughly the same shape and only shifts to the right as time goes on. Once again, we summed up the single cell secretions and compared them to the bulk ELISA results. Similar to previous experiments, we observed much lower secretion levels in the single cell experiment than in bulk cultures. Interestingly, although we do observe increases in secretion due to fibronectin and increase in time in both single and bulk experiments, the differences are much more pronounced in the single cell experiments. In bulk cultures, it seems that the cell population secretes most of its cytokines by 6 h, and only small increases in secretion is detected at 12 h and 18 h. This again may be attributed to paracrine amplification of secretion, where large group of cells together would more quickly reach saturating secretion level of the population. Together, these results show that our device can detect the effect of adhesion on single cell secretion. It proves the necessity of a single cell device that can control cell adhesion and simultaneously detect cell secretion.

*3.6.5 Single macrophage secretion with different cell shape*

Finally, we wanted to investigate the effect of cell shape on single macrophage secretion. This is in part motivated by our previous work from Chapter 2, where we discovered that elongated cell morphology promoted macrophage polarization toward a more M2, or anti-

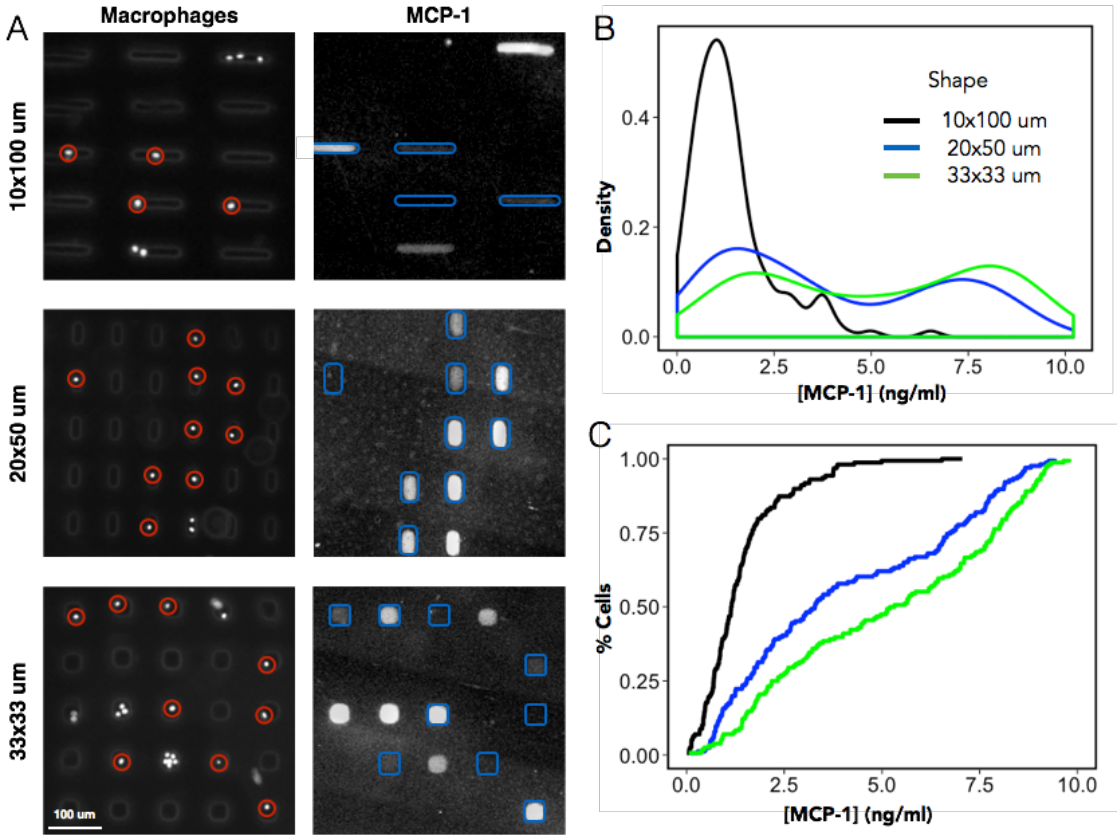


Figure 22. Single cell secretion of MCP-1 from BMDMs of different cell shape. BMDMs were seeded into microwells of the same area (1000 $\mu m^2$) but three different shapes and stimulated with 10 ng/mL LPS and IFNγ. They were interrogated for MCP-1 secretion for 6 h. (A) Representative images of Hoechst-stained BMDMs in microwells (*Left*) and corresponding MCP-1 secretion (*Right*). Red circles indicate single cells in wells, and blue outlines indicate single cell secretions of MCP-1. (B) Probability density plot of single cell secretion heterogeneity in microwells of different shapes. (C) Cumulative distribution plot of single cell secretion heterogeneity in microwells of different shapes. At least 150 cells from each shape condition were analyzed.

inflammatory phenotype. We had previously elongated populations of macrophages through micropatterning and examined their secretion using an ELISA-based cytokine array. Somewhat disappointingly, we only discovered statistically significant but moderate decreases in a few inflammatory cytokines with engineered cell elongation. We had reasoned that cellular heterogeneity and the imperfect bulk method of controlling cell shape may have confounded our results. Now that we have a validated single cell cytokine detection method where we can control

single cell shape, we have the tool to properly address that question. From our previous work, we know that the average BMDM has a spread area of about 1000 $\mu m^2$, irrespective of soluble stimulation (Fig. 4 B). So we designed microwells with different shapes but all have the same area of 1000 $\mu m^2$. This allows us to eliminate cell area as a potential factor that could influence cell secretion. To investigation cell elongation, we chose three different aspect ratios or elongation factors: 1, 2.5 , and 10. We designed these three types of microwells, which have the dimensions of 33x33 μm, 20x50 μm, and 10x100 μm (Fig. 14 B). By simply seeding single BMDM macrophages into these wells and allow them to spread into the shape of the wells, we demonstrated that we can control single cell shape and area (Fig. 14 C). Once the cells assume the shape of the wells, they were stimulated with 10 ng/mL of LPS and IFN-γ and immediately sealed against detection substrates modified with MCP-1 capturing antibodies. After 6 h of cytokine interrogation, the MCP-1 secretion of 150 single cells from each shape condition were analyzed for their MCP-1 cytokine secretion (Fig. 22 A). Interestingly, the most elongated macrophages, assuming the 1:10 aspect ratio (10x100 μm), secreted significantly less inflammatory cytokine MCP-1 than the other cell shapes (Fig. 22 B). Higher aspect ratios of cell shape seem to correlate with lower secretion of MCP-1 on a single cell level (Fig. 22 C). This corroborates with our previous conclusion that elongated macrophages assume a more anti-inflammatory phenotype. Although the 33 x 33 μm macrophages seem to secrete marginally less MCP-1 than 20 x 50 μm macrophages, the difference is much less pronounced than that between

33 x 33 μm and 10 x 100 μm cells. This result supports our previous study, where patterning macrophages on 50 μm-wide lines (leading to more or less a 20 x 50 μm cell shape), did not significantly affect macrophage activation (Fig. 7 D). This result is also interesting in that when we examined MCP-1 secretion in the bulk micropatterned cells, we did not observe any statistically significant changes in secretion between elongated and non-elongated cells (Fig. 8 D). However, with our single cell cytokine detection device, we can detect differences in cell secretion based on cell shape, which could not be detected in tradition bulk assays. This further proves the usefulness and necessity of this device.

**3.7 Discussion**

The inherent heterogeneity of immune cell populations has long been recognized, although the progress to understand has been hindered by the limitations of traditional "bulk" assays. Recent advances in single cell RNA-sequencing have revealed unique information that cannot be obtained with traditional methods, and demonstrated the importance of cellular heterogeneity as a potential strategy for controlling population level response[146]. In this light, there has been increasing demand for single cell technologies.

While single cell phenotyping (flow cytometry) and genotyping (RNA-seq) has already been established, one area that has proven difficult to advance has been secreted products. These are arguably the most important for coordinating population level response as they facilitate cell-

to-cell communication. Also, measuring secreted proteins directly rather than mRNA copies has distinct advantages. For one, proteins and mRNA content within a cell are not necessarily correlated, especially when measurements are taken in static snapshots. Both are subject to intrinsic and extrinsic noises, and different rates of production (transcription or translation) and degradation[158]. Specifically in the case of immune cells, inflammatory cytokines such as IL-1β and the mRNAs of inflammatory cytokines such as TNFα are often produced in advance and stored within cells[159]. Such design enables these cytokines to be rapidly released upon stimulation, which is why we could observe macrophage secretion of these proteins within thirty minutes of stimulation. Therefore, measuring secreted proteins from single cells provides a more accurate picture regarding how each cell may be affecting the population.

Previous work on single cell secretion have primarily used microarrayed wells for cell isolation, and secretion detection relies on immunofluorescence-based sandwich assays[149,150]. While this proves to be a viable and relatively easy to implement strategy for studying T cells and B cells, it neglects the adhesion dependence of cells such as macrophages. Especially motivated by our previous work in Chapter Two, where we demonstrated the importance of adhesion and cell morphology on macrophage activation, we sought to develop a platform to assess single cytokine secretion while controlling individual cell adhesion.

In this work, we used microfabrication techniques to create arrays of microwells that contain ECM-coated adhesive bottoms. By manipulating the microwell size and geometry, we

can control single macrophage morphology and spreading. Macrophage viability in the microwells remained relatively constant over a 24-hour period, which makes this a viable platform for monitoring single cell secretion dynamics over time. We validated the system with a few different experiments. First, we examined single macrophage secretion of inflammatory cytokine MCP-1 under different levels of soluble stimuli. As we expected, higher dose of LPS stimulation resulted in higher secretion of MCP-1, which is supported by bulk ELISA data. However, unlike ELISA, we were able to detect possible subsets within a single population in addition to obtaining the average levels of single cell secretion. We were also able to use this single cell platform to examine the effect of different adhesive substrates, which is what sets this device apart from its predecessors. Congruent to bulk ELISA data, we observed higher single macrophage secretion of MCP-1 on fibronectin than Pluronics. Interestingly, while the average single macrophage secretion on pluronics increased with increasing duration of interrogation, the secretion profiles retained relatively similar shape over the same time course. However, the secretion profile of single macrophages on fibronectin gradually widened over that time period, implying increase in secretion heterogeneity over time. This finding suggests ECM proteins as a possible explanation for observed cellular heterogeneity *in vivo*, and it can only be revealed with our single cell platform. Equally important, when comparing bulk ELISA results with the sum of the average single cell secretion, which essentially gives us the same measurement as an ELISA, there appears to be significant discrepancies. The cell secretions detected by ELISA, under the

same soluble and adhesive conditions, are consistently and dramatically higher than that detected by the single cell method. We have performed this comparison for both TNFα and MCP-1 secretions. Although the differences between bulk and summed single cell results were smaller for TNFα (~20x) than MCP-1 (~50x), they are still significant. This strongly suggest the presence of paracrine signaling in bulk cultures that could have amplified the overall population secretion. Lastly, we examined the effect of macrophage cell shape on single cell secretion, which was the original motivation behind developing this device. We kept all cell areas to be 1000 $\mu m^2$ while changing the cell aspect ratio from 1:1 to 1: 2.5 to 1:10. Intriguingly, single macrophage secretion of MCP-1 correlated with cell aspect ratio. The most elongated single macrophages, assuming the 1:10 aspect ratio, secreted the least amount of MCP-1, whereas the roundest macrophages (1:1) secreted the most MCP-1. This not only supports our previous finding that macrophage elongation promotes a more M2 or anti-inflammatory phenotype, it also links cell shape with macrophage function. More importantly, this reduction in secretion was not observed in bulk measurements, and was only possible due to the development of our single cell platform.

In conclusion, we have developed a novel single cell secretion detection platform that allows for precise control of cell adhesion. The results obtained thus far using this device clearly substantiate the necessity for it as we have demonstrated effects of adhesive cues on macrophage secretions that would not be detected otherwise. Clearly, much work remains to be done to

explore these initial findings in more depth. For instance, to tease apart the paracrine signaling effect, we have already fabricated microwells that are twice as large to enable studies of paired cell secretion. Receptor antibodies can also be used to block specific pathways of paracrine signaling and investigate their effects on cell secretion.

## CHAPTER 4: Conclusions and Future Directions

Our work with macrophage cell shape adds another piece of direct evidence in support of physical and mechanical regulation of macrophage activation. It offers a somewhat unifying explanation to some of the previously reported findings regarding topographical effects on macrophage activation. However, without a clear understanding of the underlying molecular mechanism, these findings cannot be meaningfully translated into disease therapeutics. Our investigation into the actin cytoskeleton and acto-myosin contractility is only the first step in elucidating the underlying mechanism. Following the traditional route of mechanobiology, other adhesion proteins and the Rho family of GTPases should be examined. Based on our own experience and the literature, macrophages have unique and yet indistinct actin and adhesion structures, unlike most other cells. Higher resolution or better imaging techniques may be required to reveal more information about these structures. It is known that IL-4/IL-13-induced M2 polarization is mediated by the JAK/STAT signaling pathway, which then upregulates transcription factor PPAR-γ and its target gene arginase-I[169]. Future research can explore this or other known M2 signaling pathways and their connection to mechanotransduction pathways.

One caveat with our cell shape work is that the effect by cell shape was not as dramatic as that by soluble factors that were applied. We know that *in vivo*, macrophages would be exposed to both soluble and adhesive cues simultaneously. And it is difficult to ascertain the level of

soluble simulation that would be considered physiological. We could potentially be stimulating macrophages with saturating levels of soluble factor, and thus in comparison, cell shape seemed like a much weaker regulator of phenotype. Even if soluble factors are the predominate regulators of macrophage activation, which is the prevailing sentiment in the literature, we have shown substantial evidence that cell shape could modulate cytokine-induced polarization, especially if levels of cytokines present were low. In light of the recent single cell study that had shown that coordinate immune responses may be initiated by a few precocious cells[146], there maybe be room for macrophage phenotype regulators of various "strengths". For instance, if the microenvironment contains high concentrations of soluble stimuli, the threshold for activating the few precocious cells would be reached quickly, and paracrine signaling would allow the whole population to reach an activated equilibrium very quickly. In this case, having a few "starter" cells is an efficient way for quorum sensing. On the other hand, this could also be a very dangerous strategy, for a system level response would be inescapable if the few precocious cells were accidently activated. This may be especially relevant in the absence of a strong soluble microenvironment, perhaps reminiscent of nascent stages of disease pathogenesis, where more subtle regulators such as physical and adhesive cues could nudge the macrophages into activation. Therefore, there is value in understanding all macrophage functional regulators.

However, before we could accomplish that, better tools for understanding macrophage functional regulation in the absence of confounding factors such as cellular heterogeneity, cell-

cell interactions and paracrine signaling is needed. To this end, we have developed and validated a single cell secretion detection platform that would allow us to specifically study macrophages with controlled adhesion. Although our initial findings clearly shown an effect of cell adhesion on macrophage secretion, they raise more questions than they answer. How the different ECMs and cell shapes could mechanistically activate macrophages must be explored on a single cell level.

The biggest current limitation with our single cell system is that it is not multiplexed, and there is not an immediately obvious way to make it so. In the current "omics" age, the desire to obtain a comprehensive picture of a single cell state is increasing. Even the ability to obtain information on multiple different markers or different types of markers (surface, intracellular, secreted etc.) without bias will facilitate potential discovery of new subpopulations. To address this shortcoming as well as enhancing the overall detection sensitivity of the system, we plan to conjugate detection antibodies with quantum dot (QDs) nanoparticles using bioorthogonal chemistry. The small footprint of nanoparticles allows multiple conjugations per detection antibody, thus significantly increasing fluorescence signal. QDs are chosen over organic fluorophores because they have tunable emission and high resistance to photobleaching. Different colored QDs can be modified to different detection antibodies to enable simultaneous detection of multiple target proteins. Additionally, macrophages in the microwells could be stained for different surface and intracellular markers to extract more information out of each

cell. With our current fluorescence-based detection, we are only able to detect secretion when macrophages are stimulated with soluble factors. So all the results obtained thus far are from macrophages stimulated with both soluble and adhesive cues. Increased detection limit with the incorporation of QDs will allow us to examined the pure effect of adhesive cues on secretion and ultimately better understand these factors on macrophage activation.

Recent studies clearly suggest that physical cues in the microenvironment contribute to the regulation of macrophage phenotype and function. However, we are far from reaching a consensus for how the picture looks. Contributing to the confusion and a few seemingly contradictory findings in the current body of literature are several factors. 1) There are differences between macrophages from different species. The majority of studies described in this review were performed using murine and human macrophages, with a few using rat cells. While experiments with murine systems have been extremely valuable particularly for molecular-genetic studies, and mouse and human immune systems clearly share some similarities, there are also fundamental differences[160]. Although macrophages from both species adopt a similar continuum of activation states, it has been well established that the markers for each state can be quite different[13,161]. A cross-species comparison for macrophage activation in response to physical and mechanical stimulation is still lacking. 2) Macrophages from different tissues within the same host may have different sensitivity to mechanical cues. For example, alveolar macrophages and osteoclasts naturally undergo more mechanical loading in the body,

and therefore may be more sensitive to physical stimuli. In addition, ECMs from different tissues can have dramatically different stiffness and architecture, which may result in differential responsiveness to physical signals by macrophages in those tissues. 3) The length and time scale at which the effects of mechanical cues are examined is important. It merits reiteration that there is likely a range of ECM stiffness and architecture that best supports tissue homeostasis and physiological macrophage function. Engineered materials should closely mimic the cellular niche of the intended targets of study. Additionally, macrophage secretion profile of different cytokines is likely to vary over time. Several studies have shown a temporal dependence of the effect of mechanical cues, especially substrate topography and rigidity. 4) Macrophages are very sensitive to various soluble and matrix cues, and possibly to different materials including the polymers and metals that are used as biomaterials. It has been demonstrated that adhesion to various ECM proteins can induce macrophage activation[151,152] and enhance phagocytosis[162]. Therefore, future studies should be assiduous in extricating the effects of matrix and mechanics. 5) Last but not least, immune cells including macrophages are notorious for being very heterogeneous. The ground state activation level of macrophages is known to fluctuate depending on time of the day, seasons of the year, diet and systemic conditions of the host[163], which may explain inconsistencies in studies using primary cells.

Clearly, much work is still needed in elucidating the underlying mechanism for macrophage mechanobiology. The link between adhesion, cytoskeletal dynamics and activation

remains ambiguous at best. The pathway between the cytoskeleton, nuclei and possible transcription factors is largely unknown. Topographical studies have shown that surface roughness alone can cause src-mediated FAK phosphorylation[103], which then leads to nuclear translocation of ERK1/2 and increased secretion of proinflammatory cytokines in RAW264.7 cells[48]. It has also been postulated that substrate topography can activate the NF-κB-mediated inflammatory signaling pathway via cell surface receptors found in actin-associated, lipid-enriched rafts on the cell membrane[164]. Stretch-induced inflammation in macrophages has been attributed to NF-κB[63] and NLRP3 inflammasome[165] activation. Stretch-induced MMP expressions have been linked to upregulation in transcription factors *c-jun*, *c-fos* and *PU.1*[65]. There has also been studies suggesting that mechanically sensitive potassium channels are responsible for modulating macrophage cell shape upon adherence as well as stretch-mediated activation[166]. Alternatively, macrophage activation can be regulated by epigenetic means[167]. And it has also been postulated that the physical and mechanical activation may be due to post-translational modifications that are not associated with gene expression, such as ligand-receptor interactions and cell membrane extensions[73].

Despite these limitations, there is much evidence supporting physical and mechanical regulation of macrophage phenotype polarization and function. In addition to affecting change on their own, biophysical cues can also function synergistically with soluble factors to mediate macrophage behavior. Although much of the work highlighted here is performed on engineered

substrates, with work in 3D beginning to emerge, the effects observed may very well translate to *in vivo* conditions. Tissues and various components of tissue can be conceptualized as distinct biomaterials that can possess wide range of mechanical properties and exert physical influences on macrophages in the same way engineered materials can. While soluble factors are the putative reason for abnormal macrophage polarization in diseases, physical and mechanical factors associated with ECM modification may exacerbate disease progression. Experimental approaches by means of selectively targeting macrophages with disease phenotypes or introducing beneficial ones have so far been unsuccessful[128,168]. Evidence suggests that most likely, more than one macrophage phenotype is required for complex processes such as wound healing. The key may lie in the timely transition from one phenotype to another. Leveraging the functional plasticity of macrophages, by both biochemical and physical means, to "re-educate" them to attain beneficial phenotypes in a timely manner may prove to be a more effective therapeutic strategy than complete depletion of certain populations.

## REFERENCES


1. Sieweke, M. H. & Allen, J. E. Beyond stem cells: self-renewal of differentiated macrophages. *Science* **342,** 1242974 (2013).

2. Guilliams, M. *et al.* Dendritic cells, monocytes and macrophages: a unified nomenclature based on ontogeny. *Nat. Rev. Immunol.* 1–8 (2014). doi:10.1038/nri3712

3. Ajami, B., Bennett, J. L., Krieger, C., Tetzlaff, W. & Rossi, F. M. V. Local self-renewal can sustain CNS microglia maintenance and function throughout adult life. *Nat. Neurosci.* **10,** 1538–43 (2007).

4. Mosser, D. M. & Edwards, J. P. Exploring the full spectrum of macrophage activation. *Nat. Rev. Immunol.* **8,** 958–69 (2008).

5. Gautier, E. L. *et al.* Gene-expression profiles and transcriptional regulatory pathways that underlie the identity and diversity of mouse tissue macrophages. *Nat. Immunol.* **13,** 1118–28 (2012).

6. Martinez, F. O., Gordon, S., Locati, M. & Mantovani, A. Transcriptional profiling of the human monocyte-to-macrophage differentiation and polarization: new molecules and patterns of gene expression. *J. Immunol.* **177,** 7303–7311 (2006).

7. Mantovani, A. *et al.* The chemokine system in diverse forms of macrophage activation and polarization. *Trends Immunol.* **25,** 677–86 (2004).

8. Lang, R., Patel, D., Morris, J. J., Rutschman, R. L. & Murray, P. J. Shaping gene expression in activated and resting primary macrophages by IL-10. *J. Immunol.* **169,** 2253–63 (2002).

9. Albina, J. E., Mills, C. D., Henry, W. L. & Caldwell, M. D. Temporal expression of different pathways of 1-arginine metabolism in healing wounds. *J. Immunol.* **144,** 3877–3880 (1990).

10. Gallardo-Soler, A. *et al.* Arginase I induction by modified lipoproteins in macrophages: a peroxisome proliferator-activated receptor-gamma/delta-mediated effect that links lipid metabolism and immunity. *Mol. Endocrinol.* **22,** 1394–402 (2008).

11. Stein, M., Keshav, S., Harris, N. & Gordon, S. Interleukin 4 potently enhances murine macrophage mannose receptor activity: a marker of alternative immunologic macrophage activation. *J. Exp. Med.* **176,** 287–292 (1992).

12. Brown, B. N., Ratner, B. D., Goodman, S. B., Amar, S. & Badylak, S. F. Macrophage polarization: an opportunity for improved outcomes in biomaterials and regenerative medicine. *Biomaterials* **33,** 3792–802 (2012).

13. Raes, G. et al. Arginase-1 and Ym1 are markers for murine, but not human, alternatively activated myeloid cells. *J. Immunol.* **174,** 6561–6562 (2005).

14. Lewis, C. E. & Pollard, J. W. Distinct role of macrophages in different tumor microenvironments. *Cancer Res.* **66,** 605–612 (2006).

15. Mantovani, A., Sozzani, S., Locati, M., Allavena, P. & Sica, A. Macrophage polarization: tumor-associated macrophages as a paradigm for polarized M2 mononuclear phagocytes. *Trends Immunol.* **23,** 549–55 (2002).

16. Sica, A. *et al.* Macrophage polarization in tumour progression. *Semin. Cancer Biol.* **18,** 349–55 (2008).

17. Kortylewski, M. *et al.* Inhibiting Stat3 signaling in the hematopoietic system elicits multicomponent antitumor immunity. *Nat. Med.* **11,** 1314–1321 (2005).

18. Meir, K. S. & Leitersdorf, E. Atherosclerosis in the Apolipoprotein E – Deficient Mouse A Decade of Progress. *Arterioscler. Thromb. Vasc. Biol.* **24,** 1006–1014 (2004).

19. Khallou-Laschet, J. *et al.* Macrophage Plasticity in Experimental Atherosclerosis. *PLoS One* **5,** 10 (2010).

20. Chinetti-Gbaguidi, G. *et al.* Human atherosclerotic plaque alternative macrophages display low cholesterol handling but high phagocytosis because of distinct activities of the PPARγ and LXRα pathways. *Circ. Res.* **108,** 985–95 (2011).

21. Tsimikas, S. & Miller, Y. I. Oxidative modification of lipoproteins: mechanisms, role in inflammation and potential clinical applications in cardiovascular disease. *Curr. Pharm. Des.* **17,** 27–37 (2011).

22. Li, S. *et al.* Defective phagocytosis of apoptotic cells by macrophages in atherosclerotic lesions of ob/ob mice and reversal by a fish oil diet. *Circ. Res.* **105,** 1072–1082 (2009).

23. Brancato, S. K. & Albina, J. E. Wound macrophages as key regulators of repair: origin, phenotype, and function. *Am. J. Pathol.* **178,** 19–25 (2011).

24. Lucas, T. *et al.* Differential roles of macrophages in diverse phases of skin repair. *J. Immunol.* **184,** 3964–77 (2010).

25. Anderson, J. M., Rodriguez, A. & Chang, D. T. Foreign body reaction to biomaterials. *Semin. Immunol.* **20,** 86–100 (2008).

26. Brown, B. N., Valentin, J. E., Stewart-Akers, A. M., McCabe, G. P. & Badylak, S. F. Macrophage phenotype and remodeling outcomes in response to biologic scaffolds with and without a cellular component. *Biomaterials* **30,** 1482–91 (2009).

27. Badylak, S. F. & Gilbert, T. W. Immune response to biologic scaffold materials. *Semin. Immunol.* **20,** 109–116 (2008).

28. Madden, L. R. *et al.* Proangiogenic scaffolds as functional templates for cardiac tissue engineering. *Proc. Natl. Acad. Sci. U. S. A.* **107,** 15211–15216 (2010).

29. Jaalouk, D. E. & Lammerding, J. Mechanotransduction gone awry. *Nat. Rev. Mol. Cell Biol.* **10,** 63–73 (2009).

30. Brownell, W. E., Bader, C. R., Bertrand, D. & De Ribaupierre, Y. Evoked mechanical responses of isolated cochlear outer hair cells. *Science (80-. ).* **227,** 194–196 (1985).

31. Duncan, R. L. & Turner, C. H. Mechanotransduction and the functional response of bone to mechanical strain. *Calcif. Tissue Int.* **57,** 344–358 (1995).

32. Yamamoto, K. *et al.* Proliferation, differentiation, and tube formation by endothelial progenitor cells in response to shear stress. *J. Appl. Physiol.* **95,** 2081–2088 (2003).

33. Stegemann, J. P., Hong, H. & Nerem, R. M. Mechanical, biochemical, and extracellular matrix effects on vascular smooth muscle cell phenotype. *J. Appl. Physiol.* **98,** 2321–2327

(2005).

34. Hsiai, T. K. & Wu, J. C. Hemodynamic Forces Regulate Embryonic Stem Cell Commitment to Vascular Progenitors. *Curr. Cardiol. Rev.* **4,** 269–274 (2008).

35. Engler, A. J., Sen, S., Sweeney, H. L. & Discher, D. E. Matrix elasticity directs stem cell lineage specification. *Cell* **126,** 677–89 (2006).

36. Gilbert, P. M. *et al.* Substrate elasticity regulates skeletal muscle stem cell self-renewal in culture. *Science (80-. ).* **329,** 1078–1081 (2010).

37. Folkman, J. & Moscona, A. Role of cell shape in growth control. *Nature* **273,** 345–349 (1978).

38. Chen, C. S. Geometric Control of Cell Life and Death. *Science (80-. ).* **276,** 1425–1428 (1997).

39. Yang, Y., Relan, N. K., Przywara, D. A. & Schuger, L. Embryonic mesenchymal cells share the potential for smooth muscle differentiation: myogenesis is controlled by the cell's shape. *Dev. Cambridge Engl.* **126,** 3027–3033 (1999).

40. Kilian, K. A., Bugarija, B., Lahn, B. T. & Mrksich, M. Geometric cues for directing the differentiation of mesenchymal stem cells. *Proc. Natl. Acad. Sci. U. S. A.* **107,** 4872–4877 (2010).

41. Zhang, D. & Kilian, K. a. The effect of mesenchymal stem cell shape on the maintenance of multipotency. *Biomaterials* **34,** 3962–3969 (2013).

42. Brown, B. N. *et al.* Macrophage phenotype as a predictor of constructive remodeling following the implantation of biologically derived surgical mesh materials. *Acta Biomater.* **8,** 978–987 (2012).

43. Chen, S. *et al.* Characterization of topographical effects on macrophage behavior in a foreign body response model. *Biomaterials* **31,** 3479–91 (2010).

44. Saino, E. *et al.* Effect of electrospun fiber diameter and alignment on macrophage activation and secretion of proinflammatory cytokines and chemokines.

*Biomacromolecules* **12,** 1900–1911 (2011).

45. Garg, K., Pullen, N. a, Oskeritzian, C. a, Ryan, J. J. & Bowlin, G. L. Macrophage functional polarization (M1/M2) in response to varying fiber and pore dimensions of electrospun scaffolds. *Biomaterials* **34,** 4439–4451 (2013).

46. McWhorter, F. Y., Davis, C. T. & Liu, W. F. Physical and mechanical regulation of macrophage phenotype and function. *Cell. Mol. Life Sci.* **72,** 1303–1316 (2014).

47. Rich, A. & Harris, A. K. Anomalous preferences of cultured macrophages for hydrophobic and roughened substrata. *J. Cell Sci.* **50,** 1–7 (1981).

48. Refai, A. K., Textor, M., Brunette, D. M. & Waterfield, J. D. Effect of titanium surface topography on macrophage activation and secretion of proinflammatory cytokines and chemokines. *J. Biomed. Mater. Res. Part A* **70,** 194–205 (2004).

49. Tan, K. S., Qian, L., Rosado, R., Flood, P. M. & Cooper, L. F. The role of titanium surface topography on J774A.1 macrophage inflammatory cytokines and nitric oxide production. *Biomaterials* **27,** 5170–5177 (2006).

50. Lee, S. *et al.* Analysis on migration and activation of live macrophages on transparent flat and nanostructured titanium. *Acta Biomater.* **7,** 2337–44 (2011).

51. Wójciakâ-Stothard, B., Madeja, Z., Korohoda, W., Curtis, A. & Wilkinson, C. Activation of macrophage-like cells by multiple grooved substrata. Topographical control of cell behaviour. *Cell Biol. Int.* **19,** 485 (1995).

52. Wójciak-Stothard, B., Curtis, a, Monaghan, W., MacDonald, K. & Wilkinson, C. Guidance and activation of murine macrophages by nanometric scale topography. *Exp. Cell Res.* **223,** 426–35 (1996).

53. Cao, H., McHugh, K., Chew, S. Y. & Anderson, J. M. The topographical effect of electrospun nanofibrous scaffolds on the in vivo and in vitro foreign body reaction. *J. Biomed. Mater. Res. A* **93,** 1151–9 (2010).

54. Sanders, J. E., Bale, S. D. & Neumann, T. Tissue response to microfibers of different polymers: Polyester, polyethylene, polylactic acid, and polyurethane. *J. Biomed. Mater.*

*Res.* **62,** 222–227 (2002).

55. Baker, B. M. & Chen, C. S. Deconstructing the third dimension - how 3D culture microenvironments alter cellular cues. *Journal of Cell Science* **125,** 3015–3024 (2012).

56. Bartneck, M. *et al.* Inducing healing-like human primary macrophage phenotypes by 3D hydrogel coated nanofibres. *Biomaterials* **33,** 4136–46 (2012).

57. Brown, E. *et al.* Dynamic imaging of collagen and its modulation in tumors in vivo using second-harmonic generation. *Nat. Med.* **9,** 796–800 (2003).

58. Guiet, R. *et al.* The process of macrophage migration promotes matrix metalloproteinase-independent invasion by tumor cells. *J. Immunol.* **187,** 3806–14 (2011).

59. Van Goethem, E., Poincloux, R., Gauffre, F., Maridonneau-Parini, I. & Le Cabec, V. Matrix architecture dictates three-dimensional migration modes of human macrophages: differential involvement of proteases and podosome-like structures. *J. Immunol.* **184,** 1049–61 (2010).

60. Liu, M. & Post, M. Invited review: mechanochemical signal transduction in the fetal lung. *J. Appl. Physiol.* **89,** 2078–2084 (2000).

61. Klein-Nulend, J., Bacabac, R. G. & Mullender, M. G. Mechanobiology of bone tissue. *Pathol. Biol. (Paris).* **53,** 576–80 (2005).

62. Kurata, K. *et al.* Mechanical strain effect on bone-resorbing activity and messenger RNA expressions of marker enzymes in isolated osteoclast culture. *J. Bone Miner. Res.* **16,** 722–730 (2001).

63. Pugin, J. *et al.* Activation of human macrophages by mechanical ventilation in vitro. *Am J Physiol* **275,** L1040–L1050 (1998).

64. Wehner, S. *et al.* Mechanical strain and TLR4 synergistically induce cell-specific inflammatory gene expression in intestinal smooth muscle cells and peritoneal macrophages. *Am. J. Physiol. Gastrointest. Liver Physiol.* **299,** G1187–G1197 (2010).

65. Yang, J. H., Sakamoto, H., Xu, E. C. & Lee, R. T. Biomechanical regulation of human

monocyte/macrophage molecular function. *Am. J. Pathol.* **156,** 1797–804 (2000).

66. Ballotta, V., Driessen-Mol, A., Bouten, C. V. C. & Baaijens, F. P. T. Strain-dependent modulation of macrophage polarization within scaffolds. *Biomaterials* **35,** 4919–4928 (2014).

67. Lo, C. M., Wang, H. B., Dembo, M. & Wang, Y. L. Cell movement is guided by the rigidity of the substrate. *Biophys. J.* **79,** 144–152 (2000).

68. Paszek, M. J. *et al.* Tensional homeostasis and the malignant phenotype. *Cancer Cell* **8,** 241–254 (2005).

69. Huynh, J. *et al.* Age-related intimal stiffening enhances endothelial permeability and leukocyte transmigration. *Sci. Transl. Med.* **3,** 112ra122 (2011).

70. Blakney, A. K., Swartzlander, M. D. & Bryant, S. J. The effects of substrate stiffness on the in vitro activation of macrophages and in vivo host response to poly(ethylene glycol)-based hydrogels. *J. Biomed. Mater. Res. A* **100,** 1375–86 (2012).

71. Nemir, S., Hayenga, H. N. & West, J. L. PEGDA hydrogels with patterned elasticity: Novel tools for the study of cell response to substrate rigidity. *Biotechnol. Bioeng.* **105,** 636–644 (2010).

72. Irwin, E. F. *et al.* Modulus-dependent macrophage adhesion and behavior. *J. Biomater. Sci. Polym. Ed.* **19,** 1363–82 (2008).

73. Patel, N. R. *et al.* Cell elasticity determines macrophage function. *PLoS One* **7,** e41024 (2012).

74. Pelham, R. J. & Wang, Y. Cell locomotion and focal adhesions are regulated by substrate flexibility. *Proc. Natl. Acad. Sci. U. S. A.* **94,** 13661–13665 (1997).

75. Discher, D. E., Janmey, P. & Wang, Y.-L. Tissue cells feel and respond to the stiffness of their substrate. *Science (80-. ).* **310,** 1139–1143 (2005).

76. Liu, W. F. Mechanical regulation of cellular phenotype: implications for vascular tissue regeneration. *Cardiovasc. Res.* **95,** 215–22 (2012).

77. Chen, C. S., Alonso, J. L., Ostuni, E., Whitesides, G. M. & Ingber, D. E. Cell shape provides global control of focal adhesion assembly. *Biochem. Biophys. Res. Commun.* **307,** 355–361 (2003).

78. Parsons, J. T., Martin, K. H., Slack, J. K., Taylor, J. M. & Weed, S. A. Focal adhesion kinase: a regulator of focal adhesion dynamics and cell movement. *Oncogene* **19,** 5606–5613 (2000).

79. Hall, A. Rho GTPases and the Actin Cytoskeleton. *Science (80-. ).* **279,** 509–514 (1998).

80. Kozma, R., Sarner, S., Ahmed, S. & Lim, L. Rho family GTPases and neuronal growth cone remodelling: relationship between increased complexity induced by Cdc42Hs, Rac1, and acetylcholine and collapse induced by RhoA and lysophosphatidic acid. *Mol. Cell. Biol.* **17,** 1201–1211 (1997).

81. Aepfelbacher, M., Essler, M., Huber, E., Czech, A. & Weber, P. C. Rho is a negative regulator of human monocyte spreading. *J. Immunol.* **157,** 5070–5075 (1996).

82. Postma, F. R. *et al.* Serum-induced membrane depolarization in quiescent fibroblasts: activation of a chloride conductance through the G protein-coupled LPA receptor. *Eur. Mol. Biol. Organ. J.* **15,** 63–72 (1996).

83. Allen, W. E., Jones, G. E., Pollard, J. W. & Ridley, A. J. Rho, Rac and Cdc42 regulate actin organization and cell adhesion in macrophages. *J. Cell Sci.* **110 ( Pt 6,** 707–720 (1997).

84. McBeath, R., Pirone, D. M., Nelson, C. M., Bhadriraju, K. & Chen, C. S. Cell shape, cytoskeletal tension, and RhoA regulate stem cell lineage commitment. *Dev. Cell* **6,** 483–95 (2004).

85. DeMali, K. a, Wennerberg, K. & Burridge, K. Integrin signaling to the actin cytoskeleton. *Curr. Opin. Cell Biol.* **15,** 572–582 (2003).

86. Machesky, L. M. & Hall, A. Role of actin polymerization and adhesion to extracellular matrix in Rac- and Rho-induced cytoskeletal reorganization. *J. Cell Biol.* **138,** 913–26 (1997).

87. Amano, M., Nakayama, M. & Kaibuchi, K. Rho-kinase/ROCK: A key regulator of the cytoskeleton and cell polarity. *Cytoskeleton* **554,** 545–554 (2010).

88. Féréol, S. *et al.* Sensitivity of alveolar macrophages to substrate mechanical and adhesive properties. *Cell Motil. Cytoskeleton* **63,** 321–40 (2006).

89. Vereyken, E. J. F. *et al.* Classically and alternatively activated bone marrow derived macrophages differ in cytoskeletal functions and migration towards specific CNS cell types. *J. Neuroinflammation* **8,** 58 (2011).

90. McWhorter, F. Y., Wang, T., Nguyen, P., Chung, T. & Liu, W. F. Modulation of macrophage phenotype by cell shape. *Proc. Natl. Acad. Sci. U. S. A.* **110,** 17253–8 (2013).

91. Block, M. R. *et al.* Podosome-type adhesions and focal adhesions, so alike yet so different. *Eur. J. Cell Biol.* **87,** 491–506 (2008).

92. Leporatti, S. *et al.* Elasticity and adhesion of resting and lipopolysaccharide-stimulated macrophages. *FEBS Lett.* **580,** 450–454 (2006).

93. Pi, J. *et al.* Detection of lipopolysaccharide induced inflammatory responses in RAW264.7 macrophages using atomic force microscope. *Micron* 1–9 (2014). doi:10.1016/j.micron.2014.03.012

94. Féréol, S. *et al.* Mechanical and structural assessment of cortical and deep cytoskeleton reveals substrate-dependent alveolar macrophage remodeling. *Biomed. Mater. Eng.* **18,** S105–S118 (2008).

95. Tee, S. Y., Fu, J., Chen, C. S. & Janmey, P. A. Cell shape and substrate rigidity both regulate cell stiffness. *Biophys. J.* **100,** (2011).

96. Friedl, P. & Weigelin, B. Interstitial leukocyte migration and immune function. *Nat. Immunol.* **9,** 960–969 (2008).

97. Gowen, B. B., Borg, T. K., Ghaffar, a & Mayer, E. P. Selective adhesion of macrophages to denatured forms of type I collagen is mediated by scavenger receptors. *Matrix Biol.* **19,** 61–71 (2000).

98. El Khoury, J. *et al.* Macrophages adhere to glucose-modified basement membrane collagen IV via their scavenger receptors. *J. Biol. Chem.* **269,** 10197–10200 (1994).

99. Santiago-García, J., Kodama, T. & Pitas, R. E. The class A scavenger receptor binds to proteoglycans and mediates adhesion of macrophages to the extracellular matrix. *J. Biol. Chem.* **278,** 6942–6946 (2003).

100. Kirkham, P. A., Spooner, G., Ffoulkes-Jones, C. & Calvez, R. Cigarette smoke triggers macrophage adhesion and activation: Role of lipid peroxidation products and scavenger receptor. *Free Radic. Biol. Med.* **35,** 697–710 (2003).

101. Duong, L. T. & Rodan, G. A. Pyk2 is an adhesion kinase in macrophages, localized in podosomes and activated by B2-integrin ligation. *Cell Motil. Cytoskeleton* **47,** 174–188 (2000).

102. Pfaff, M. & Jurdic, P. Podosomes in osteoclast-like cells: structural analysis and cooperative roles of paxillin, proline-rich tyrosine kinase 2 (Pyk2) and integrin alphaVbeta3. *J. Cell Sci.* **114,** 2775–2786 (2001).

103. Ghrebi, S., Hamilton, D. W., Douglas Waterfield, J. & Brunette, D. M. The effect of surface topography on cell shape and early ERK1/2 signaling in macrophages; linkage with FAK and Src. *J. Biomed. Mater. Res. A* **101,** 2118–28 (2013).

104. Collin, O. *et al.* Self-organized podosomes are dynamic mechanosensors. *Curr. Biol.* **18,** 1288–94 (2008).

105. Van Goethem, E. *et al.* Macrophage podosomes go 3D. *Eur. J. Cell Biol.* **90,** 224–236 (2011).

106. Berton, G. & Lowell, C. Integrin signalling in neutrophils and macrophages. *Cell. Signal.* **11,** 621–635 (1999).

107. Zaveri, T. D., Lewis, J. S., Dolgova, N. V, Clare-Salzler, M. J. & Keselowsky, B. G. Integrin-directed modulation of macrophage responses to biomaterials. *Biomaterials* **35,** 3504–15 (2014).

108. Ory, S., Brazier, H., Pawlak, G. & Blangy, A. Rho GTPases in osteoclasts: orchestrators of

podosome arrangement. *Eur. J. Cell Biol.* **87,** 469–77 (2008).

109. Hoppe, A. D. & Swanson, J. A. Cdc42, Rac1, and Rac2 display distinct patterns of activation during phagocytosis. *Mol. Biol. Cell* **15,** 3509–3519 (2004).

110. Wheeler, A. P. *et al.* Rac1 and Rac2 regulate macrophage morphology but are not essential for migration. *J. Cell Sci.* **119,** 2749–2757 (2006).

111. Joshi, S., Singh, A., Zulcic, M., Bao, L. & Messer, K. Rac2 Controls Tumor Growth, Metastasis and M1-M2 Macrophage Differentiation In Vivo. *PLoS One* **9,** (2014).

112. Murray, P. J. *et al.* Macrophage Activation and Polarization: Nomenclature and Experimental Guidelines. *Immunity* **41,** 14–20 (2014).

113. Wheeler, A. R., Smith, S. D. & Ridley, A. J. CSF-1 and PI 3-kinase regulate podosome distribution and assembly in macrophages. *Cell Motil. Cytoskeleton* **63,** 132–140 (2006).

114. Cougoule, C. *et al.* Blood leukocytes and macrophages of various phenotypes have distinct abilities to form podosomes and to migrate in 3D environments. *Eur. J. Cell Biol.* **91,** 938–949 (2012).

115. Pradip, D., Peng, X. & Durden, D. L. Rac2 specificity in macrophage integrin signaling: potential role for Syk kinase. *J. Biol. Chem.* **278,** 41661–41669 (2003).

116. Daley, J. & Reichner, J. Modulation of macrophage phenotype by soluble product (s) released from neutrophils. *J. Immunol.* **174,** 2265–2272 (2005).

117. Nelson, C. & Bissell, M. Of extracellular matrix, scaffolds, and signaling: tissue architecture regulates development, homeostasis, and cancer. *Annu. Rev. cell Dev. …* (2006). doi:10.1146/annurev.cellbio.22.010305.104315.Of

118. Goetz, J. G. *et al.* Biomechanical remodeling of the microenvironment by stromal caveolin-1 favors tumor invasion and metastasis. *Cell* **146,** 52–67 (2010).

119. Sharma, V. et al. Reconstitution of in vivo macrophage-tumor cell pairing and streaming motility on one-dimensional micro-patterned substrates. *IntraVital* **1,** 77–85 (2012).

120. Stöger, J., Gijbels, M. & Velden, S. Van Der. Distribution of macrophage polarization markers in human atherosclerosis. *Atherosclerosis* **225,** 461–468 (2012).

121. Matheson, L. a, Fairbank, N. J., Maksym, G. N., Paul Santerre, J. & Labow, R. S. Characterization of the Flexcell Uniflex cyclic strain culture system with U937 macrophage-like cells. *Biomaterials* **27,** 226–33 (2006).

122. Hanisch, U.-K. & Kettenmann, H. Microglia: active sensor and versatile effector cells in the normal and pathologic brain. *Nat. Neurosci.* **10,** 1387–1394 (2007).

123. Neubrand, V. E. *et al.* Mesenchymal stem cells induce the ramification of microglia via the small RhoGTPases Cdc42 and Rac1. *Glia* 1–11 (2014). doi:10.1002/glia.22714

124. Lee, H.-S. *et al.* Correlating macrophage morphology and cytokine production resulting from biomaterial contact. *J. Biomed. Mater. Res. A* **101,** 203–12 (2013).

125. Li, F., Li, B., Wang, Q.-M. & Wang, J. H.-C. Cell shape regulates collagen type I expression in human tendon fibroblasts. *Cell Motil. Cytoskeleton* **65,** 332–41 (2008).

126. Thakar, R. G. *et al.* Cell-shape regulation of smooth muscle cell proliferation. *Biophys. J.* **96,** 3423–32 (2009).

127. Alford, P. W., Nesmith, A. P., Seywerd, J. N., Grosberg, A. & Parker, K. K. Vascular smooth muscle contractility depends on cell shape. *Integr. Biol. (Camb).* **3,** 1063–70 (2011).

128. Mirza, R., DiPietro, L. A. & Koh, T. J. Selective and specific macrophage ablation is detrimental to wound healing in mice. *Am. J. Pathol.* **175,** 2454–62 (2009).

129. Pesce, J. T. *et al.* Arginase-1-expressing macrophages suppress Th2 cytokine-driven inflammation and fibrosis. *PLoS Pathog.* **5,** (2009).

130. Waldo, S. W. *et al.* Heterogeneity of human macrophages in culture and in atherosclerotic plaques. *Am. J. Pathol.* **172,** 1112–26 (2008).

131. Aderem, a & Underhill, D. M. Mechanisms of phagocytosis in macrophages. *Annu. Rev. Immunol.* **17,** 593–623 (1999).

132. Amato, P. A., Unanue, E. R. & Taylor, D. L. Distribution of actin in spreading macrophages: A comparative study on living and fixed cells. *J. Cell Biol.* **96,** 750–761 (1983).

133. DeFife, K. M., Jenney, C. R., Colton, E. & Anderson, J. M. Disruption of filamentous actin inhibits human macrophage fusion. *FASEB J.* **13,** 823–832 (1999).

134. Dupont, S. *et al.* Role of YAP/TAZ in mechanotransduction. *Nature* **474,** 179–83 (2011).

135. Versaevel, M., Grevesse, T. & Gabriele, S. Spatial coordination between cell and nuclear shape within micropatterned endothelial cells. *Nature Communications* **3,** 671 (2012).

136. Li, Y. *et al.* Biophysical regulation of histone acetylation in mesenchymal stem cells. *Biophys. J.* **100,** 1902–1909 (2011).

137. Sica, A. & Mantovani, A. Macrophage plasticity and polarization: in vivo veritas. *J. Clin. Invest.* **122,** 787–95 (2012).

138. Lin, C. Q. & Bissell, M. J. Multi-faceted regulation of cell differentiation by extracellular matrix. *FASEB J.* **7,** 737–43 (1993).

139. Bissell, M. J. & Radisky, D. Putting tumours in context. *Nat. Rev. Cancer* **1,** 46–54 (2001).

140. Chen, S. *et al.* Characterization of topographical effects on macrophage behavior in a foreign body response model. *Biomaterials* **31,** 3479–3491 (2010).

141. Proserpio, V. & Mahata, B. Single-cell technologies to study the immune system. *Immunology* n/a–n/a (2015). doi:10.1111/imm.12553

142. Mosser, D. M. The many faces of macrophage activation. *J. Leukoc. Biol.* **73,** 209–212 (2003).

143. Chattopadhyay, P. K., Gierahn, T. M., Roederer, M. & Love, J. C. Single-cell technologies for monitoring immune systems. *Nat. Immunol.* **15,** 128–35 (2014).

144. Sindrilaru, A. *et al.* An unrestrained proinflammatory M1 macrophage population

induced by iron impairs wound healing in humans and mice. *J. Clin. Invest.* **121,** 985–997 (2011).

145. Peine, M. *et al.* Stable T-bet(+)GATA-3(+) Th1/Th2 hybrid cells arise in vivo, can develop directly from naive precursors, and limit immunopathologic inflammation. *PLoS Biol.* **11,** e1001633 (2013).

146. Shalek, A. K. *et al.* Single-cell RNA-seq reveals dynamic paracrine control of cellular variation. *Nature* **509,** 363–9 (2014).

147. Shalek, A. K. *et al.* Single-cell transcriptomics reveals bimodality in expression and splicing in immune cells. *Nature* **498,** 236–240 (2013).

148. Bershadsky, A. D. & Futerman, A. H. Disruption of the Golgi apparatus by brefeldin A blocks cell polarization and inhibits directed cell migration. *Proc. Natl. Acad. Sci.* **91 ,** 5686–5689 (1994).

149. Love, J. C., Ronan, J. L., Grotenbreg, G. M., van der Veen, A. G. & Ploegh, H. L. A microengraving method for rapid selection of single cells producing antigen-specific antibodies. *Nat. Biotechnol.* **24,** 703–7 (2006).

150. Lu, Y. *et al.* Highly multiplexed profiling of single-cell effector functions reveals deep functional heterogeneity in response to pathogenic ligands. *Proc. Natl. Acad. Sci.* 201416756 (2015). doi:10.1073/pnas.1416756112

151. Okamura, Y. *et al.* The extra domain A of fibronectin activates Toll-like receptor 4. *J. Biol. Chem.* **276,** 10229–33 (2001).

152. Smiley, S. T., King, J. A. & Hancock, W. W. Fibrinogen stimulates macrophage chemokine secretion through toll-like receptor 4. *J. Immunol.* **167,** 2887–2894 (2001).

153. Deshmane, S. L., Kremlev, S., Amini, S. & Sawaya, B. E. Monocyte chemoattractant protein-1 (MCP-1): an overview. *J. Interferon Cytokine Res.* **29,** 313–326 (2009).

154. Leonard, E. J. & Yoshimura, T. Human monocyte chemoattractant protein-1 (MCP-1). *Immunol. Today* **11,** 97–101 (1990).

155. Villena, J. & Kitazawa, H. Modulation of intestinal TLR4-inflammatory signaling pathways by probiotic microorganisms: Lessons learned from Lactobacillus jensenii TL2937. *Front. Immunol.* **4,** 1–5 (2013).

156. Hopkins, P. N. Molecular biology of atherosclerosis. *Physiol. Rev.* **93,** 1317–542 (2013).

157. Wittenburg, G., Lauer, G., Oswald, S., Labudde, D. & Franz, C. M. Nanoscale topographic changes on sterilized glass surfaces affect cell adhesion and spreading. *J. Biomed. Mater. Res. A* **102,** 2755–66 (2014).

158. Taniguchi, Y. *et al.* Quantifying E. coli proteome and transcriptome with single-molecule sensitivity in single cells. *Science* **329,** 533–538 (2010).

159. Carpenter, S., Ricci, E. P., Mercier, B. C., Moore, M. J. & Fitzgerald, K. a. Post-transcriptional regulation of gene expression in innate immunity. *Nat. Rev. Immunol.* **14,** 361–76 (2014).

160. Mestas, J. & Hughes, C. C. W. Of Mice and Not Men: Differences between Mouse and Human Immunology. *J. Immunol.* **172,** 2731–2738 (2004).

161. Raes, G. *et al.* Differential expression of FIZZ1 and Ym1 in alternatively versus classically activated macrophages. *J. Leukoc. Biol.* **71,** 597–602 (2002).

162. Newman, S. L. & Tucci, M. A. Regulation of Human Monocyte / Macrophage Function by Extracellular Matrix by Activation of Complement Receptors and Enhancement of Fc Receptor Function Monocyte / Mrb bactericidal assay. *J. Clin. Invest.* **86,** 703–714 (1990).

163. Huang, E. & Wells, C. A. The Ground State of Innate Immune Responsiveness Is Determined at the Interface of Genetic, Epigenetic, and Environmental Influences. *J. Immunol.* **193,** 13–19 (2014).

164. Waterfield, J. D., Ali, T. a, Nahid, F., Kusano, K. & Brunette, D. M. The effect of surface topography on early NFκB signaling in macrophages. *J. Biomed. Mater. Res. A* **95,** 837–47 (2010).

165. Wu, J. *et al.* Activation of NLRP3 inflammasome in alveolar macrophages contributes to mechanical stretch-induced lung inflammation and injury. *J. Immunol.* **190,** 3590–9

(2013).

166. Martin, D., Bootcov, M., Campell, T., French, P. & Breit, S. Human macrophages contain a stretch-sensitive potassium channel that is activated by adherence and cytokines. *J. Membr. Biol.* **315,** 305–315 (1995).

167. Ishii, M. *et al.* Epigenetic regulation of the alternatively activated macrophage phenotype. *Blood* **114,** 3244–3254 (2009).

168. Jetten, N. *et al.* Wound administration of m2-polarized macrophages does not improve murine cutaneous healing responses. *PLoS One* **9,** e102994 (2014).

169. Bensinger, S. J. & Tontonoz, P. Integration of metabolism and inflammation by lipid-activated nuclear receptors. *Nature* **454,** 470–7 (2008).